centre for radio science

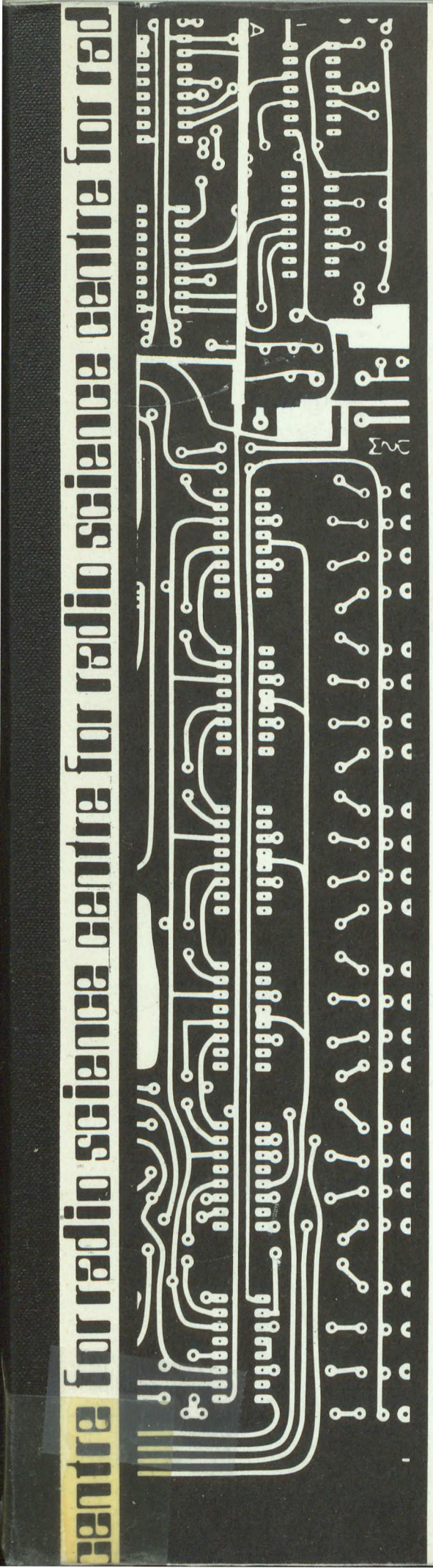

MARCH 1979

HA-28

MEASUREMENTS OF ANOMALOUS PROPOGATION OF UHF/VHF USING TV TRANSMITTERS

D.S.S. CONTRACT
OSU78-00140

02SU 3610-8-9509

THE UNIVERSITY OF WESTERN ONTARIO
LONDON CANADA.

MARCH 1979

HA-28

(1)

MEASUREMENTS OF ANOMALOUS PROPOGATION OF UHF/VHF USING TV TRANSMITTERS

D.S.S. CONTRACT
OSU78-00140

02SU 3610-8-9509

DD 4589403
DL 4589447

UHF/VHF TV MONITORING

Introduction and Acknowledgements:

The primary purpose of the contract was to gather data on the propagation of signals in the UHF/VHF frequency band. The statistical data from this study was to be used in support of decisions on land mobile frequency allocation in the border region of Canada-U.S.A.

A major portion of this contract activity was therefore in support of the routine collection and analysis of propagation data. Some of the programming for data reduction is described in section "C" of this report.

Other activities associated with this contract were (a), a detailed study of height-gain effects on propagation and (b), midpath measurements to enable a more detailed look at atmospheric effects on propagation.

The height gain measurements are described in section "A". The results given here are still somewhat preliminary since the equipment component of this study has only recently been completed.

The midpath measurements are described in section "B". In this study data on atmospheric conditions was obtained from an acoustic sounder and from routine weather maps and the weather logs from London. Also a midpath monitor on the over-water path to Erie channels 24 and 12 was operated for several months. An attempt has been made in section "B" to present some of the highlights of these studies.

Acknowledgements:

A special acknowdedgement is to Professor Z.Kucerovsky who voluntarily put a great deal of time and effort into the acoustic sounder study.

The height-gain study is by Mr.E.Lau who prepared part"A" of this report.

The computer programming is by Dr. S.K.Chan who, based on previous programming by Dr.F.C.Choo, prepared part"C" of this report.

Many people were associated with the midpath studies described in part "B". Prof. Kucerovsky, and mentioned above, operated the acoustic sounder and helped prepare this report. Ms.S.Frank and Mr.J.Haycock did the routine operation of the midpath station. The Canada Centre for Inland Waters generously allowed us to use their site near Port Burwell for our midpath recording activity. Atmospheric Environment Services provided routine atmospheric charts and data.

Also associated with this contract were the conscientous routine operation of the London monitor by Mr.S.Symons and Ms.S.Frank. Data reduction support were by Mrs.S.Fulford.Mrs.M.Meighen provided bookkeeping and secretarial support, and lastly Dr.A.Fulford and Dr. J.MacDougall were the contract co-investigators.

INDEX

PART A

HEIGHT-GAIN MEASUREMENTS

PROPAGATION OF ULTRA HIGH FREQUENCY IN TROPOSPHERE

Chapter 1. Background

The troposphere is an atmospheric region at a height of ground up to about 10 Km . When a radio wave is propagated in this region it is influenced by the properties of this region as well as the properties of the earth. The earth is considered as an inhomogeneous body and its electromagnetic properties vary from one point to another. The troposphere is a dynamic medium and its properties vary with pressure, temperature and humidity. All these variations can alter the direction, velocity and properties of the wave and result in interference effect and fading phenomenom. Figure 1.1 shows radio-wave propagation in the troposphere.

There is a line-of-sight path from the transmitter T to the receiver R and this direct wave is determined by the free space pattern of the antenna. Another wave-path is by the reflection from the earth's surface and is called reflected wave. The amplitude of this wave is governed by the properties of the earth in the region of interest. There is a third wave called tropospheric wave and this bending wave is due to the inhomogeneous medium of the troposphere.

1.1 Ground Wave.

Referring to Figure 1.1, the ground wave can be considered to be composed of the direct wave, the reflected wave and the surface wave. The complex analytical results for the propagation of these waves had been derived by K. Norton[1]. and simplified by K. Bullington[2].

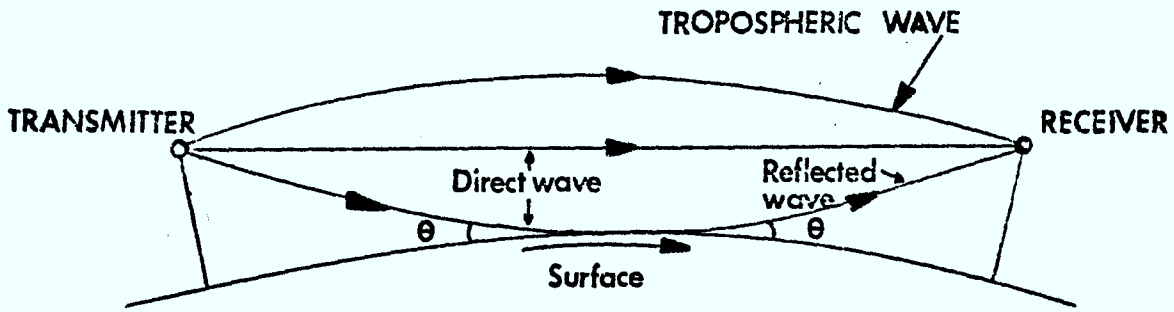

Fig. 1.1 Radio-wave Propagation

This expression is:

$$\frac{E}{E_0} = 1 + Re^{j\Delta} + (1 - R)Ae^{j\Delta} + \ldots\ldots\ldots\ldots\ldots \quad (1)$$

where E - received field intensity in volts per metre

E_0 - free space field intensity in volts per metre

R - reflection coefficient of the ground

A - 'surface wave' attenuation factor

Δ - phase difference between the direct and reflected path in radians

The first term (unity) represents the direct wave, the second term represents the reflected wave, the third term represents the surface wave and the remaining terms represent the induction field and the secondary effects of the ground.

The reflection coefficient of the ground, R, is determined by the angle of incidence θ, polarization of the wave and the ground characteristics. It is given by:

$$R = \frac{\text{Sin } \theta - z}{\text{Sin } \theta + z} \quad (2)$$

where $z = \dfrac{\sqrt{\varepsilon_0 - \text{Cos}^2\theta}}{\varepsilon_0}$ for vertical polarization

$z = \sqrt{\varepsilon_0 - \text{Cos}^2\theta}$ for horizontal polarization

$\varepsilon_0 = \varepsilon - j60\sigma\lambda$

and ε - dielectric constant of the ground relative to unity in the free space

σ - conductivity of the ground in mhos per metre

λ - wave-length in metres

when $\theta << |z|$, the reflection coefficient approaches -1,

when $\theta >> |z|$, which happens in vertical polarization, the reflection

coefficient approaches +1. In practice, the angle θ between the reflected wave and the direct wave is small, so R approaches -1 independent of the polarization.

The phase difference Δ can be expressed as (See Appendix 1):

$$\Delta = \frac{2\pi}{\lambda}\left[\left(\frac{hT + hR}{d}\right)^2 + 1\right]^{1/2} - \frac{2\pi d}{\lambda}\left[\left(\frac{hT - hR}{d}\right)^2 + 1\right]^{1/2} \qquad (3)$$

for a distance d between antennas greater than about five times the sum of the two antenna height hT and hR, that is, d>5hThR, the angle becomes:

$$\Delta \simeq 4\pi\left(\frac{hT \cdot hR}{\lambda d}\right) \qquad (4)$$

In Equation (1), there is a surface-wave term because the earth is not a perfect conductor. Some energy is transmitted into the ground and is absorbed. This results in setting up of ground currents that distort the electromagnetic field distribution relative to what it would have been over a perfectly reflecting surface. The surface wave attenuation factor, A, depends on frequency, polarization and the ground constants. It is never greater than unity and decreases with increasing frequency and distances. An approximate expression is given by:

$$A = \frac{-1}{1 + j\,\frac{2\pi d}{\lambda}\,(\mathrm{Sin}\theta + z)^2} \qquad (5)$$

with same notations as in Equation (2).

More accurate values are given by K. Norton[1]. This effect is only significant in a region a few wavelengths above the ground and it becomes approximately equal to unity at frequencies above about 300 MHz.

1.2 Tropospheric Wave.

Due to the intrinsic properties of the troposphere, propagation in this region can be resolved into three phenomena, namely, refraction, reflection and scattering. Refraction and reflection are caused by the sudden changes in the direction of the phase front while scattering is the result of irregular reflections. When considering propagation over the horizon these phenomena, along with another phenomenon, diffraction, play an important role. Diffraction is an edge effect that occurs when the phase surface is not infinite.

1.2.1 Refraction.

The formula for the index of refraction of the atmosphere is given by:

$$(n - 1)10^6 = \frac{79\rho}{T} - \frac{11e}{T} + \frac{3.8 \times 10^5 e}{T^2} \qquad (6)$$

where n - index of refraction of the atmosphere

ρ - barometric pressure in millibars

T - temperature in degrees Kelvin

e - water vapor pressure in millibars

This equation shows that the index of reflection depends upon temperature, pressure and water vapor content. In an average atmosphere the decrement in moisture content and temperature with height is uniform, so the index of refraction decreases linearly with height and this results in bending of the rays toward the earth.

Under abnormal atmospheric conditions the gradient of the index of refraction is not uniform and the rays will bend away from the earth or conversely toward the earth more strongly. Sometimes,

under this condition, a 'duct' is formed in the atmosphere and this guides the waves over the surface of the earth. Large signals at ranges beyond the line-of-sight are then obtained.

The radius of curvature of the ray path in the troposphere is given by (see Appendix 2):

$$p = \frac{-1}{\frac{dn}{dh}} \qquad (7)$$

where p - radius of curvature

n - refraction index

h - height

Therefore, in the troposphere the radius of curvature of ray path is determined by the rate of change of refractive index with height.

1.2.2 Diffraction.

1.2.2(a) Smooth Sphere Diffraction.

Diffraction is another phenomenon that can transmit a radio wave beyond the horizon. It is an edge effect that occurs when the phase surface is not infinite and the curved surface of the earth is considered to be the edge of an object. It is possible to obtain analytic expressions for the diffraction over an ideal conducting sphere, neglecting the factors such as frequency, antenna height, distance, conductivity of the earth. Bullington[2] had reduced the involved factors to various asymptotic form and the nomograph derived from his approximation is shown in Appendix 3.

1.2.2(b) Knife Edge Diffraction.

When the wave path is obscured by obstructions such as trees, hills and buildings, their effect on the propagation is complicated.

In order to simplify the calculation it is possible to treat these objects as absorbing knife edge, to estimate the amount of signal attenuation. The diffraction of plane wave over a knife edge can be represented by:

$$\frac{E}{E_0} = Ae^{j\Delta} \qquad (8)$$

where E - electric field strength

E_0 - value of electric field strength at knife edge

A - amplitude

Δ - phase angle with respect to the direct path

The expression for A and Δ can be expressed in terms of Fresnel integrals and

$$A = \frac{S+\frac{1}{2}}{\sqrt{2}\,\mathrm{Sin}(\Delta+\frac{\pi}{4})} \quad , \quad \Delta = \tan^{-1}\left(\frac{S+\frac{1}{2}}{C+\frac{1}{4}}\right) - \frac{\pi}{4}$$

where

$$C = \int_0^{h_0} \mathrm{Cos}\left(\frac{\pi}{2}v^2\right)dv \quad , \quad S = \int_0^{h_0} \mathrm{Sin}\left(\frac{\pi}{2}v^2\right)dv \quad , \quad h_0 = h\sqrt{\frac{2}{\lambda}\left(\frac{1}{d_1}+\frac{1}{d_2}\right)}$$

and d_1 and d_2 are the distance from the obstructions to the transmitter and receiver

h - height of the obstruction

Bullington[2] had derived a nomograph and this is shown in Appendix 4. In the cases where the curvature of the earth is considered the result is more complicated. A simplified method of computing such cases is given by Anderson and Trolese[3].

1.3 Field Strength Attenuation Characteristics.

When a radio wave is transmitted from the transmitter T with antenna height h_t to the receiver R, with antenna height h_r separated by a distance d in the atmosphere, the received field intensity is determined by the properties of the atmosphere and the terrain. Also, the antenna height, separated distance and frequency are considered to have some effect on the line-of-sight and over-the-horizon propagation. In practice, it is desirable to estimate the signal strength by controlling these parameters.

1.3.1 Line-of-Sight Propagation.

1.3.1(a) Distance.

In free space, field intensity E_o at a distance d meters from the transmitting antenna is given by:

$$E_0 = \frac{\sqrt{30 G_t P_t}}{d} \qquad (9)$$

where P_t - radiated power in watts

G_t - power gain ratio of transmitting antenna

In the receiving site the maximum power P_r that can be delivered to a matched receiver is

$$P_r = \left(\frac{E\lambda}{2\pi} \right) \frac{G_r}{120} \qquad (10)$$

where E - received field intensity in volts per meter

λ - wavelength in meters

G_r - power gain ratio of receiving antenna

Combining Equation (9) and Equation (10),

$$\frac{P_r}{P_t} = \left(\frac{\lambda}{4\pi d} \right)^2 G_t G_r \left(\frac{E}{E_0} \right)^2 \qquad (11)$$

For free space transmission $\frac{E}{E_o} = 1$

Therefore, Equation (11) becomes

$$P_r = P_t \left(\frac{\lambda}{4\pi d} \right)^2 G_t G_r \qquad (12)$$

It predicts the received power decreases 6dB for each doubling of the distance in free space.

In practice, the received signal level decrease with disrance does not follow the relationship predicted in free space. There is a general trend for the signal to decrease more rapidly when the receiving antenna is far from the transmitter. The graph showing the received power level versus distance, as measured by independent workers in three different cities - New York[4], Philadelphia[5] and Tokyo[6] - is shown in Figure 1.2. It is also found, by Okumura[6] in Tokyo, the rate-of-signal decreases with distance but does not appear to change significantly with increasing antenna height. However, raising the antenna height results in decreasing the attenuation relative to free space. (See Figure 1.3)

1.3.1(b) Frequency.

The attenuation as a function of distance can be expressed in the terms of n, that is:

$$P_r \propto f^{-n} \qquad (13)$$

where P_r - average received signal power

From the equation it is shown that signal attenuation increases as frequency increases. A graph showing the n versus distance at different frequency, given by Okumura[6], is shown in Figure 1.4. n is constant for distance under 10 Km from the transmitter and

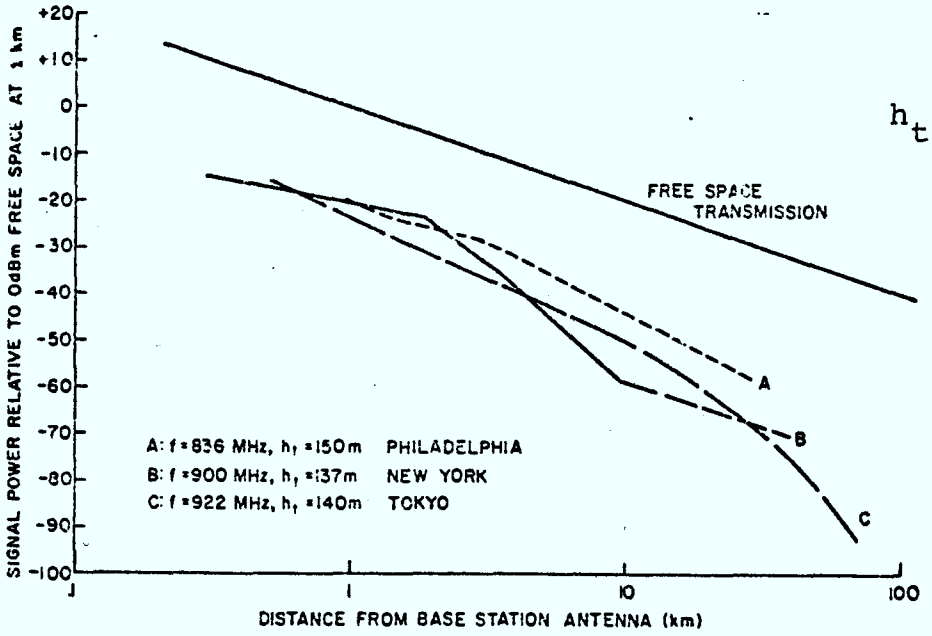

h_t = height of transmitting antenna.

Fig. 1.2 Transmission Loss with Distance

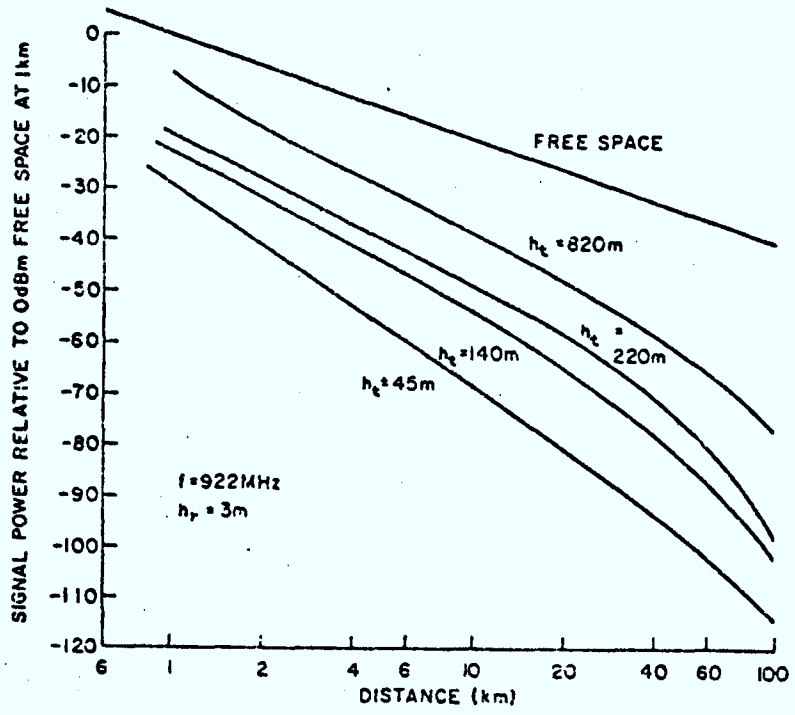

h_t = height of transmitting antenna.

h_r = height of receiving antenna.

Fig. 1.3 Median Field Strength for Various Antenna Heights

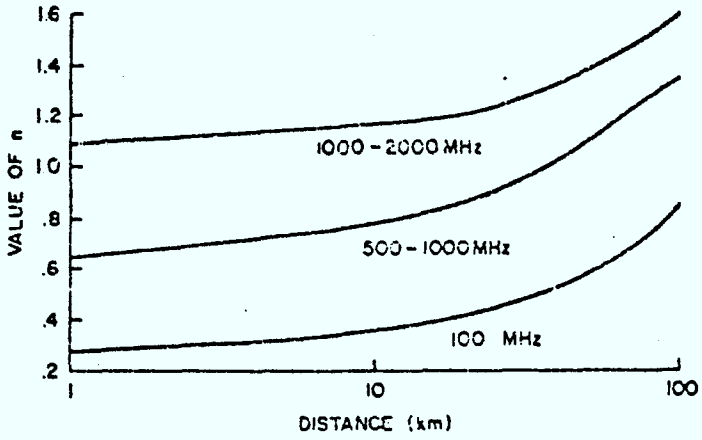

Fig. 1.4 Frequency Dependance of Median Field Strength

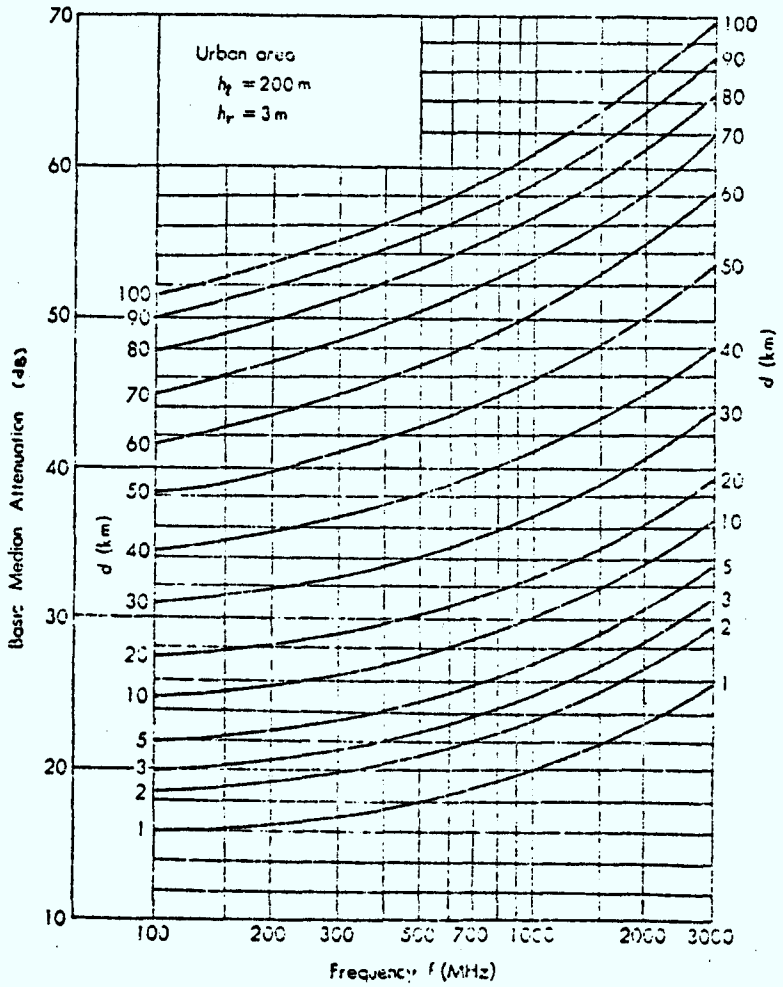

h_t = height of transmitting antenna.

h_r = height of receiving antenna.

Fig. 1.5 Prediction Curve for Basic Median Attenuation Relative to Free Space

decreasing in signal strength with frequency becomes more rapid with separation. A prediction curve for the basic median attenuation relative to free space versus frequency and distance is also given by him. See Figure 1.5.

1.3.1(c) Antenna Height.

In free space, the transmission formula is (See Equation (12))

$$P_r = P_t\left(\frac{\lambda}{4\pi d}\right)^2 G_t G_r$$

where P_r - expected power over a free space path

and substituting into Equation (1)

$$P = P_t\left(\frac{\lambda}{4\pi d}\right)^2 G_t G_r \left|1 + Re^{j\Delta} + (1-R)Ae^{j\Delta} + \cdots\cdots\cdots\right|^2 \qquad (14)$$

where P - received power

For $\Delta = \frac{4\pi h_t h_r}{\lambda d}$ $R = -1$ and neglecting A

$$P = 4P_r \sin^2\left(\frac{2\pi h_t h_r}{\lambda d}\right) \qquad (15)$$

Since Δ is very small $\sin^2\Delta = \Delta^2$

$$P = 4P_r\left(\frac{2\pi h_t h_r}{\lambda d}\right)^2 \qquad (16)$$

Substituting $P_r = P_t\left(\frac{\lambda}{4\pi d}\right)^2 G_t G_r$ into Equation (16)

$$P = P_t G_t G_r\left(\frac{h_t h_r}{d^2}\right)^2 \qquad (17)$$

It predicts a 6dB gain in received power for a doubling of the height of either antenna. In a real-life situation the effect of changing either antenna is different and should be treated separately.

1.3.1(d) Transmitting Antenna Height.

In the work of Okumura[6] he observed the variation of receiver signal with height for frequencies from 200 - 2,000 MHz. For an antenna separation distance less than 10 Km the field strength tends to be increased uniformly at 6dB per doubling of height. It rises

to 9 dB as the antenna separation becomes greater than 30 Km. (See Figure 1.6)

1.3.1(e) Receiving Antenna Height.

For the receiving antenna height less than 5 metres, Okumura[6] observed a height gain of 3dB advantage of a 3-metre high antenna over a 1.5-metre high antenna. When the antenna is above 5 metres the high gain factor depends upon the frequency and environment. In a medium sized city, and for frequency 200 MHz, the height gain factor may be 14 dB per octave. In a very large city, and for frequency under 1,000 MHz, the height gain factor may be as low as 4dB per octave. (See Figure 1.7)

1.3.2. Propagation over the Horizon.

1.3.2(a) Distance Dependance.

Receiving of signals beyond the horizon greatly depends on the mixture of the atmosphere. As previously shown, the tropospheric path is controlled by the refraction index of the atmosphere. Sometimes, under abnormal conditions, 'ducts' can be formed and the attenuation characteristics are altered. Although it is difficult to derive an analytical expression to predict the attenuation characteristics it is possible to predict the trend of the attenuation characteristics by long-term statistical measurement. A typical experiment was that conducted by Chisholm[7] over a period of two years. A transmitting signal of 400 MHz was monitored over the distances ranging from 98 to 618 miles. The distance dependence curve is shown in Figure 1.8. The following attenuation rates are obtained from this curve.

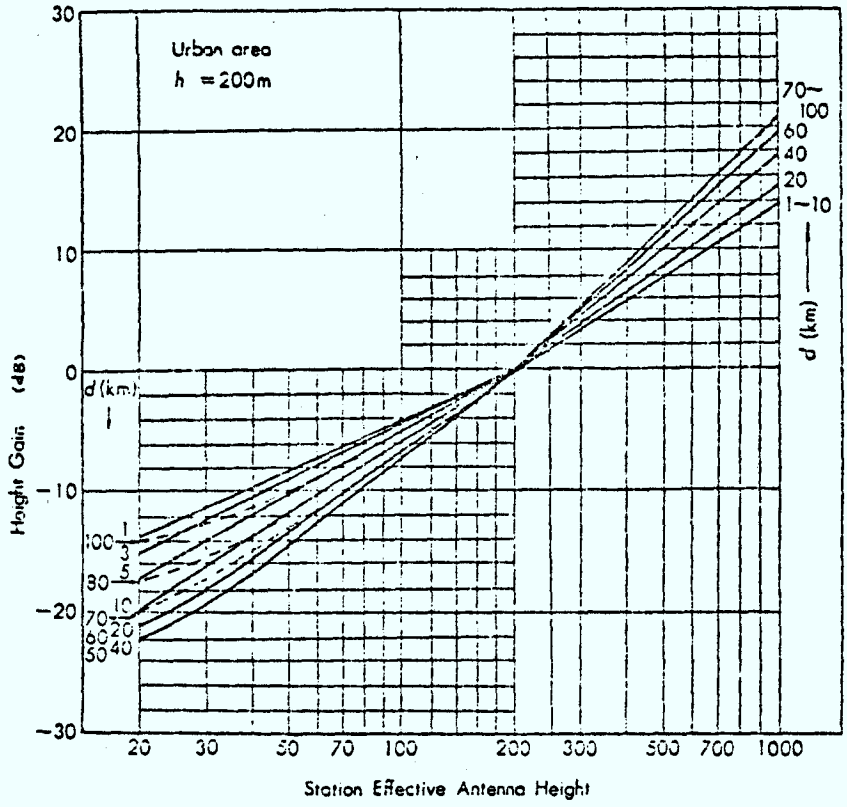

Fig. 1.6 Prediction Curve for Height-gain Measurement (Transmitting antenna height fixed at 200 M)

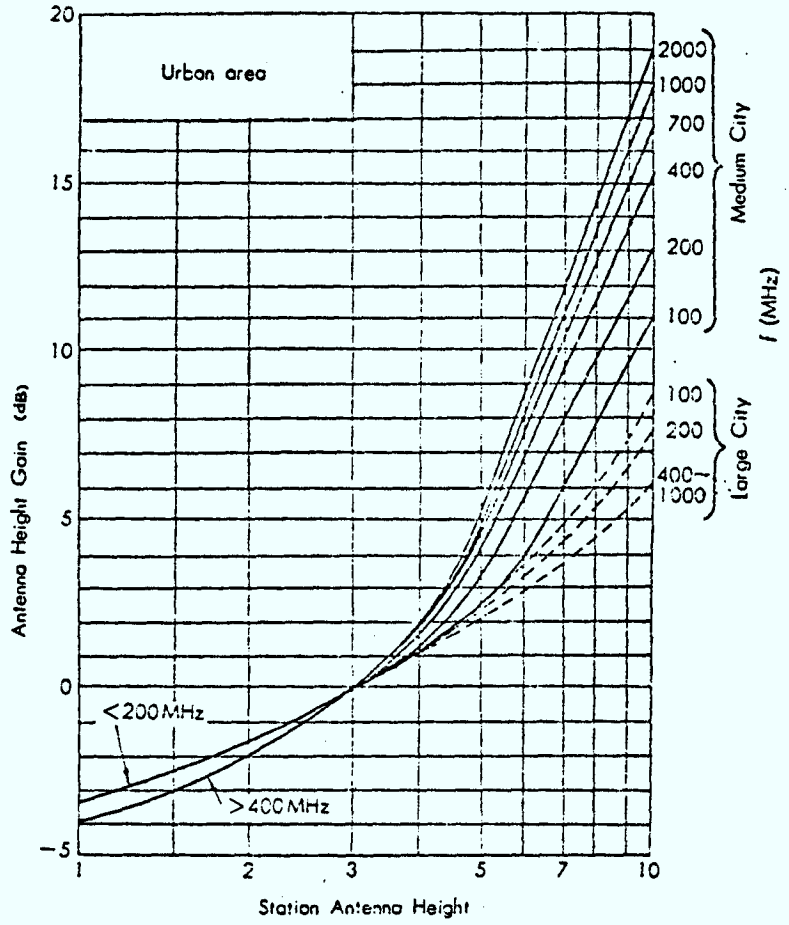

Fig. 1.7 Prediction Curve for Height-gain Measurement (Receiving Antenna)

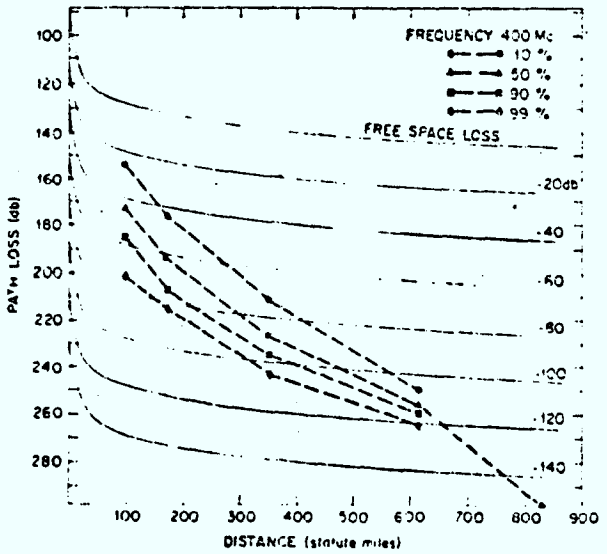

Fig. 1.8 Distance Dependance Curve

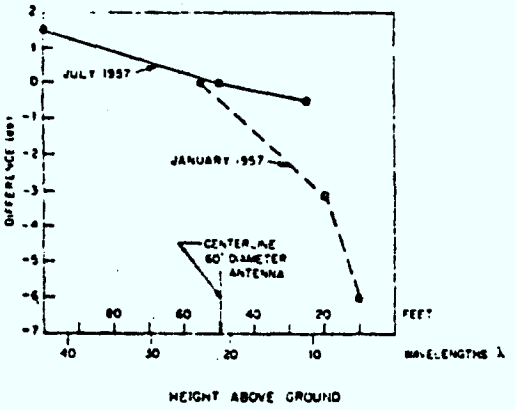

Fig. 1.9 Antenna Height-gain Measurement

Range (miles)	Attenuation Rate (dB/mile)
90 - 180	0.22
180 - 350	0.18
350 - 630	0.11
630 - 840	0.22

Therefore, an increasing of attenuation rate beyond 600 miles is indicated.

1.3.2(b) Antenna Height.

For height dependance Chisholm[7]. made a series of measurements with heights of 10, 20, 55 and 100 feet and the following graph (Figure 1.9) was constructed.

It is observed that a substantial height gain is achieved for the first ten wavelengths of height (approximately 25 feet) and this decreases to a small rate of height gain above 20 wavelengths.

Very little other data on height-gain for over-the-horizon propagation was found in the available literature.

Chapter 2. The London Height-gain Measurement

For line-of-sight transmission, signal attenuation is characterised by the properties of the terrain as well as the antenna height, separation distance and frequency. For transmission over the horizon these factors, along with the properties of the troposphere, are important. Some of the past experiments concerning the attenuation characteristic measurements for line-of-sight propagation which have been done are described in Chapter 1. In this experiment all results are for propagation over the horizon. The main purpose of this experiment is to carry out height-gain measurements and to compare the results to those obtained in the line-of-sight measurements.

The transmitting signal makes use of existing U.H.F. television stations. At the receiving site, four antennas at different height positions are used to monitor the signal. The incoming signal levels are recorded and processed by a microprocessor. The average signal strength of each individual channel and their correlations are then calculated.

2.1 System Design.

For the transmitting signals, television station Erie Channel 24 is monitored. It transmits a video frequency of 531.25 MHz. Monitoring the video carrier rather than the audio carrier results in a high signal to noise ratio because the video ERP is higher. Figure 2.1 lists the specifications of the transmitter and bearing location of the channel. Figure 2.2 shows the map location of transmitting and receiving sites.

City: Erie

Channel: 24

Freq.(Video): 531.25MHz

Call: WJET

Latitude(N): 42.04

Longitude(W): 80.07

Bearing(Deg): 136.7 (from London)

Distance(mile): 90.3

Eff. Height: 740 ft.

Actual Height: 600 ft.

ERP: 1.10 MW

Fig. 2.1 Location of Transmitting Station

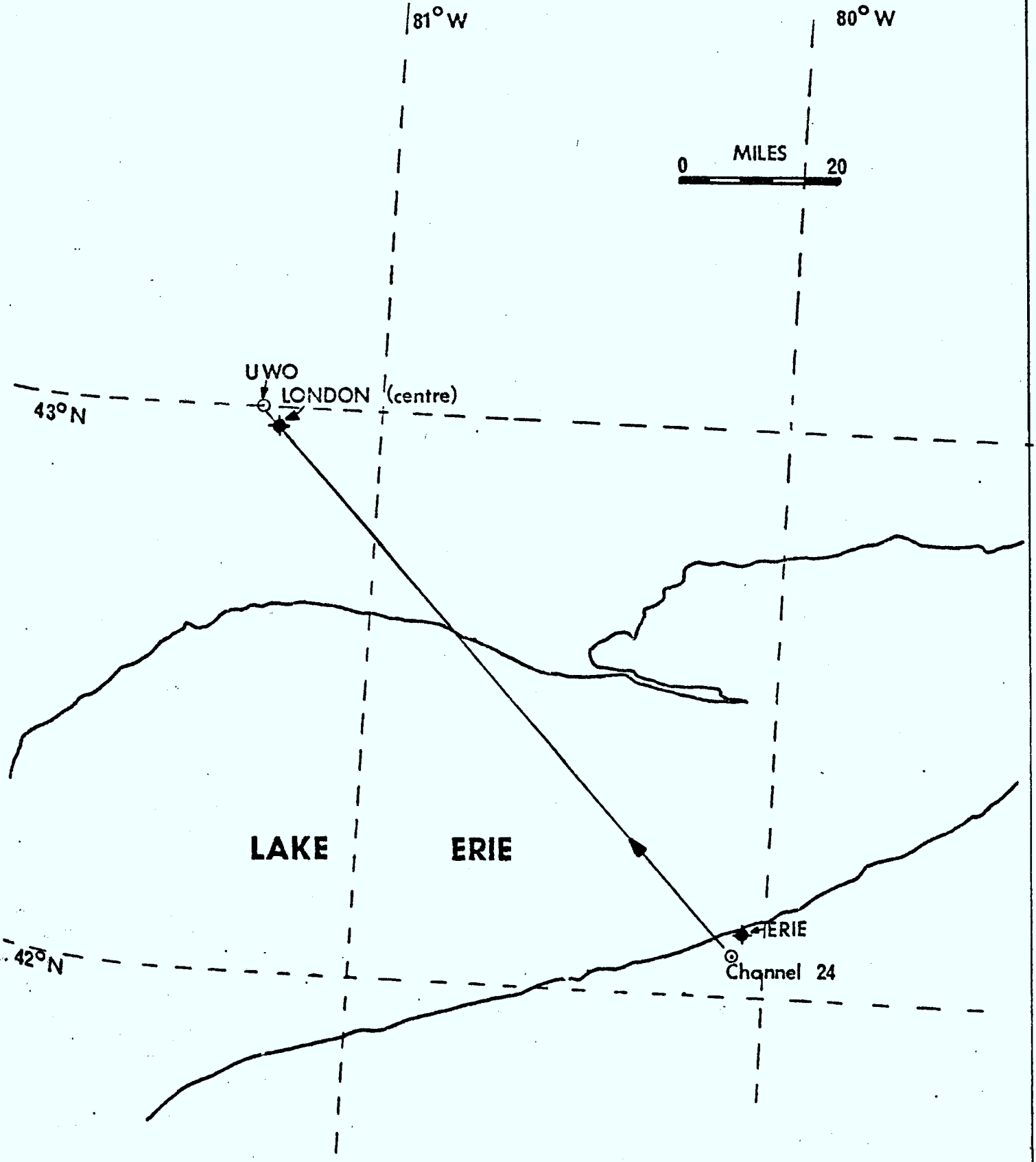

Fig. 2.2 Ray-path Map

The receiving site is located at the Physics building of the University of Western Ontario, London, Ontario. An antenna tower of 70 feet was built and placed beside the three-storey building. Figure 2.3 shows the location of the antenna tower and the four antennas. Four RG-59 cables, each 50 feet in length, are used to connect the antennas and the equipment which is located in the Centre for Radio Science Laboratory in the Physics building. The incoming signal levels are recorded on a four-channel recorder and a Motorola MEK6800D2 microprocessor is used to do all the necessary calculations. As designed, the microprocessor will do the calculations in twenty-minute intervals and the individual average result will be recorded for about three minutes on the chart recorder. A printer is also used to print out the time and the correlation coefficient.

The system consists of two main sections, receiving section and calculation section, and the block diagrams of these are shown in Figure 2.4 and Figure 2.5.

In the receiving section, the four signals coming from the four antennas are multiplexed through a coaxial switch to the converter. The rate of sampling is controlled by the control section and is set to 8 msec per sample. This will be explained later. The converter brings the incoming signal 531.25 MHz down to 30 MHz and it then passes to the receiver. The gain control in the circuit is used to control the incoming signal strength while the delay circuit in the demultiplex section is used to compensate the non-ideal response of the receiver. In order to extract the multiplex signals in d.c. form in the demultiplex circuit the best way is to extract

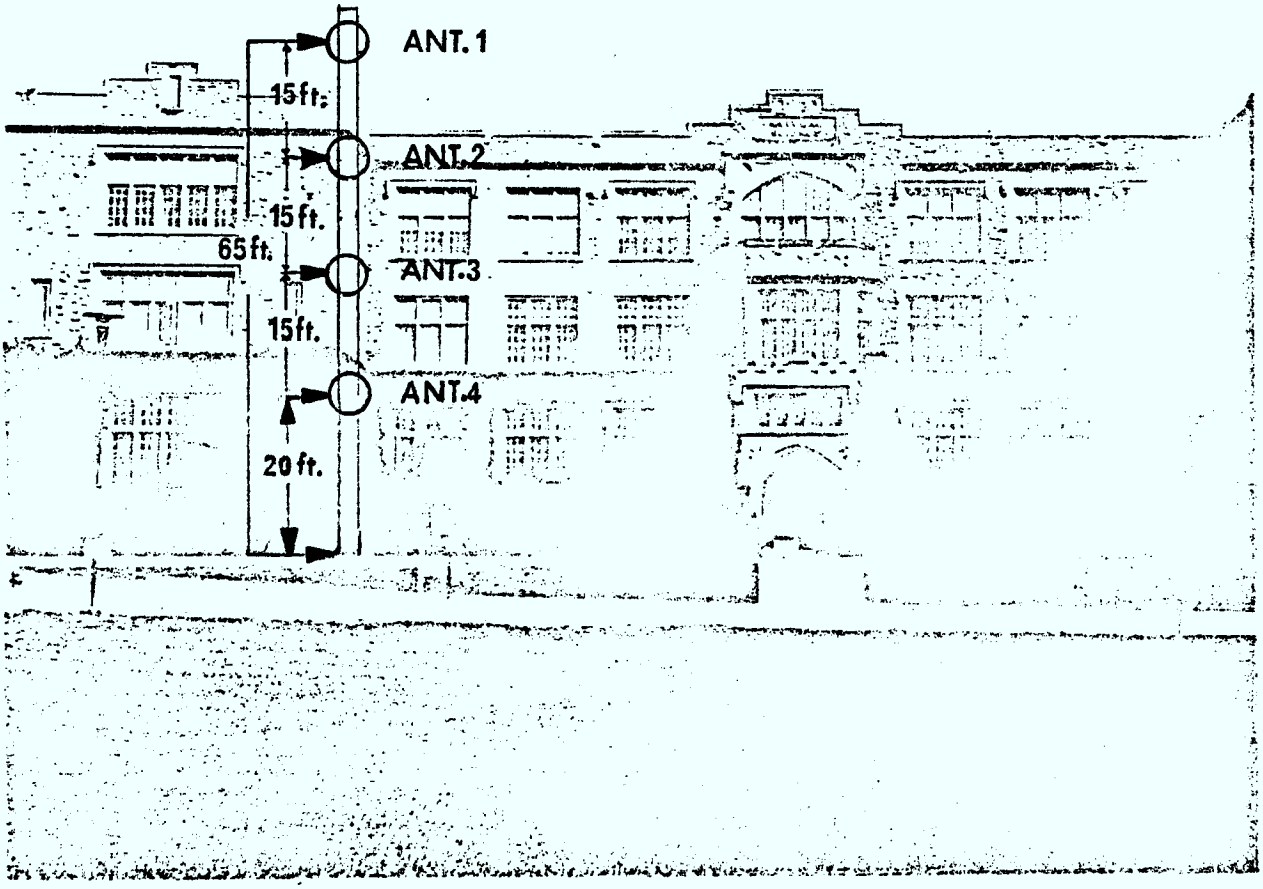

Fig. 2.3 Location of Antenna Tower

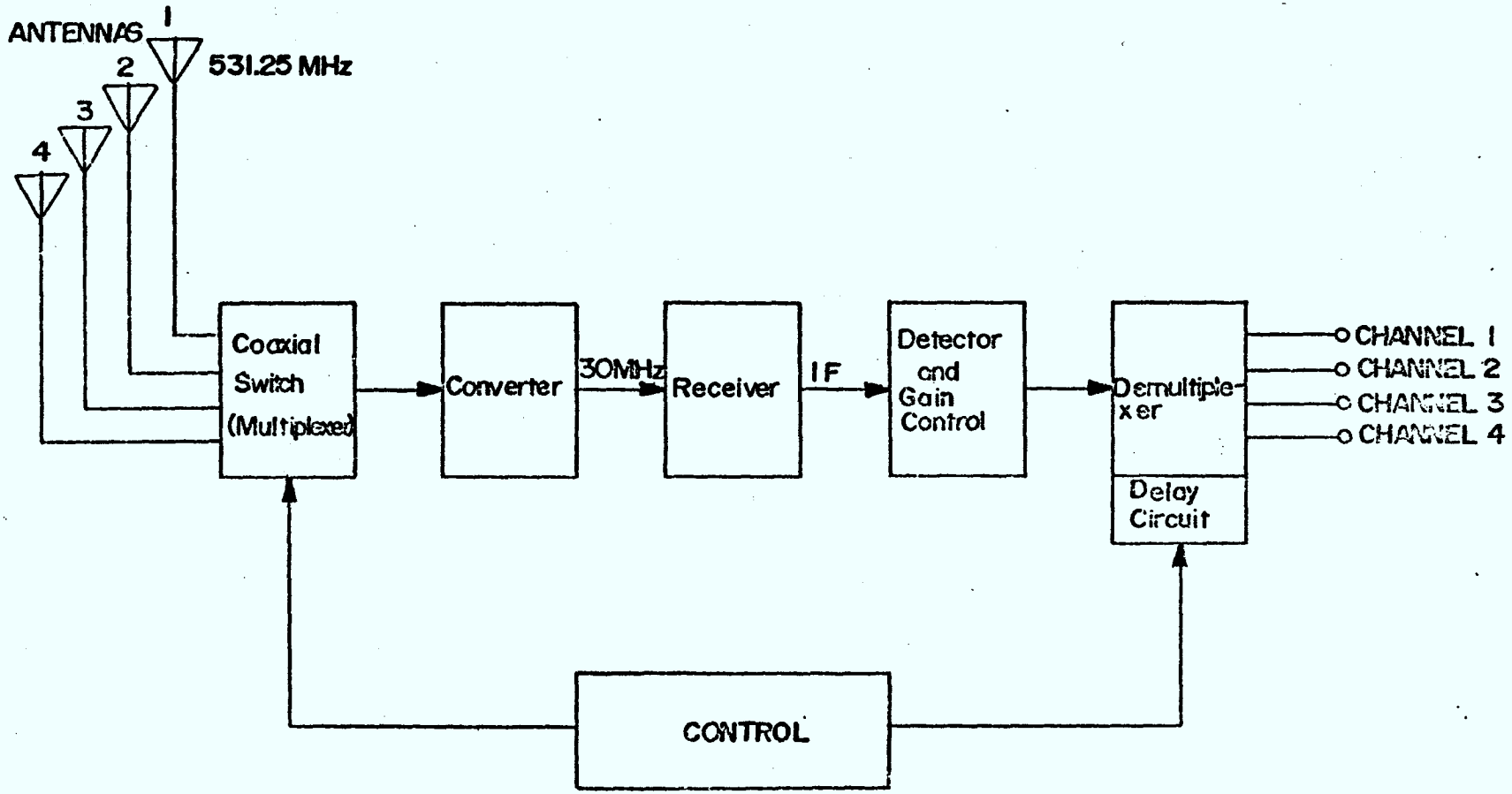

Fig. 2.4 System Block Diagram

(Receiving Section)

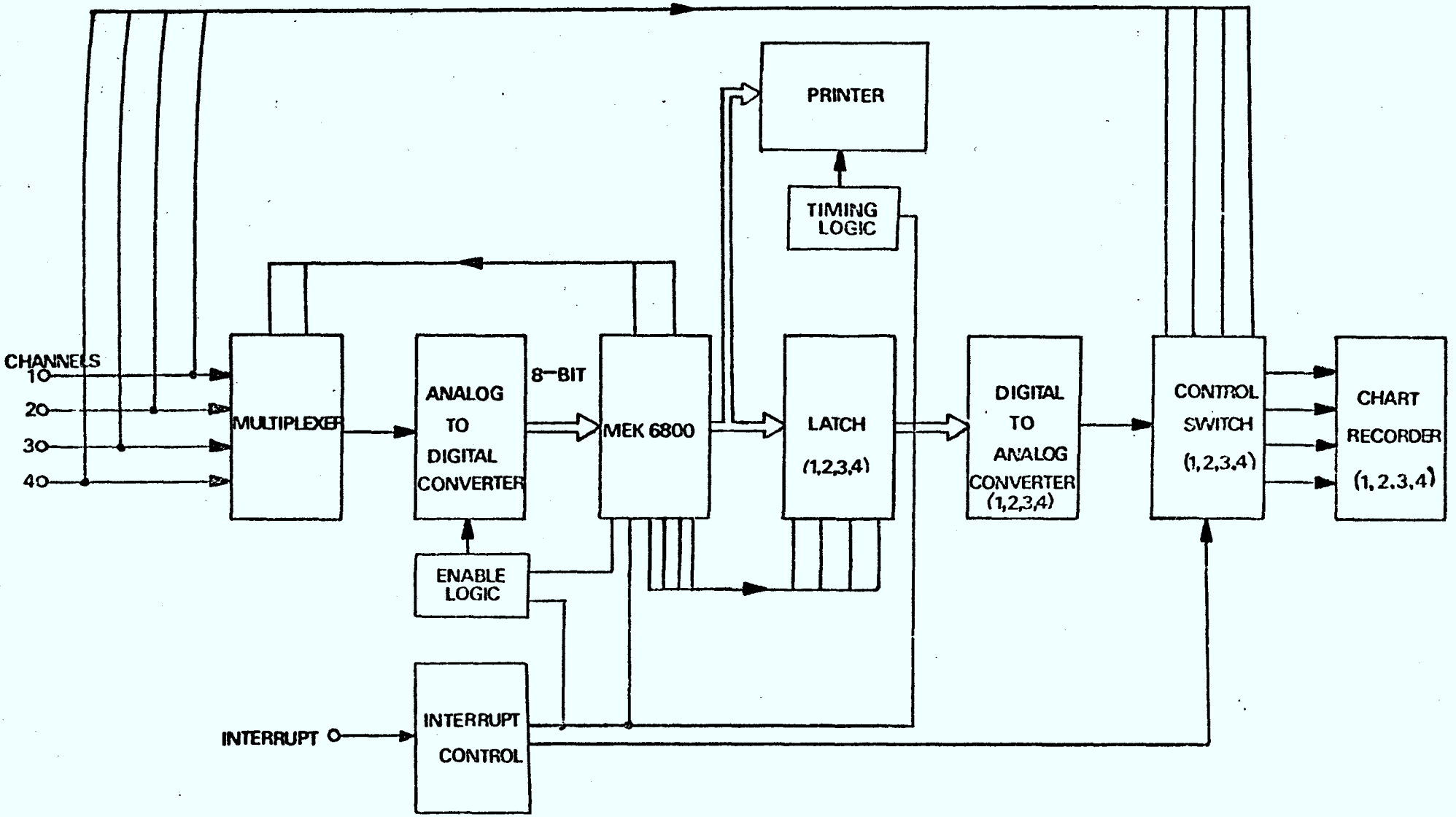

Fig. 2.5 System Block Diagram

(Calculation Section)

them from the IF of the receiver. The IF multiplexed signal is demodulated and demultiplexed. The four demultiplexed signals are then recorded on the chart recorder via the control switches in the calculation section.

Motorola MEK6800D2 microprocessor is the heart of the calculation section. It is used to control the input/output data and do all the calculations. Four signals coming from the receiving sections are passed to the multiplexer. Channel selection in the multiplexer is controlled by the microprocessor. An analog-to-digital converter converts the multiplex analog signal into digital form readable by the microprocessor. Once every twenty minutes an interrupt pulse is generated in the interrupt control section. This will interrupt the microprocessor and perform calculations of averaging input signal for each individual channel and correlation coefficient between channels 1,2, 1,3 and 1,4. The calculated correlation coefficients are output to the printer while the individual average result is latched in the latch section. Four digital-to-analog converters bring the latched digital data into analog form and they are recorded on the chart recorder through the control switches. A sample of the recording chart is shown in Figure 2.6.

2.2 Circuit Design.

2.2.1 Receiving Section.

The main function of this section is to receive four different signals using multiplexing. It comprises seven parts: antenna, coaxial switch, converter, receiver, gain and detector

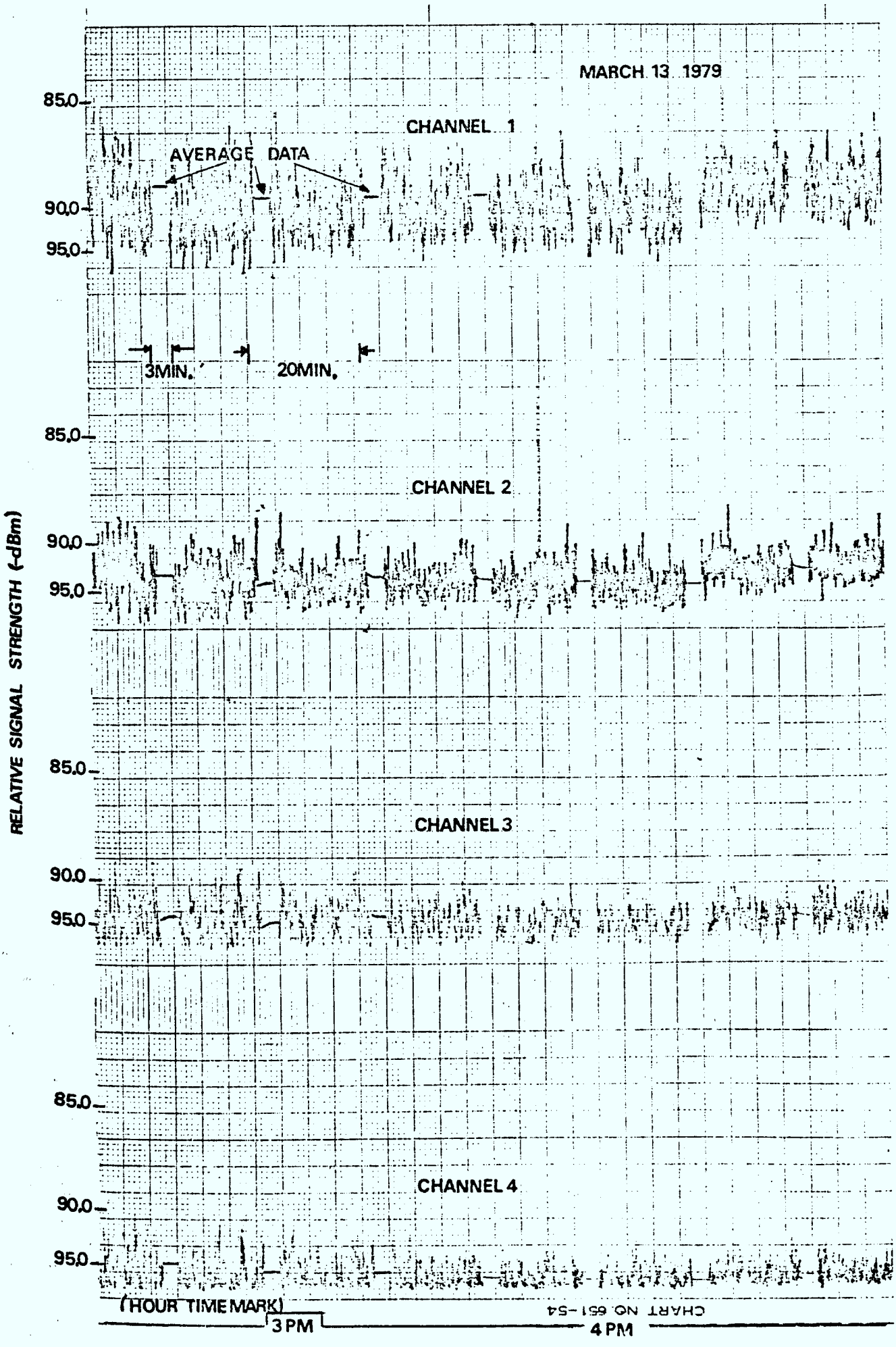

Fig. 2.6 Sample of Recording Chart

circuit, delay and demultiplex circuit and, finally, control circuit. See Figure 2.4.

2.2.1(a) Antenna.

Four antennas mounted at different heights (See Figure 2.3.) are used to receive the signals. The antennas used are Delhi VHF parabolic TV antenna, model 'Super Para 5'. It has a gain of about 18 dB. A balun is used in the antenna to step down the antenna impedance from balanced 300 ohm to unbalanced 75 ohm suitable for coaxial cable connection. Figure 2.7 shows the close-up of the antenna and Figure 2.8 shows the pointing direction of the antenna.

2.2.1(b) Coaxial Switch.

The circuit diagram is shown in Figure 2.9. It is a four-channel coaxial switch and has four control inputs, four signal inputs and one signal output. The output signal will correspond to any one of the inputs when a positive 5V is applied to the appropriate control input, provided the other control inputs are grounded. Considering the case when a 5V is applied to control 1 and other control lines are grounded: D_1 will be forward biased through the path L_5, D_1, L_9, R_2, D_6, L_6, or L_5, D_1, L_9, R_4, D_8, L_8, or L_5, D_1, L_9, R_3, D_7, L_7 and results in a d.c. component in the output of the diode D_1. This is the only output signal because other control inputs are grounded. The d.c. component of the output signal is removed by C_{17} at the output port. It should be noticed that, for proper operation, only one control input is activated and others should be tied to ground.

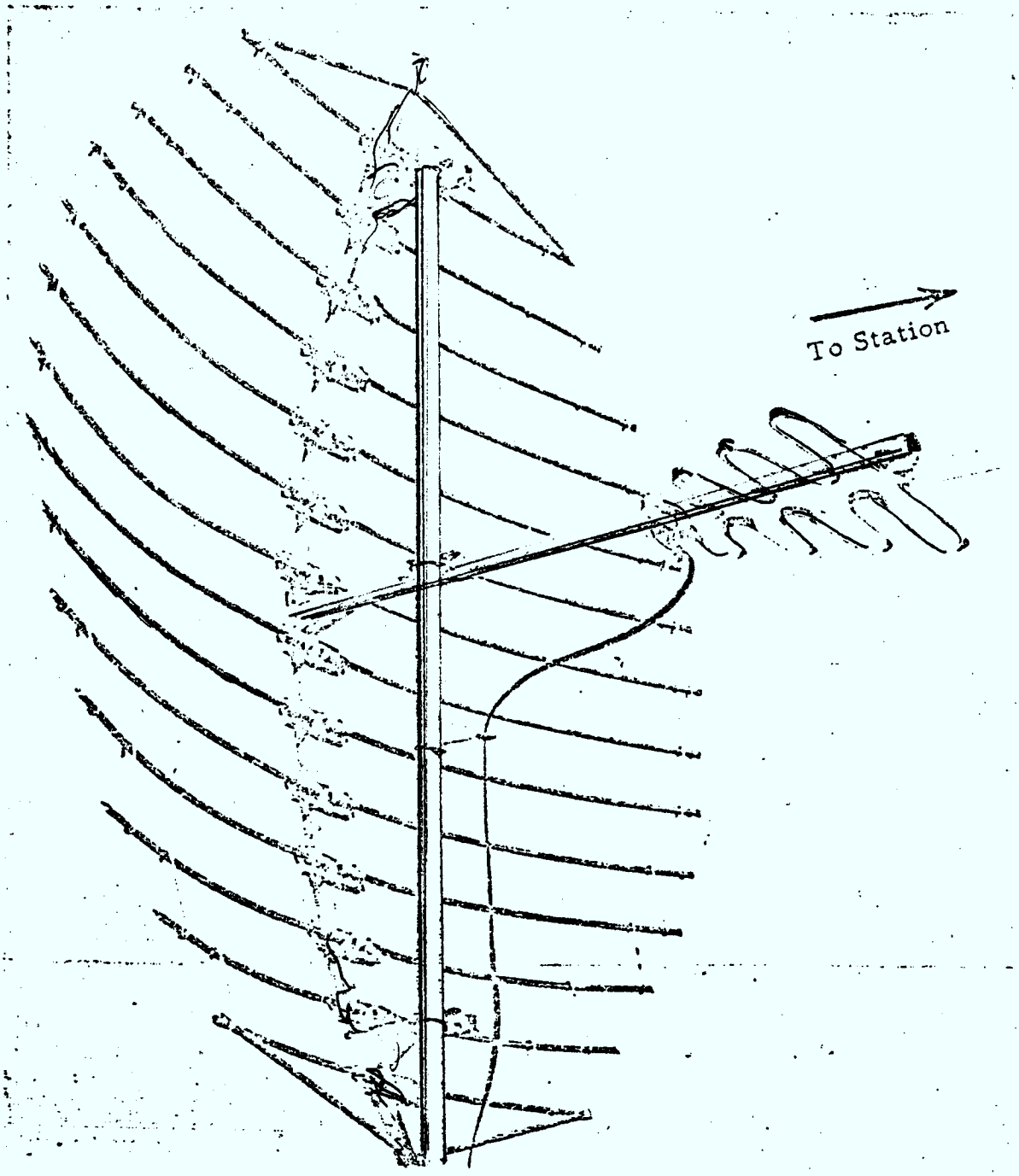

DELHI

UHF PARABOLIC

TV ANTENNAS

Models

SUPER PARA-5 G

Fig. 2.7 Close-up Diagram of Antenna

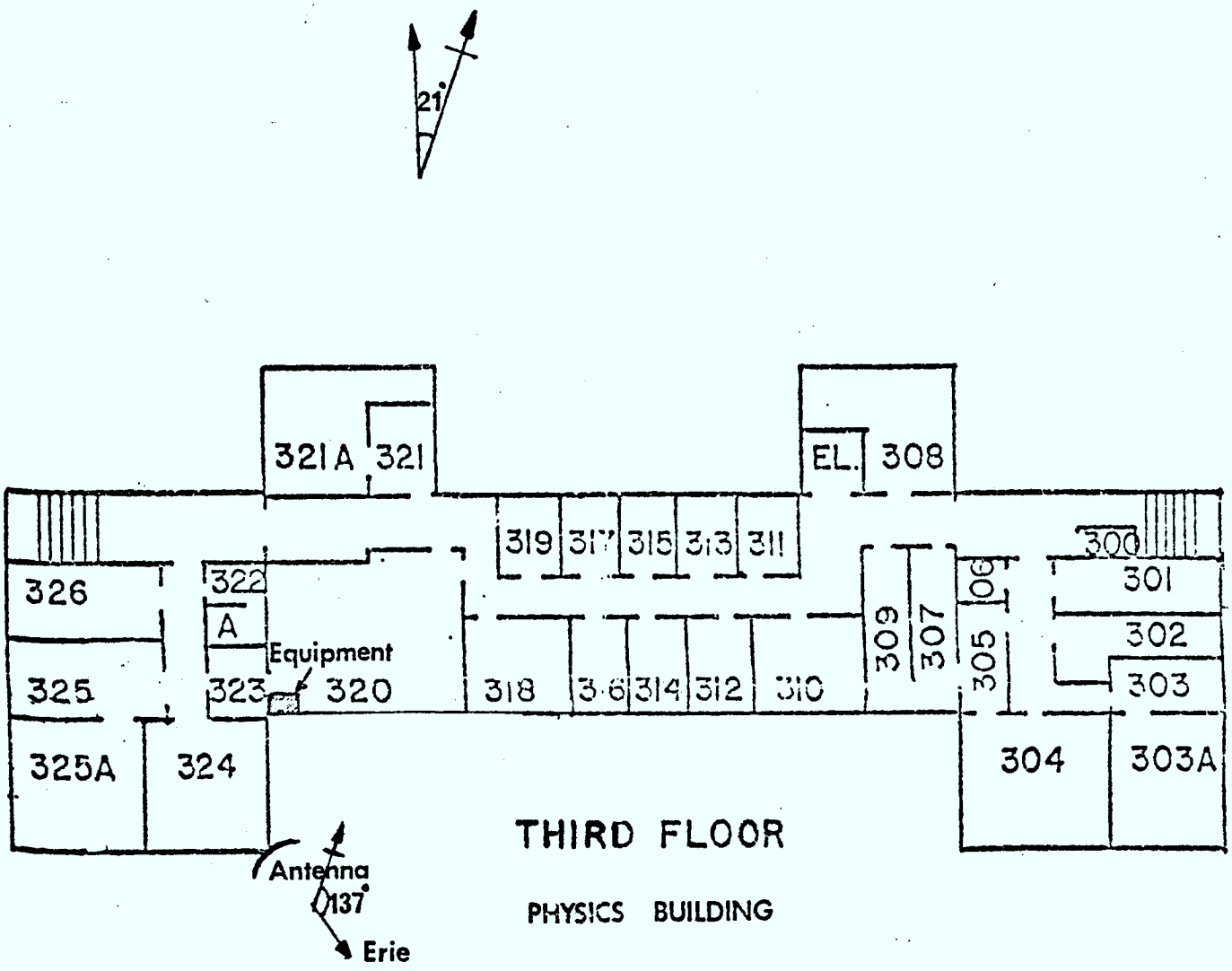

Fig. 2.8 Pointing Direction of Antenna

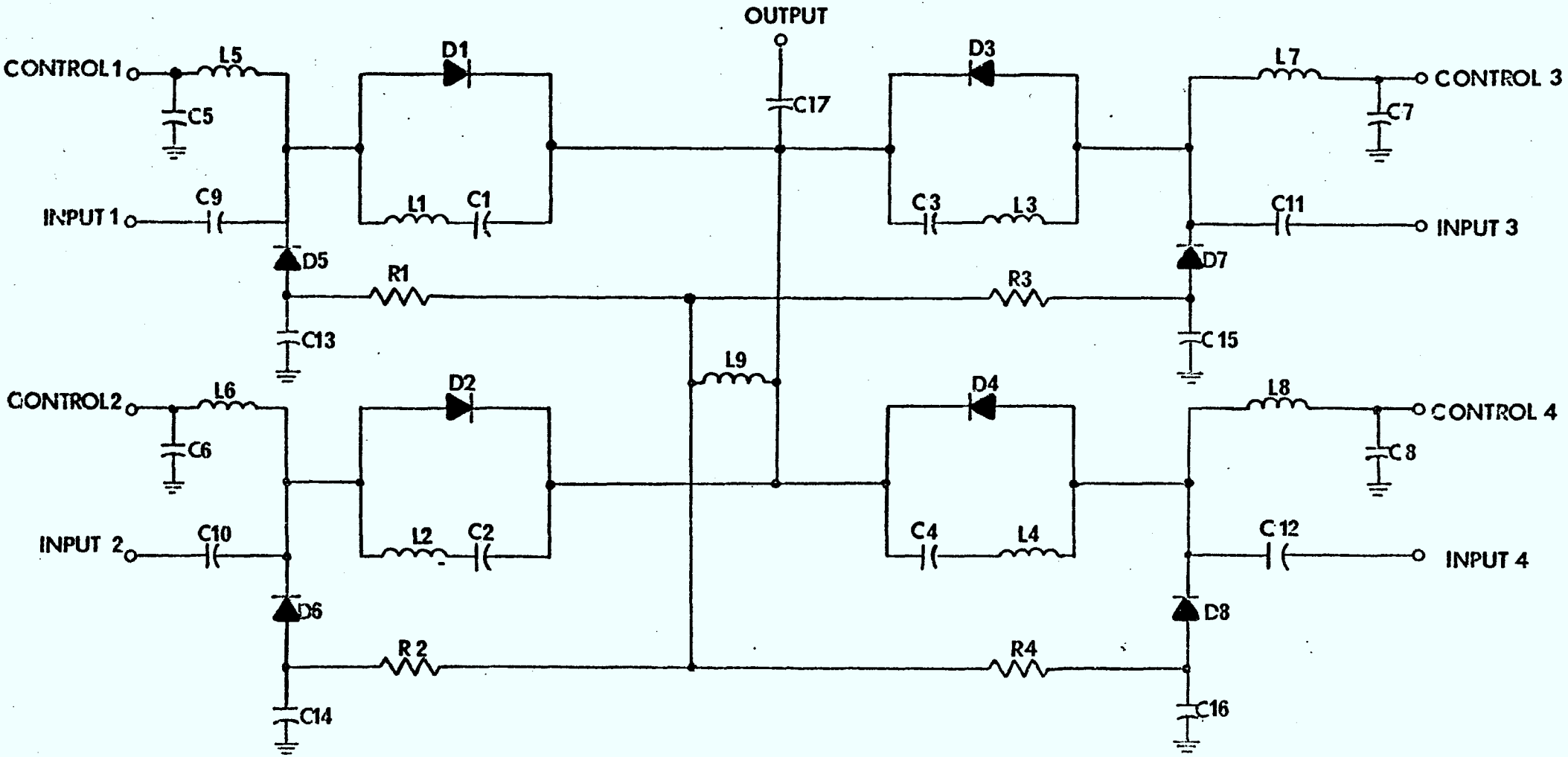

Fig. 2.9 Schematic Diagram of Coaxial Switch

2.2.1(c) Converter.

In this experiment a converter is used to convert the 531.25 MHz signal into 30 MHz. A commercial signal converter (Microwave Modules Ltd., England) was modified and used. Its oscillator was replaced by a new design which oscillates at a frequency of 41.7709 MHz. After tripling, doubling and redoubling the signal in the converter the required specification is met. Figure 2.10 shows the circuitry of the modified oscillator and converter. The specification of the converter is listed in Appendix 5.

2.2.1(d) Receiver.

A commercial receiver (Drake model DSR-1) is used. The specifications are listed in Appendix 6.

In order to obtain the good signal strengths in terms of d.c. voltage to be recorded on the chart recorder the received multiplexed signal is taken out at the 50 KHz IF of the receiver. This 50KHz signal is later demodulated in the detector section.

2.2.1(e) Detector and Gain Control.

In order to obtain a linear signal strength response of the receiver, automatic gain control in the receiver is disconnected. The gain of the receiver is controlled by the outside circuitry. The external gain control has three ranges (20, 40 and 100). Demodulation of the signal is obtained by the diode detector, as shown in Figure 2.11.

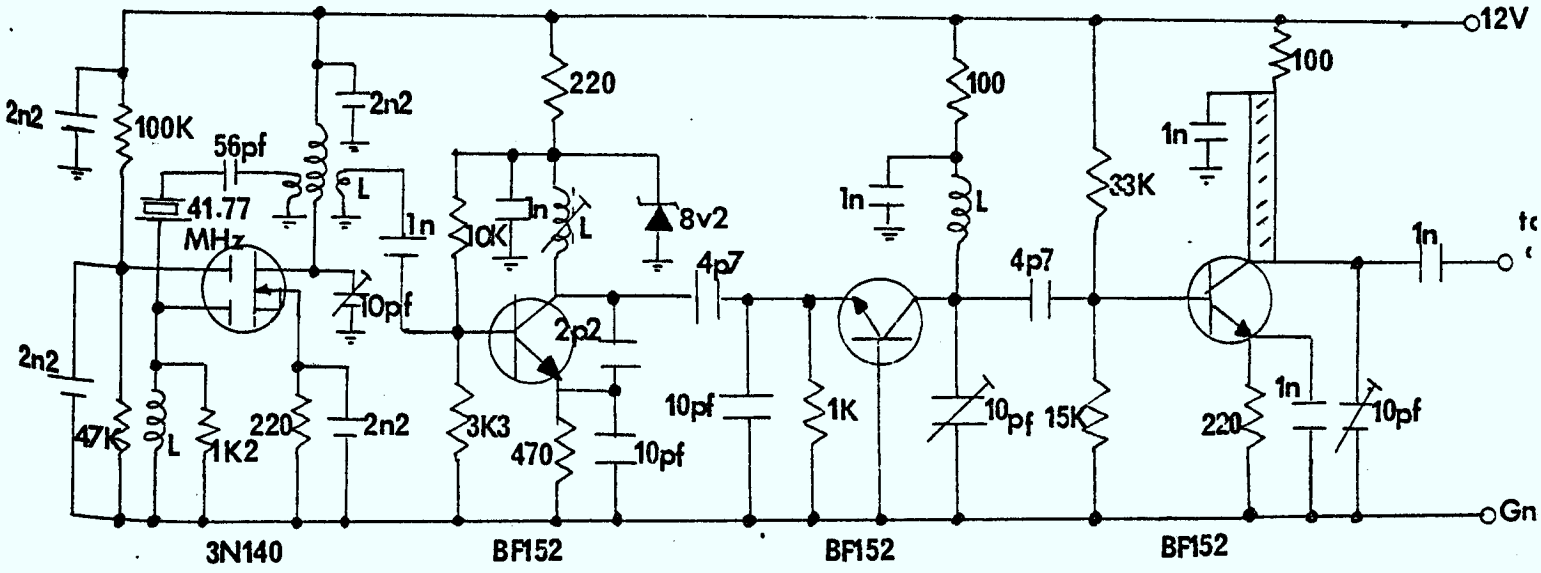

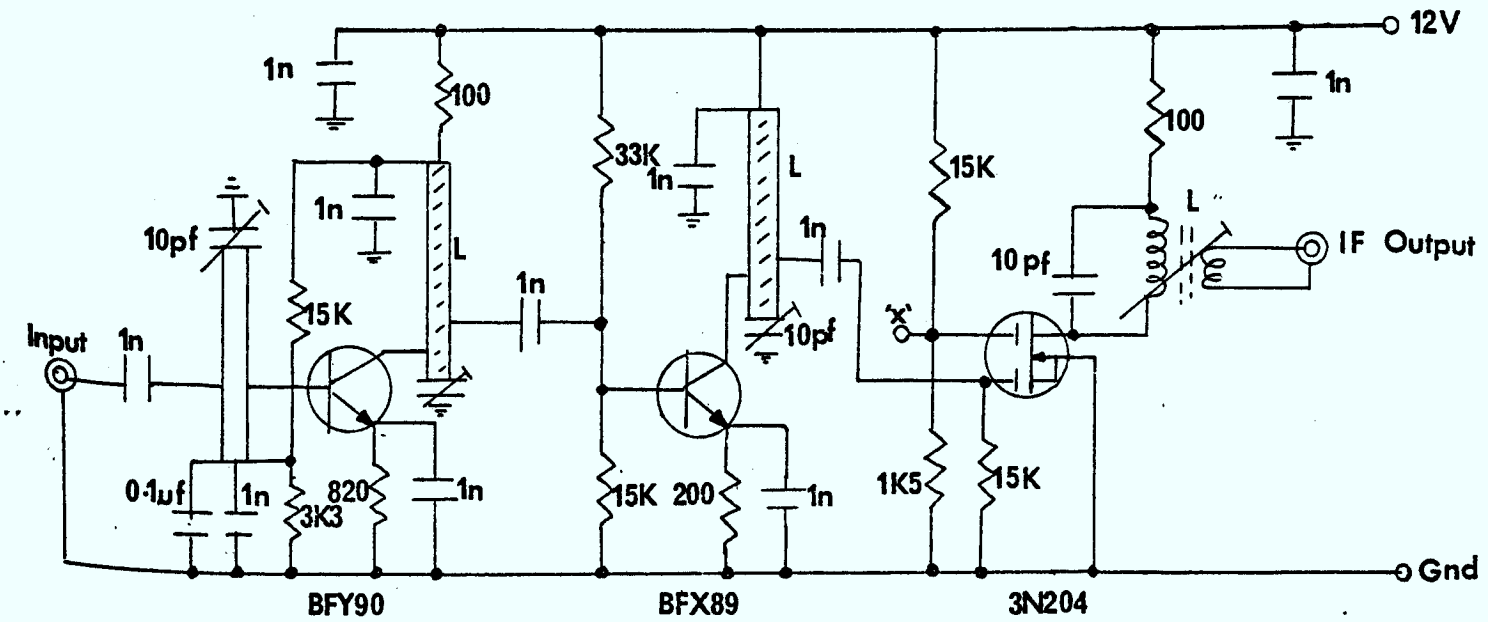

Fig. 2.10 Schematic Diagram of Converter

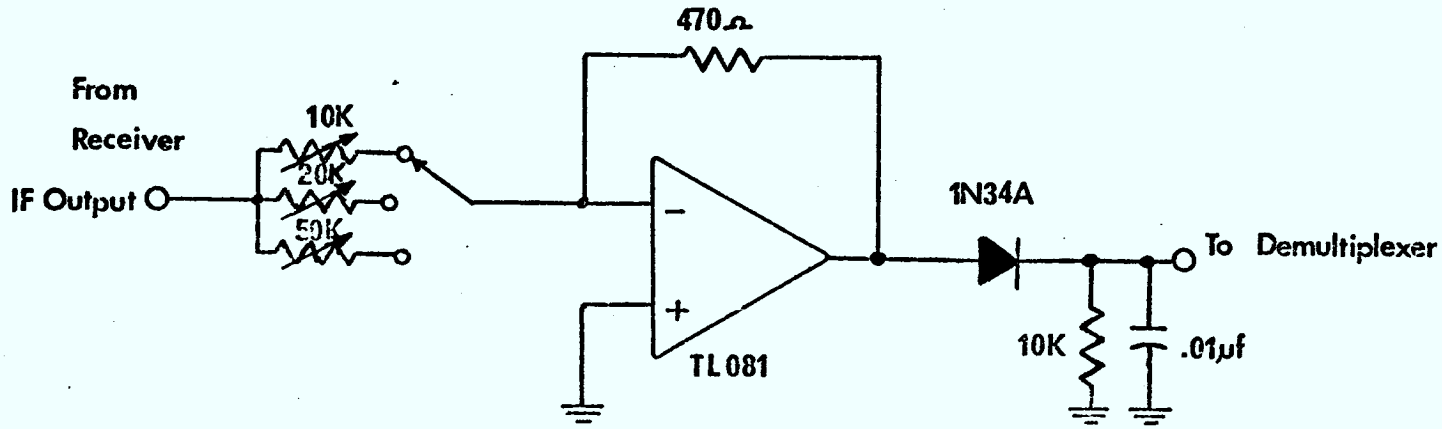

Fig. 2.11 Schematic Diagram of Detector and Gain-control Circuits

2.2.1(f) Delay and Demultiplex Circuit.

Demultiplexing of signal is achieved by using four analog switches and obtaining the controlling pulses from the control section. Due to the non-ideal response of the receiver and detector the output pulse-signal will follow an exponential decay curve (τ = .1msec). Therefore the first portion of the sample in each channel overlaps with the preceding channel. This faulty reading can be avoided when demultiplexing be delaying of the positive edge of the controlling pulse (see Figure 2.12). A delay of 0.75msec is needed in this circuit. The schematic and timing diagrams of this section are shown in Figure 2.13 A by-pass capacitor is connected to the output to remove any AC component in the demodulated signal.

2.2.1(g) Control Circuit.

Sampling pulses for the coaxial switch are produced in this circuit. Two JK flip-flop generate the control pulses and these are decoded by the decoder to obtain the required sampling pulses. High frequency multiplexing is desirable. However, due to the limitation of the receiver, the sampling rate is set to only 8 msec per sample, which is enough to be able to see the higher fading rates of the received signal. Figure 2.14 shows the schematic and timing diagrams. Also, the control pulses for the demultiplexer are obtained from this section.

Figure 2.15 describes the operation of this section. It shows how outputs can be obtained from channels with different fading signals.

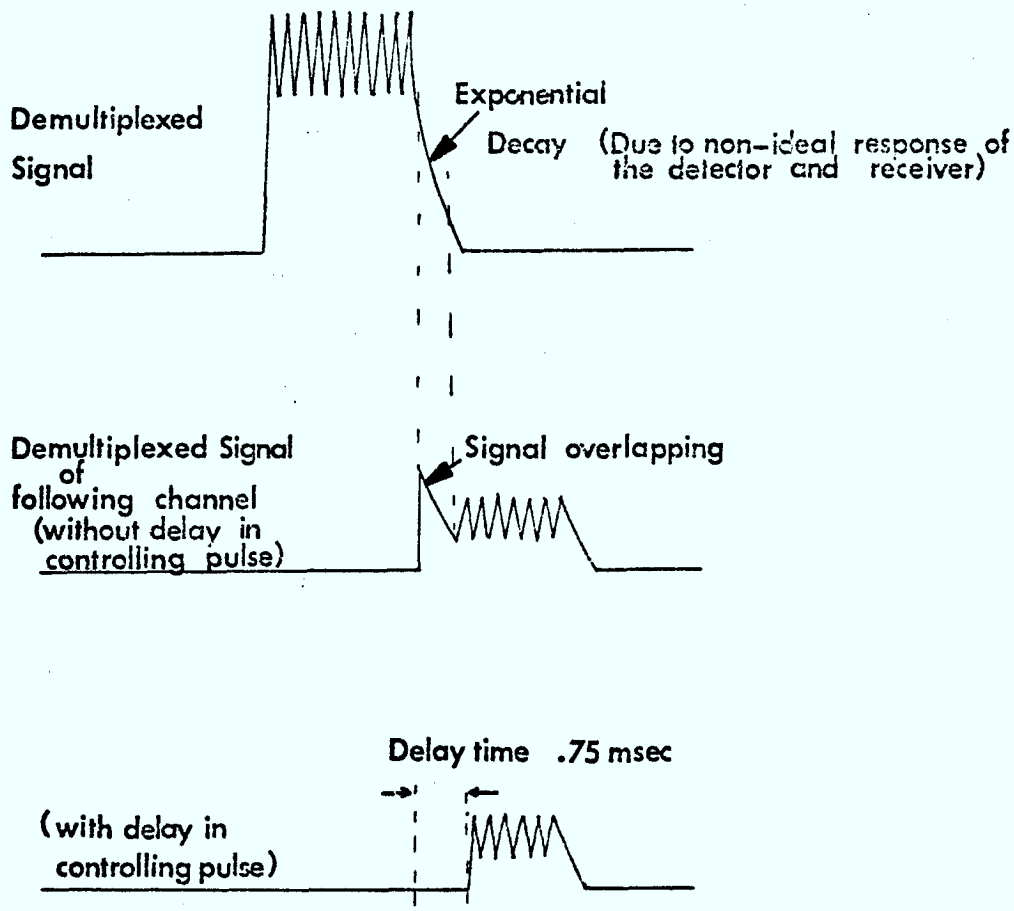

Fig. 2.12 Signal Overlapping of Demultiplexed Signal

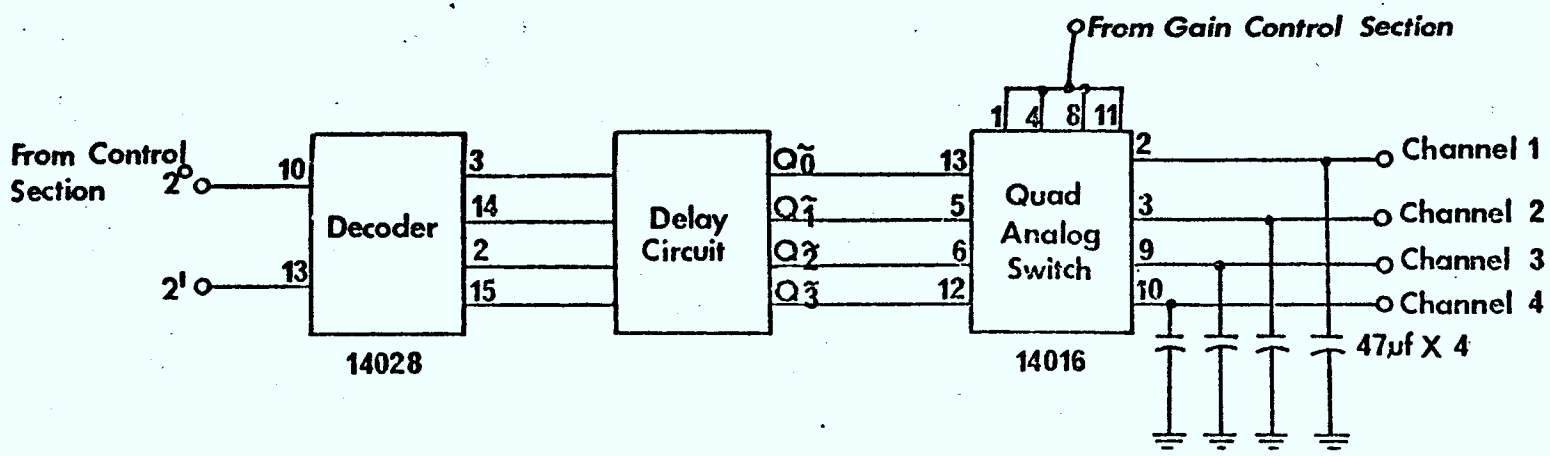

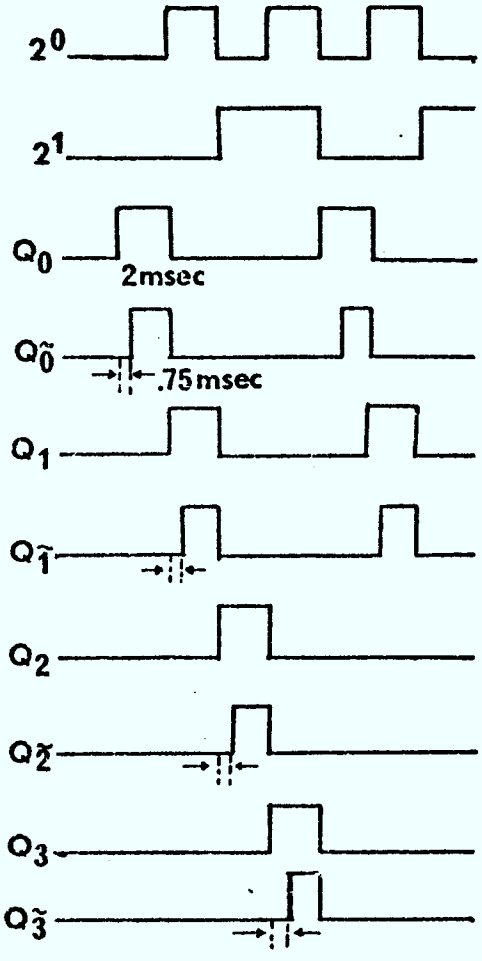

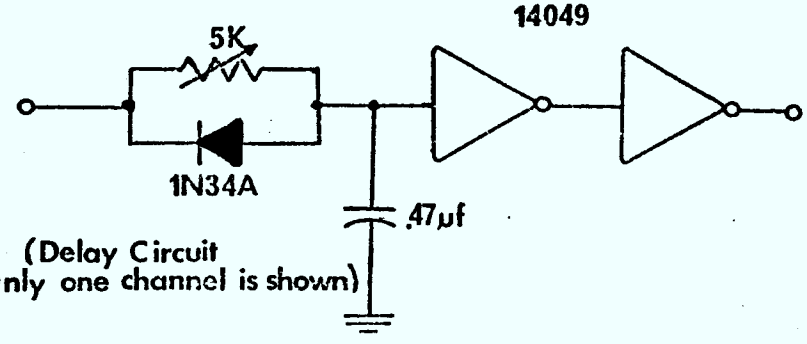

Fig. 2.13 Schematic and Timing Diagrams of Delay and Demultiplex Circuits

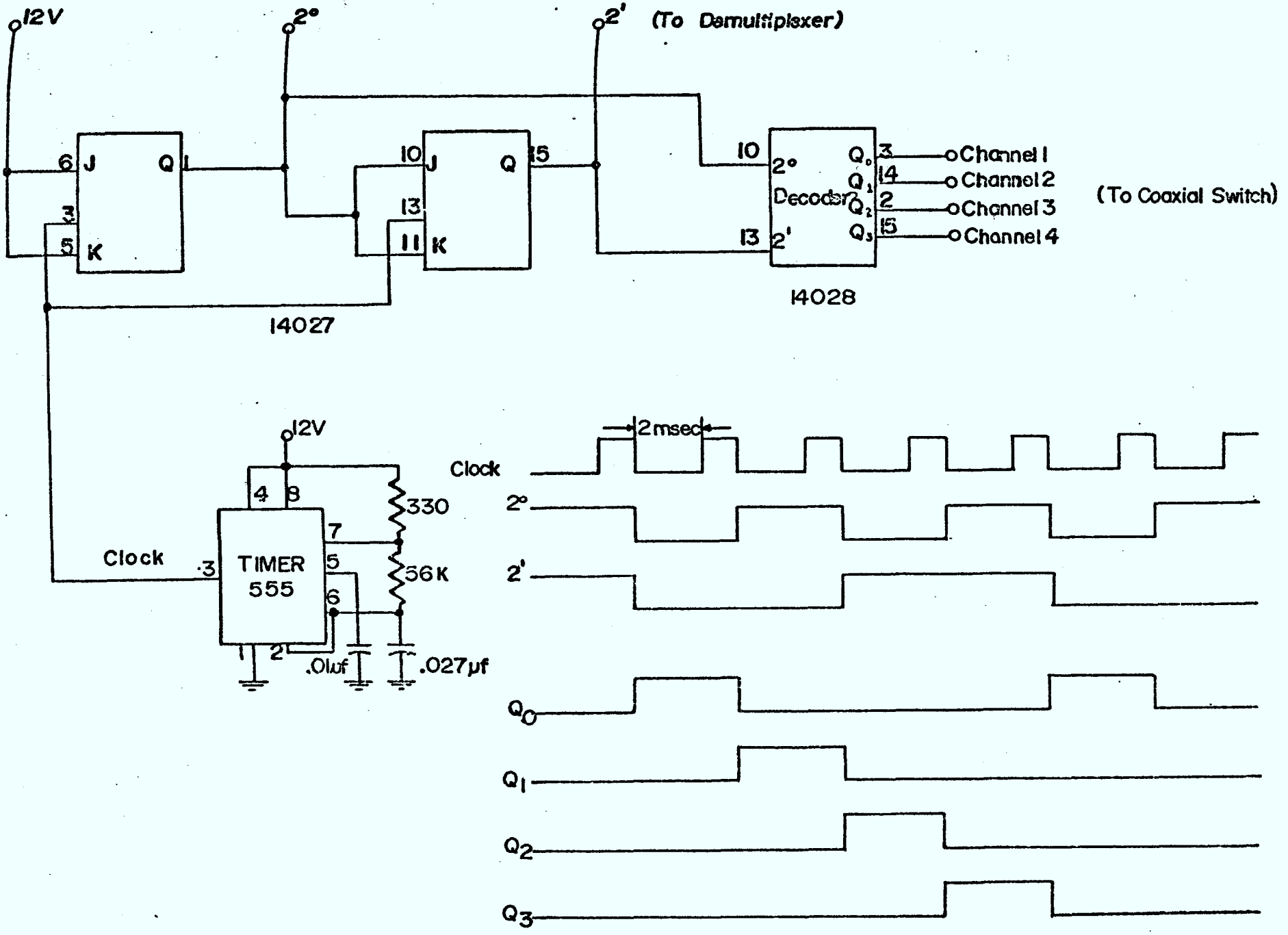

Fig. 2.14 Schematic Diagram of Control Circuit

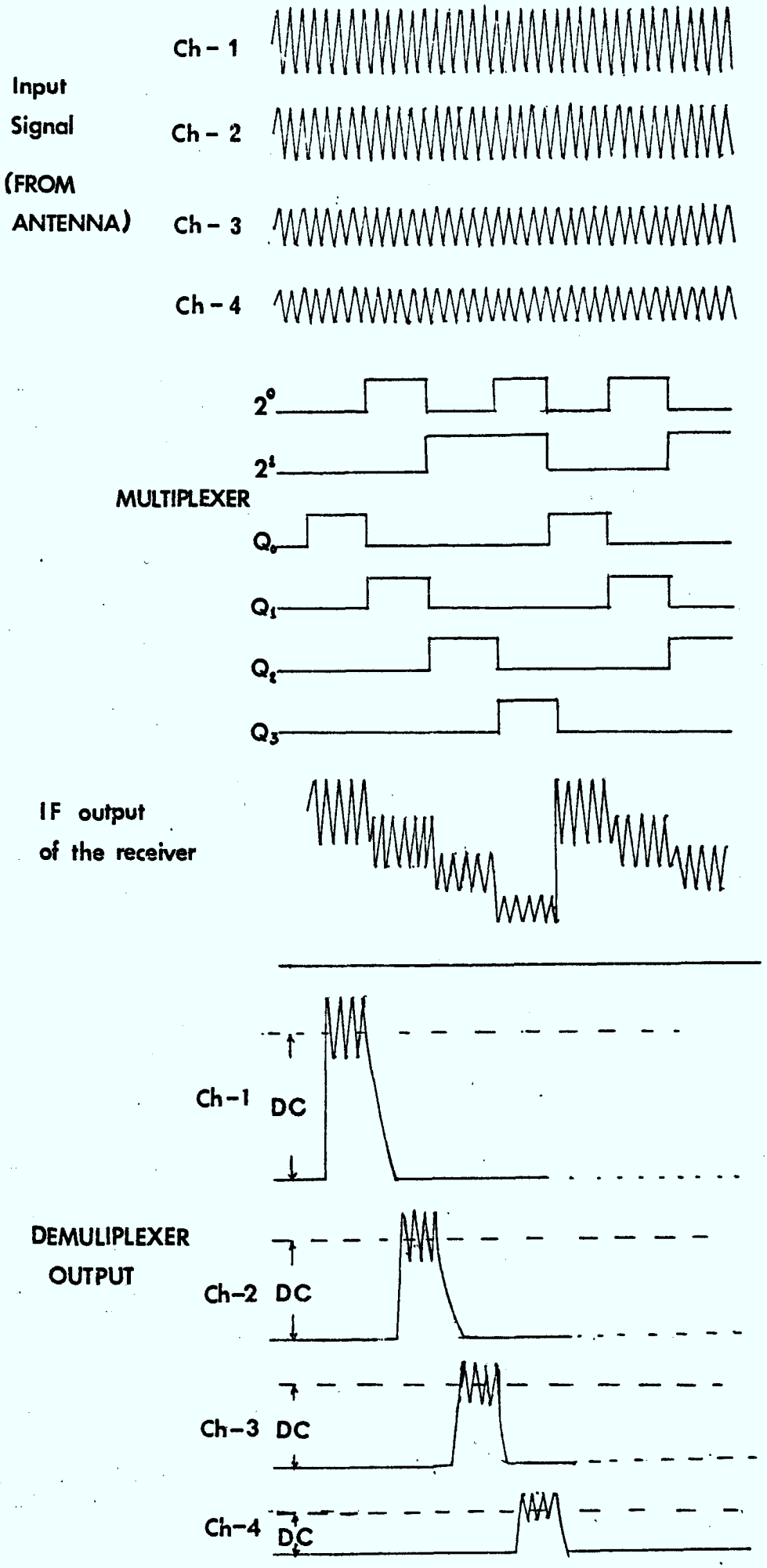

Fig. 2.15 Overall Timing Diagram (Receiving Section)

2.2.2 Calculation Section.

The function of this section is to analyze the input data. Motorola MEK6800D2 is chosen to do this job. It controls, collects the input data, does the calculations and outputs the results. This section also includes the following criteria: multiplexer, analog-to-digital converter, enable logic, interrupt control, printer, timing logic, latch, digital-to-analog converter, control switch and chart recorder. The block diagram is shown in Figure 2.5. Only the hardware of the microprocessor is considered in this section and the software is described in the next chapter.

2.2.2(a) Computer Hardware.

Motorola MEK6800D2 is an 8-bit microprocessor. It has two input-output devices but one is reserved for the keyboard display in the microprocessor. The other input-output lines (Port A and Port B) are brought out at the edge connector of the microprocessor for interfacing the outside peripherals. In this experiment, Port A is programmed as data bus and Port B is programmed as control lines. In Port B, PB_0 and PB_1 are programmed as channel selectors. PB_2 is connected to start-conversion and PB_7 is used to test end-of-conversion pulse in the analog-to-digital converter. PB_3 to PB_6 are programmed for outputting latching pulses to the latching circuitry. Figure 2.16 describes the connections of input and output ports.

2.2.2(b) Multiplexer.

The main function of this circuit is to multiplex the four

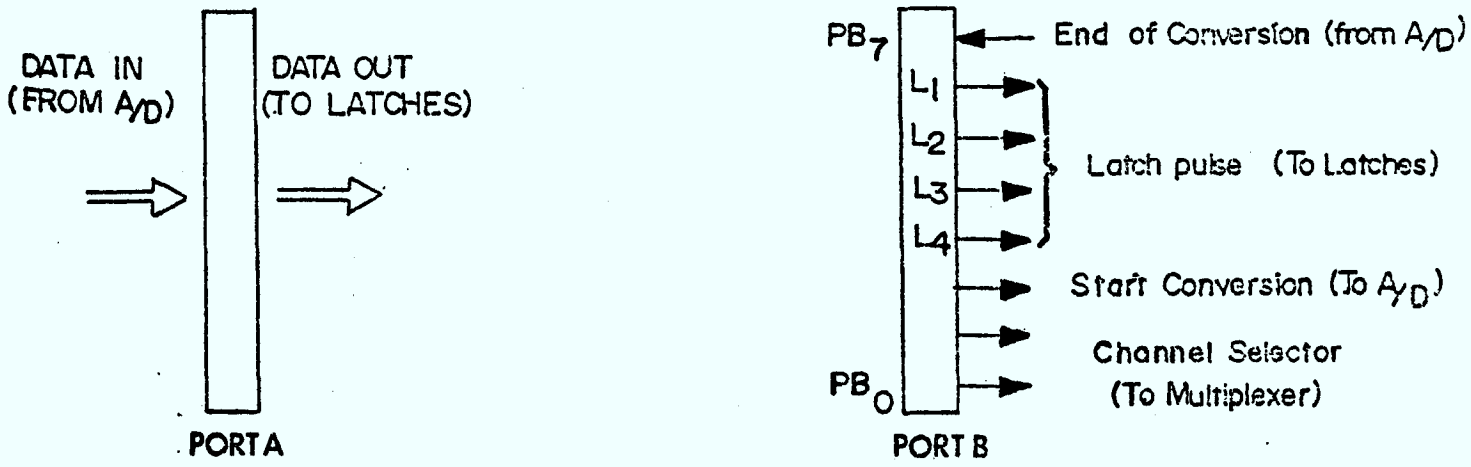

Fig. 2.16 Connections of Input/Output Port

analog signals from the receiving section into the analog-to-digital converter. It consists of four analog switches acting as a four-channel multiplexer. The controlling pulses in the multiplexer are controlled by the microprocessor and described in the Software section while a decoder is used to generate the sampling pulses. Figure 2.17 shows the circuit and timing diagrams. Buffers are added to avoid loading of the microprocessor.

2.2.2(c) Analog-to-Digital Converter.

This is an 8-bit converter using successive approximation techniques. Conversion is performed when a positive pulse is applied to the start-conversion input. After completing conversion the logic loads the binary word corresponding to the input voltage into the output latch and end-of-conversion logic level appears. The output latch is tri-state and a positive logic applied to the enable will permit the outputting of the data.

In this experiment a positive 5V is applied to the V_{ref} and gives the full scale reading. It should be noticed that this converter will give a complementary data result and can be corrected by using software in the microprocessor. A clock frequency of 2.5 KHz is used. Figure 2.18 shows the schematic and timing diagrams. The start-conversion pulse and end-of-conversion pulse are controlled and monitored by the microprocesssor, and described in the Software section, while the enable is controlled by the enable circuit described in the next section.

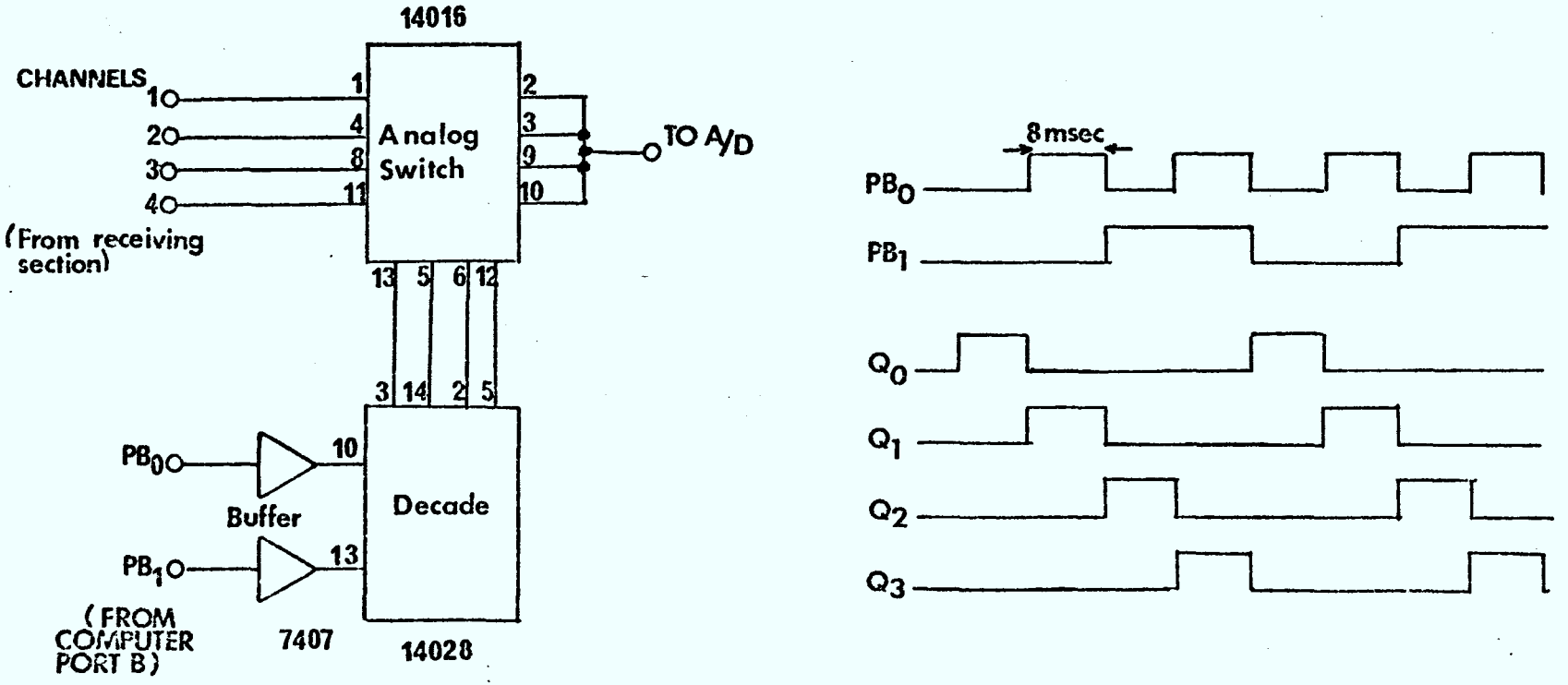

Fig. 2.17 Schematic Diagram of Multiplex Circuit

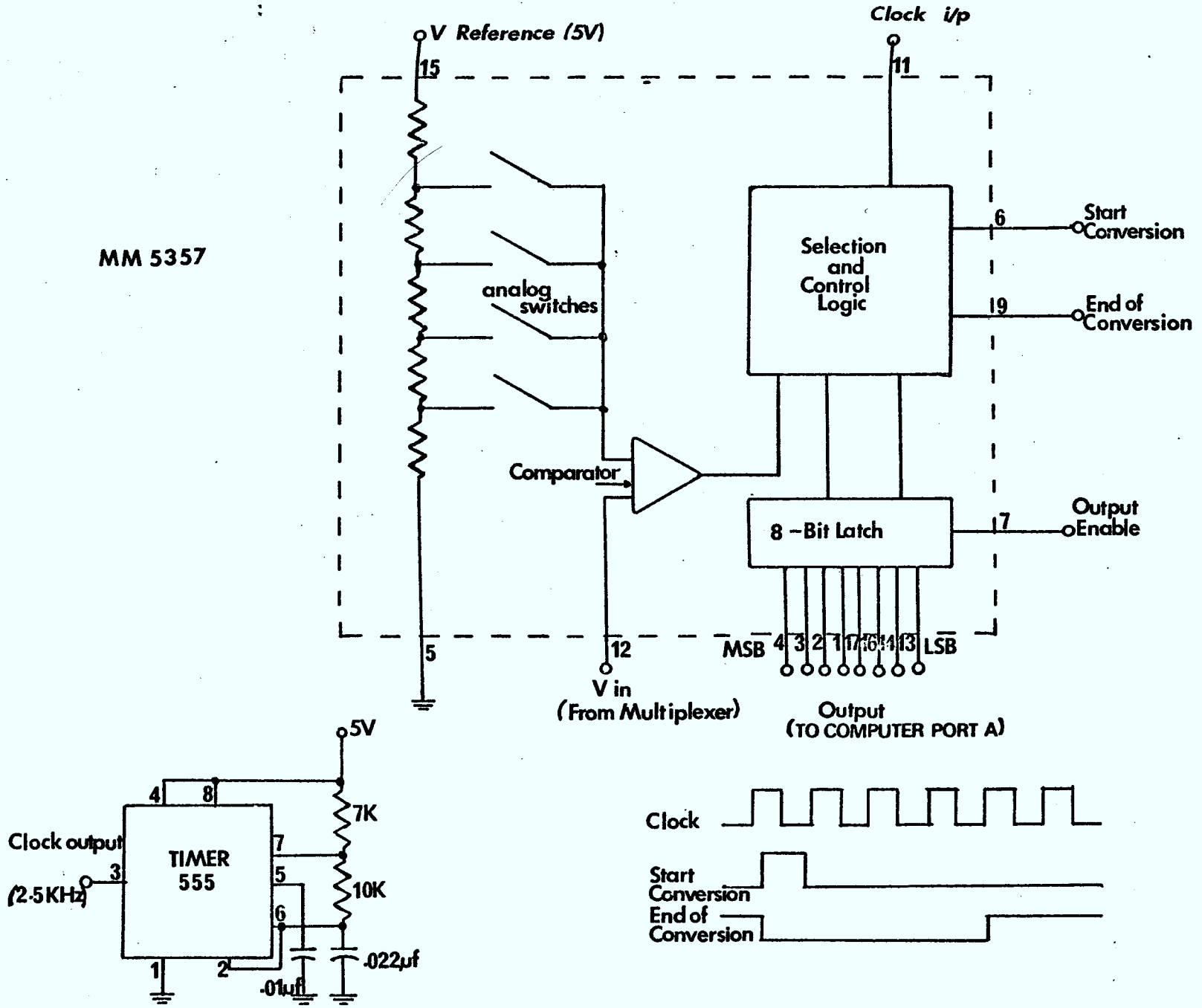

Fig. 2.18 Schematic Diagram of A/D Converter

2.2.2(d) Enable Logic.

Port A of the microprocessor is programmed as a common bus for input and output data. It reads data from the analog-to-digital converter and outputs calculated results to the latching circuit. When outputting the data the analog-to-digital converter should be isolated from the bus, to avoid loading effect. This can be done by applying a low logic at the enable input. This low logic level should start when an interrupt pulse appears (start calculation) and ends when the last latching pulse appears (end calculation). The circuit and timing diagrams are shown in Figure 2.19.

Timer 555 is used to extend the interrupt pulse. The time to be extended should exceed the total time of calculation, about 5 seconds in this experiment. The extended pulse is gated with the last latching pulse to form the input pulse to the flip-flop. Thus the desired output is obtained at the $\bar{Q}$ output of the flip-flop. A delay circuit is inserted to ensure the last calculation is completed before reading in the new data.

2.2.2(e) Latch.

After calculating the average input signal in one channel the result is latched and recorded on the chart recorder. This can be done by assigning the individual latch control to different control line locations in Port B. (See Figure 2.16) The control lines are then programmed to act as demultiplexers and, after finishing calculations in one channel, a latching pulse is generated in the appropriate control line. A full description of the latching

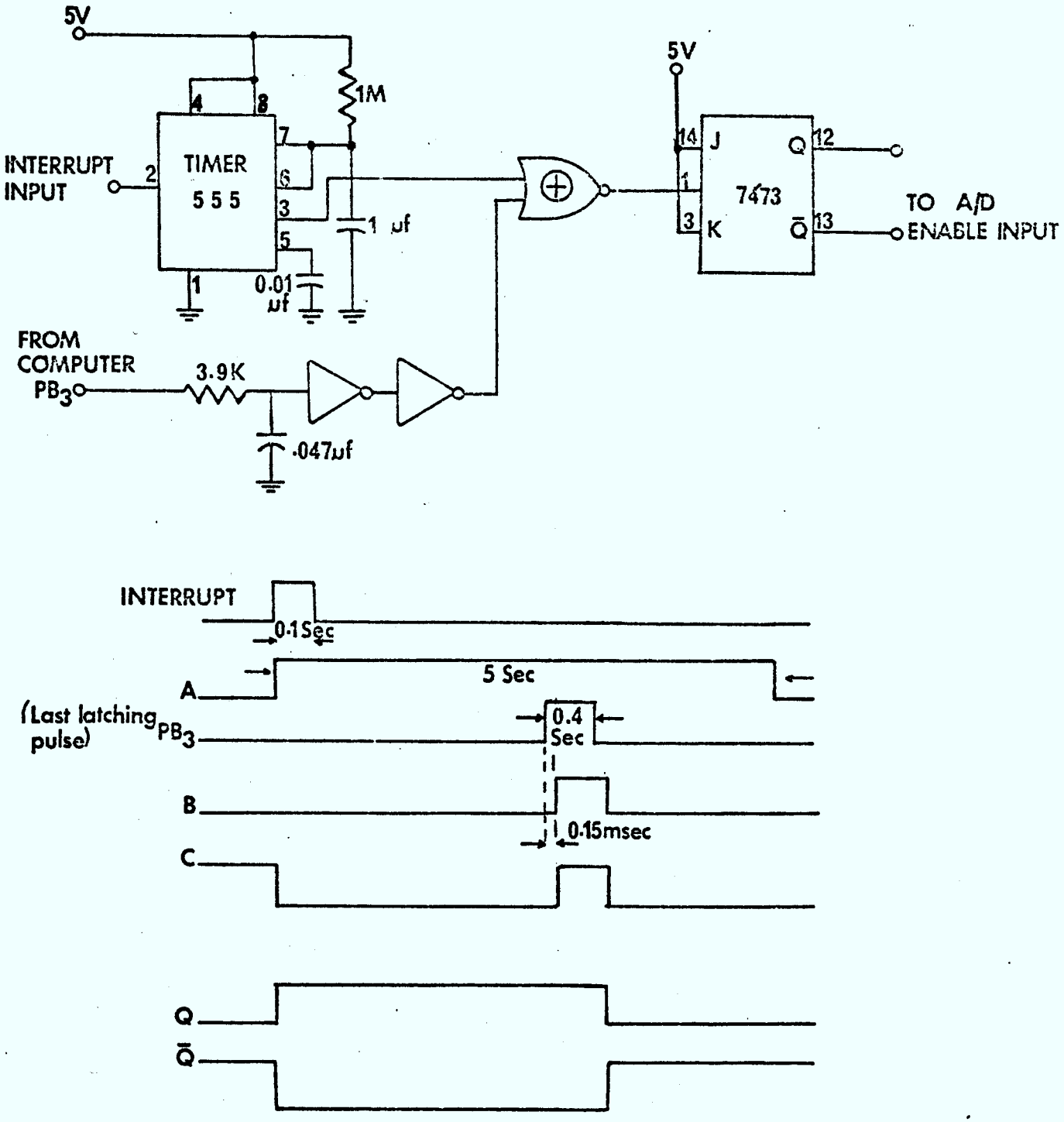

Fig. 2.19 Schematic and Timing Diagrams of Enable Logic

pulses is given in the Software section.

2.2.2(f) Digital-to-Analog Converter.

The function of this circuit is to convert the digital signal back to analog signal, to be recorded on the chart recorder. An MC1408 8-bit digital-to-analog converter is used. A 5V is applied to the V_{ref} in order to have the same reference used in analog-to-digital converter. A TL081 is used as current-to-voltage converter. Figure 2.20 shows the latching and digital-to-analog schematic diagrams.

2.2.2(g) Interrupt Control.

Once in every twenty-minute interval an interrupt pulse is generated to interrupt the microprocessor and various calculations are performed. A motor with one revolution per hour is used as a timing device and a disk, with three holes arranged in an equilateral triangle, is mounted on it. Above the disk there is placed a light source and a photo cell is placed under it. When lights shine on the cell, which happens once in every twenty-minute interval, the impedance of the cell is lowered and this activates the relay. This results in generating line pulses from the 74121 and 555 respectively. The short pulse, approximately 100 msec, is used as interrupt pulse while the 3-minutes-long pulse is used as latching pulse in the control switch section. Figure 2.21 shows the schematic and timing diagrams.

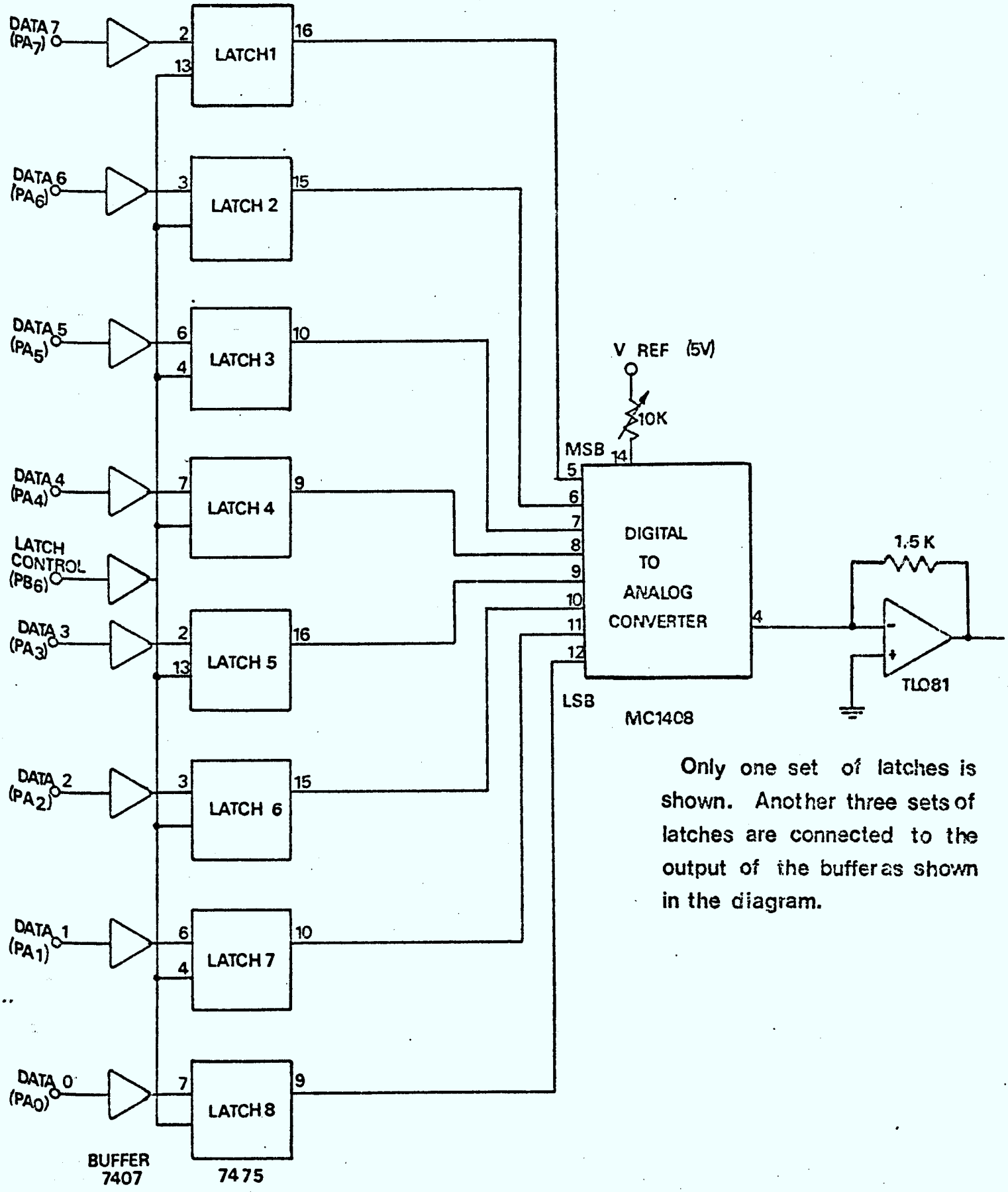

Fig. 2.20 Schematic Diagram of Latching and D/A Converter Circuits

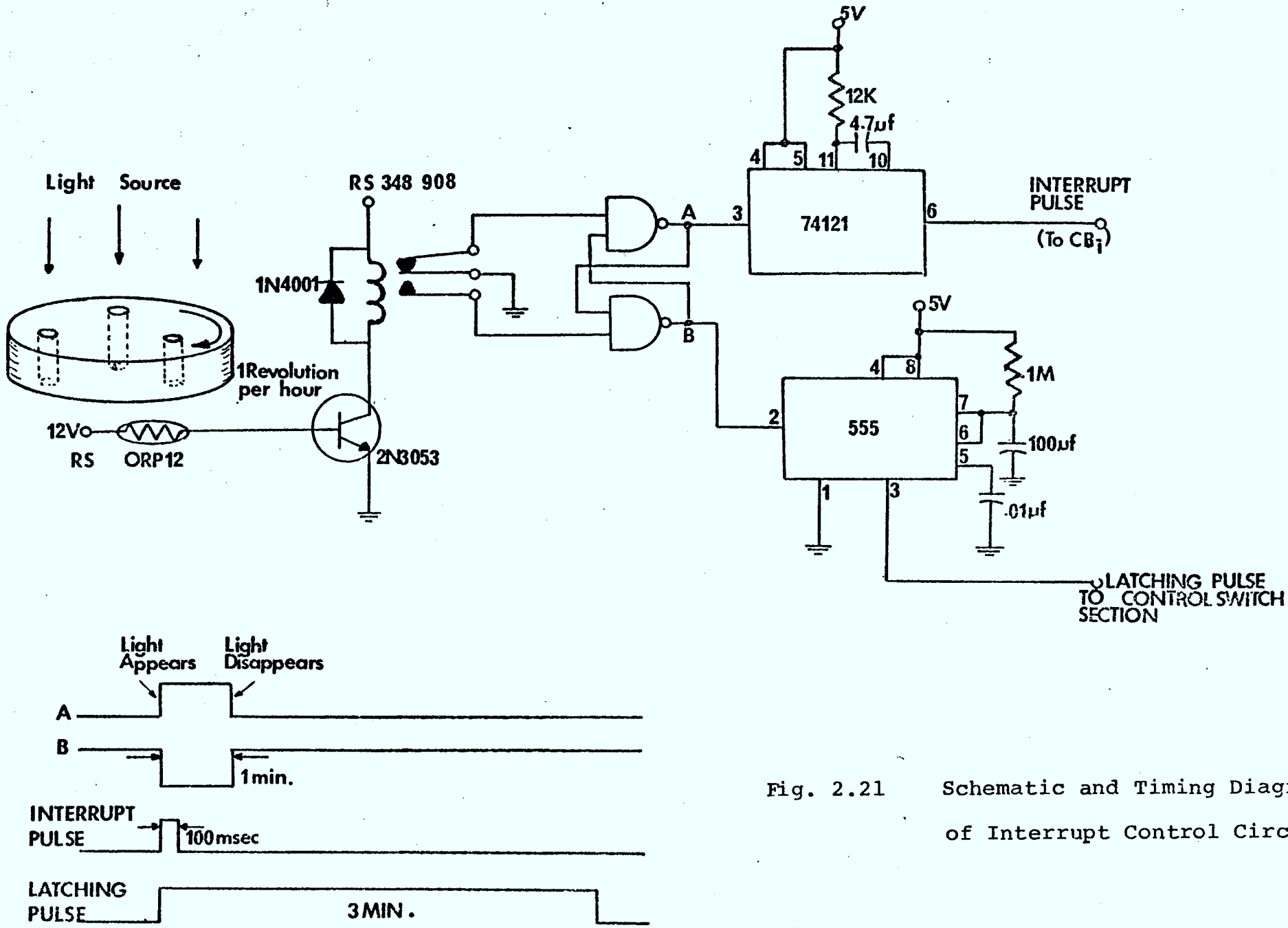

Fig. 2.21 Schematic and Timing Diagrams of Interrupt Control Circuit

2.2.2(h) Control Switch.

The incoming signal or the calculated average signal which is to be recorded on the chart recorder is controlled by this switch. It consists of a relay with four sets of one pole double throw contacts. One output is connected to the output of the receiving section while the other is connected to the output of digital-to-analog converter (See Figure 2.22). Under normal conditions the relay is not activated, so the signal strength is recorded on the chart recorder. Whenever an interrupt occurs the pulse from the interrupt control circuit activates the relay and results in three minutes of recording the average signal from the digital-to-analog converter.

2.2.2(i) Printer.

A commercial printer (Monsanto, Model 511A) is used to print out the data and the correlation coefficients between channels 1,2, 1,3 and 1,4. The printing pulse used in this printer is the positive going edge and can make use of any of the first three latching pulses in the latching circuit. They are used to generate a "print" command and the circuit diagram is shown in Figure 2.23. A full description of the printing pulse is given in the Software section. The timing logic is hardware connected to the printer and described in the next section. The specifications of the printer are listed in Appendix 7.

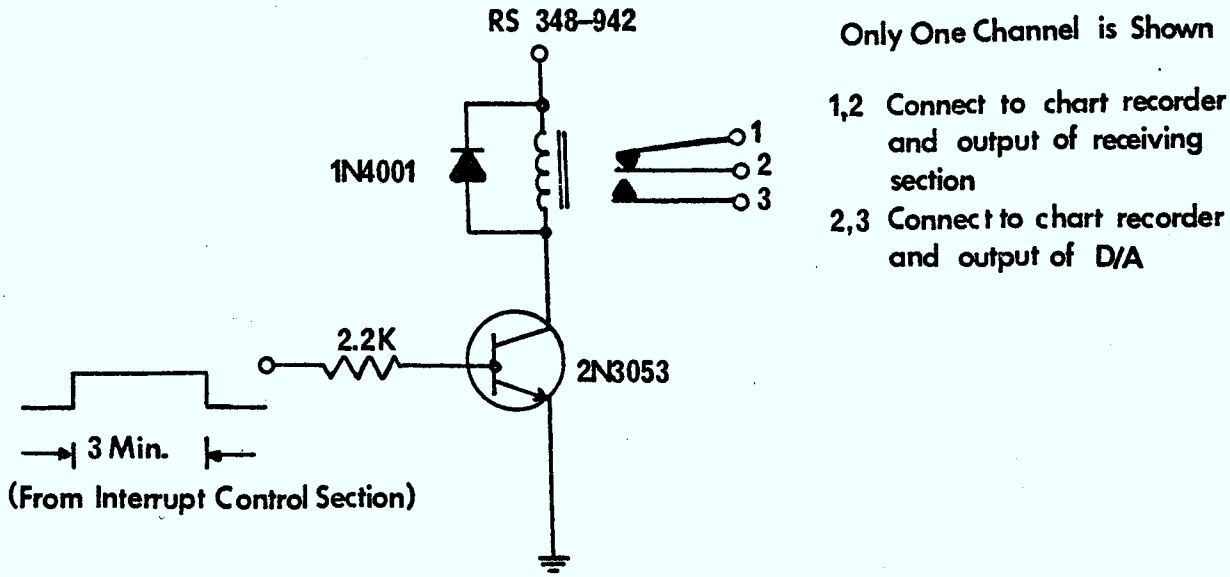

Fig. 2.22 Schematic Diagram of Control Switch Circuit

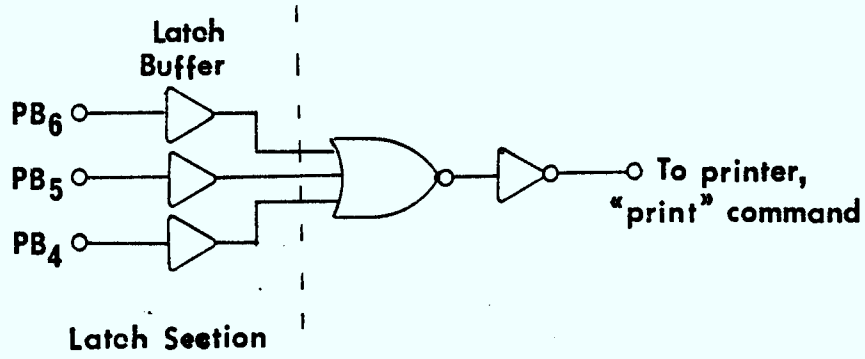

Fig. 2.23 Schematic Diagram of Input Pulse Logic to Printer

2.2.2(j) Timing Logic.

Time printing format is chosen from 0 to 23 hours, with increments of twenty minutes. The input format of the printer is in BCD and the first 8-bit word is chosen as hour input with the next 8-bit word chosen as minute input. The twenty minute increment print-out can be easily achieved by constructing a divide-by-three counter and connecting the MSB output to the 7th bit, and LSB output to the 6th bit, of the assigned word. All the other bits are grounded. Two BCD counters connecting in series are used for hour counting. A reset circuit is included to reset the counter when a count of 24 is reached. Figure 2.24 shows the schematic diagram.

2.2.2(k) Chart Recorder.

A commercial 4-channel chart recorder (MFE model M24CR) is used. The specifications are listed in Appendix 8. Usually, chart speed is set to 1mm per minute and sensitivity is set to 100mv/mm. An overall timing diagram for this section is shown in Figure 2.25.

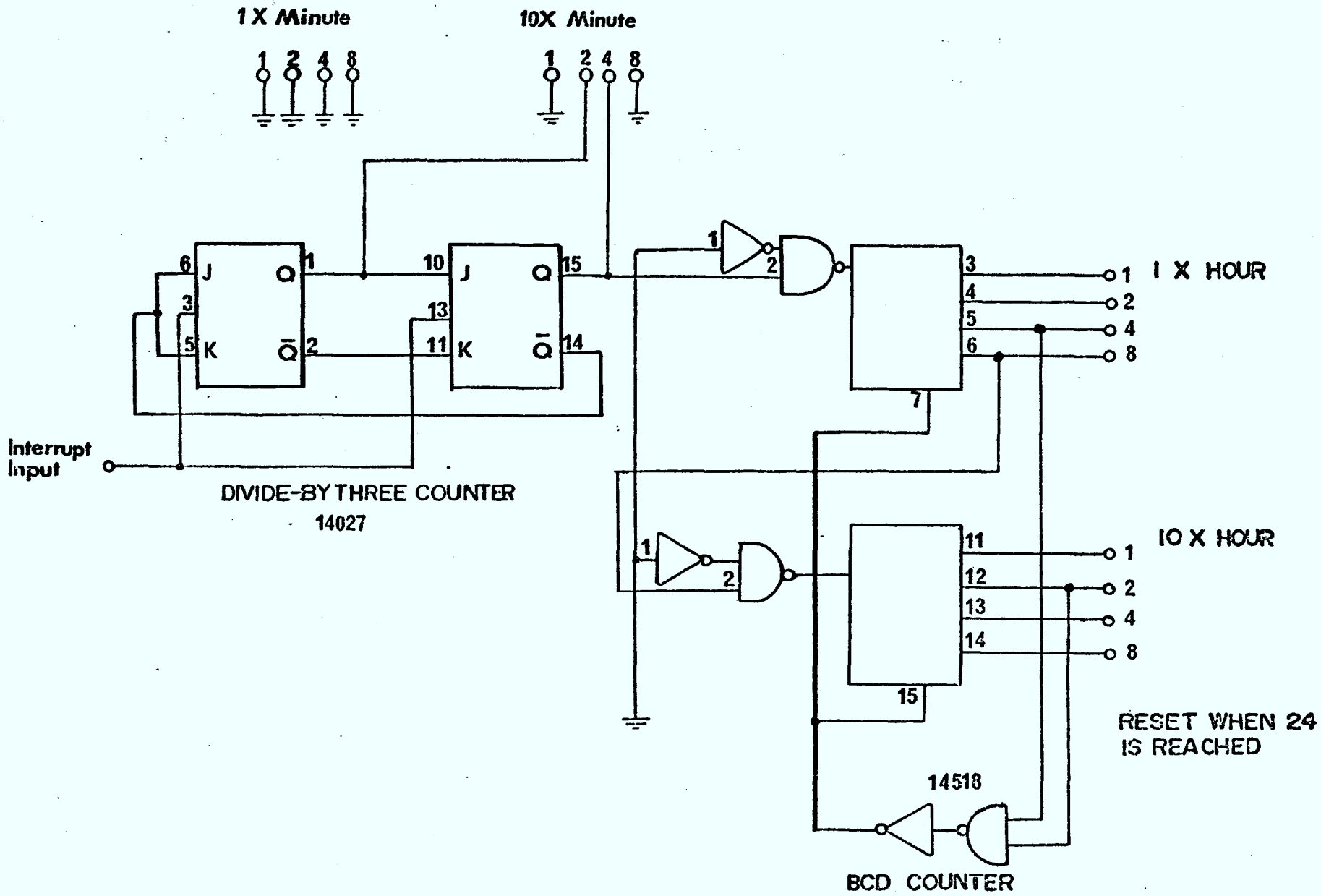

Fig. 2.24 Schematic Diagram of Timing Logic

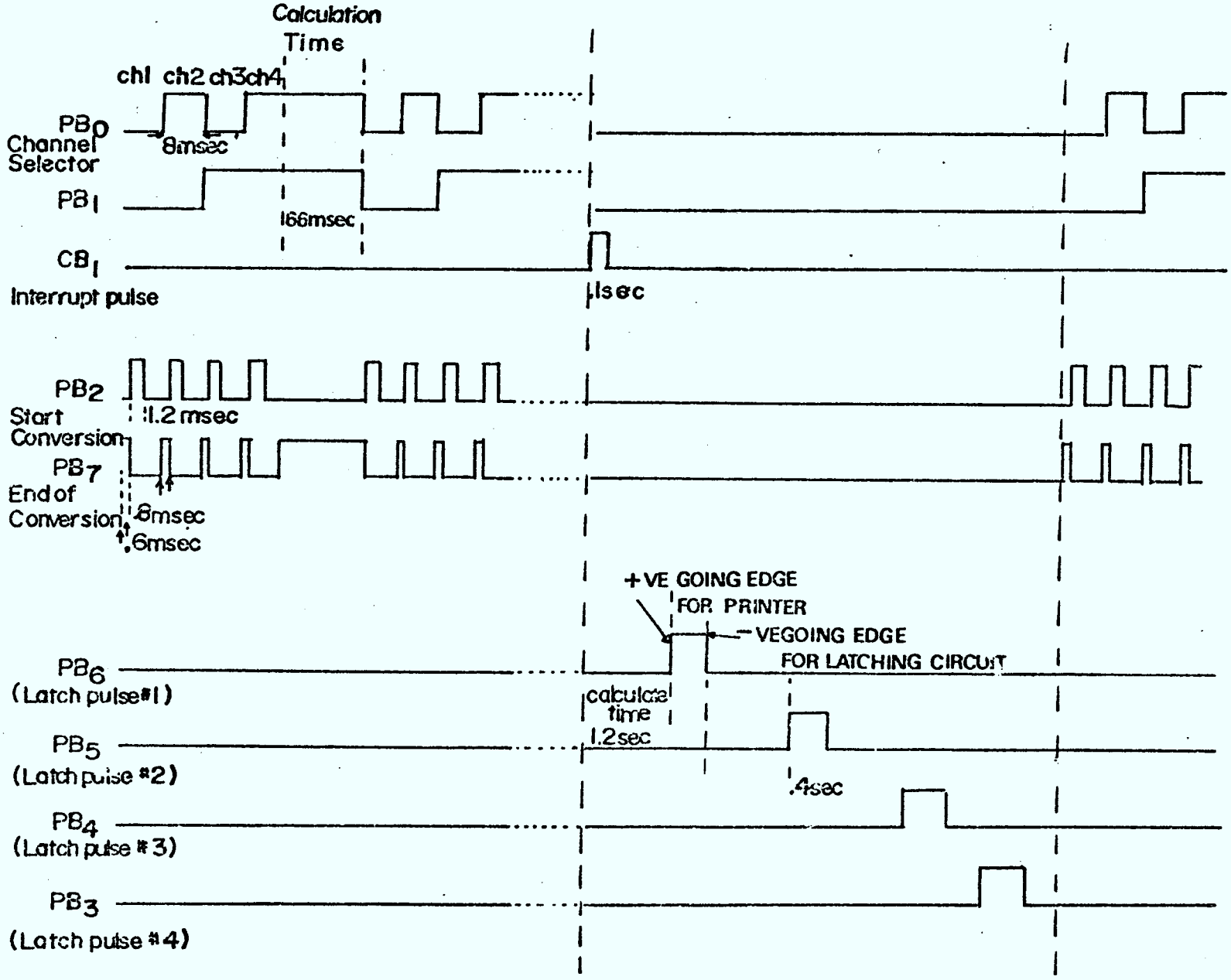

Fig. 2.25 Overall Timing Diagram (Calculation Section)

Chapter 3. Software Description

3.1 General Description.

Data control and analysis are provided by the program stored in the microprocessor. This program can be divided into two parts. Part one is used to collect data and perform necessary preliminary calculations during normal operation. Part two is used to do the main calculations during interrupt. The main calculations include averaging the input signal for each individual channel and calculating correlation coefficients between channels 1,2, 1,3 and 1,4. Subroutine programs such as multiplication, division, clearing, data conversion and square root are needed to support the program and will be discussed later. Two EPROMS (type 2708) are used to store these programs and RAM locations from 0000-0090 are needed for temporary data storage.

3.2 Program I.

This program comprises five sections, namely, setting input and output data registers, setting control pulses for multiplexer and analog-to-digital converter, summation of input data, data square and data product. As previously shown, reading in of data is done with this program and Port A is programmed as input data register. For Port B, PB_0 - PB_6 are programmed as output data register while PB_7 is programmed as input data register. Interrupt input is programmed through CB_1. Figure 3.1 shows the diagram of Port A and Port B. PB_0 and PB_1 are programmed as channel selector and the following codes are used.

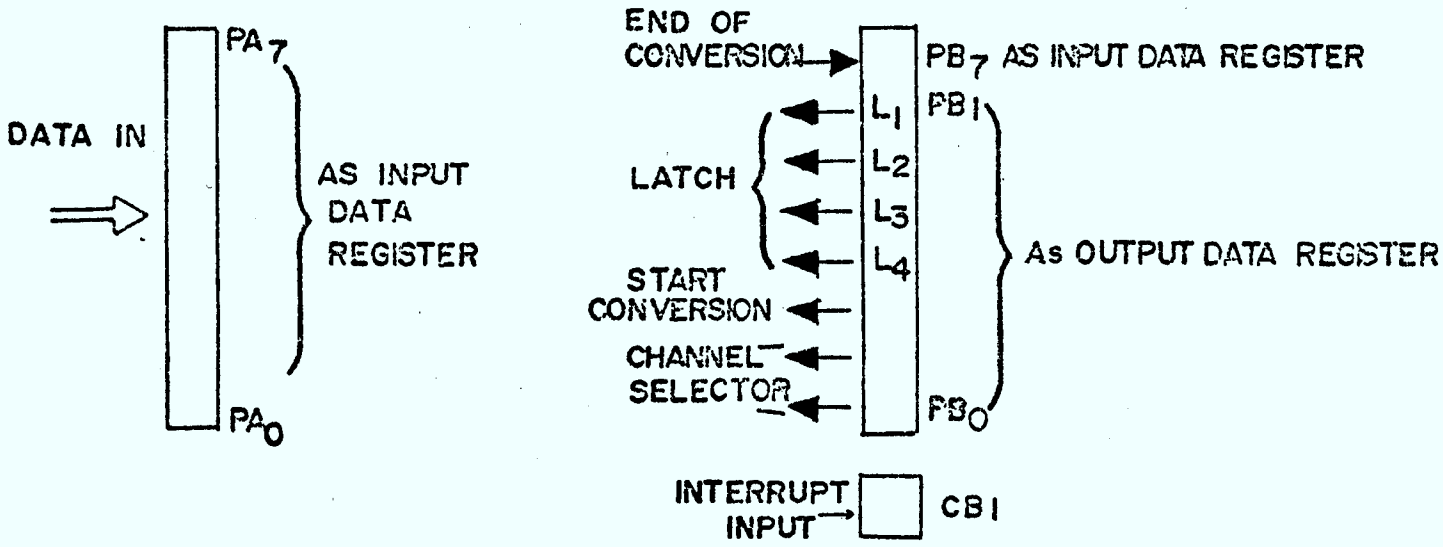

Fig. 3.1 Input/Output Port

PB_0	PB_1	Channel Selector
0	0	1
0	1	2
1	0	3
1	1	4

The cycle begins when reading in data from channel 1. This is achieved by outputting the appropriate code to the multiplexer. After delaying for about 0.6 msec, to compensate for the time delay in the multiplexer, a start pulse is supplied to the A/D converter for starting conversion. When an E.O.C. pulse appears in PB_7 data is read and summed, then the next channel is fetched. Before starting a new cycle, after reading in all channels, precalculations for the correlation coefficient are performed. This includes summing of the data square and data product. The starting location of this program is location 6000 and Figure 3.2 shows the flow chart diagram.

3.3 Program II.

Data averaging and correlation calculation are performed in this program. Port A is programmed as an output data register and PB_3 to PB_6 are programmed as output control lines. When an interrupt pulse occurs in CB1 the microprocessor will fetch the interrupt starting location C000. Interrupt program starts with calculations of variance and co-variance of channels 1,2, 1,3 and 1,4. A 2's complement program is included in the calculation because only the absolute value is used. Calculation of the correlation between

channel 1,2 is followed by outputting the result to the printer. This is done by a positive going edge pulse in PB_6. Averaging the data of channel 1 is next performed and the result is latched to the latching circuitry making use of the -ve going edge of the printing pulse. The procedures for calculation of correlation and averaging data are repeared for channels 1,3; 1,4 and channels 2, 3, 4, respectively, during which the control pulses are obtained from $PB_{5, 4, 3.}$ Before returning to 'interrupt', (Program I), the program counter is set to 6000, starting location of Program I, thus making sure a new cycle is begun. Figure 3.3 shows the flow chart diagram of this program.

3.4 Subroutines.

There are five subroutines used in the program: multiplication, clearing, division, square root and data conversion.

3.4.1 Multiplication Subroutine.

This is a 32 x 32 bit unsigned multiplication, using a shift and add algorithm. It takes 4-byte factors and yields an 8-byte product. Before multiplication the least significant four bytes of product hold the multiplier and the most significant four bytes are set to zero. After multiplication the multiplier is replaced by the least significant four bytes of product and an 8-byte result is formed. Figure 3.4 shows the flow chart diagram. Thirty-three interations are required to form the product while the thirty-fourth iteration performs a final shift to position it properly. Each iteration starts with a right shift of all eight bytes of

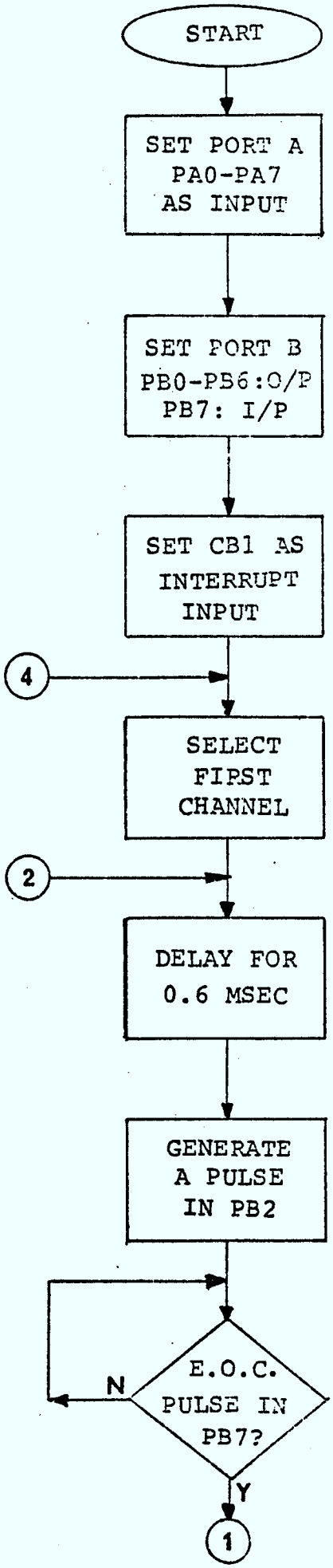

Fig. 3.2(a)

Flow Chart Diagram of

Program I

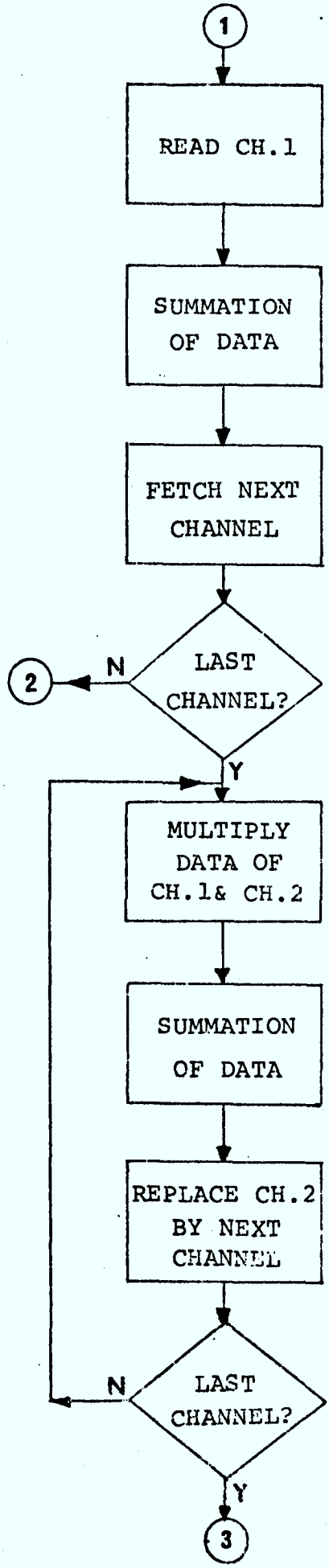

Fig. 3.2(b)

Flow Chart Diagram of Program I

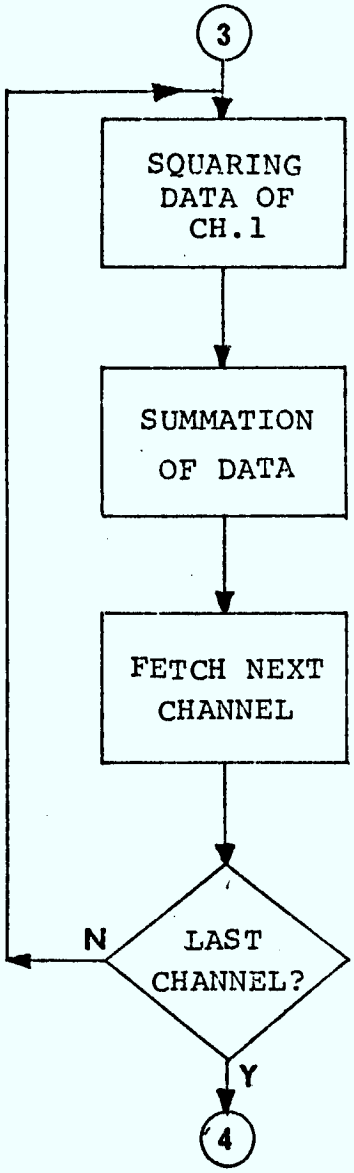

Fig. 3.2(c) Flow Chart Diagram of Program I

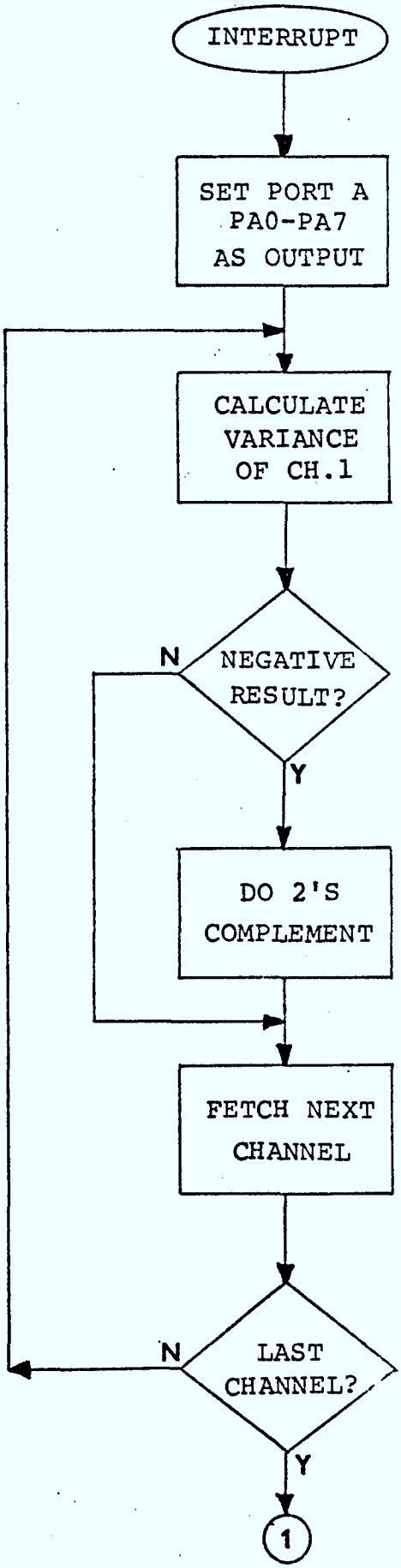

Fig. 3.3(a)

Flow Chart Diagram of Program II

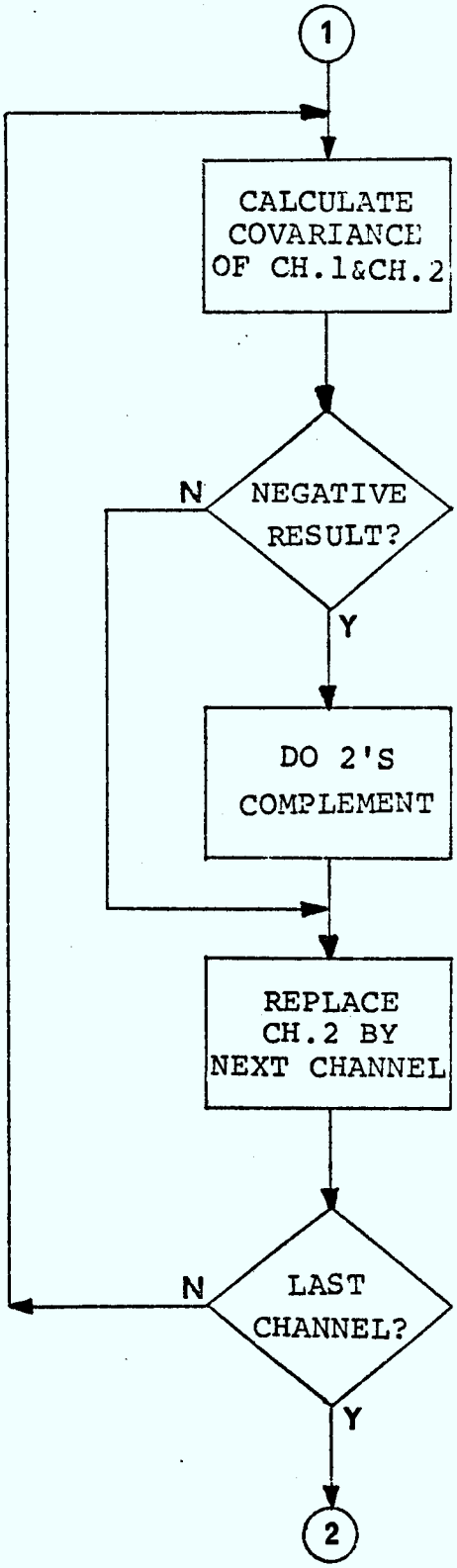

Fig 3.3(b)

Flow Chart Diagram

of Program II

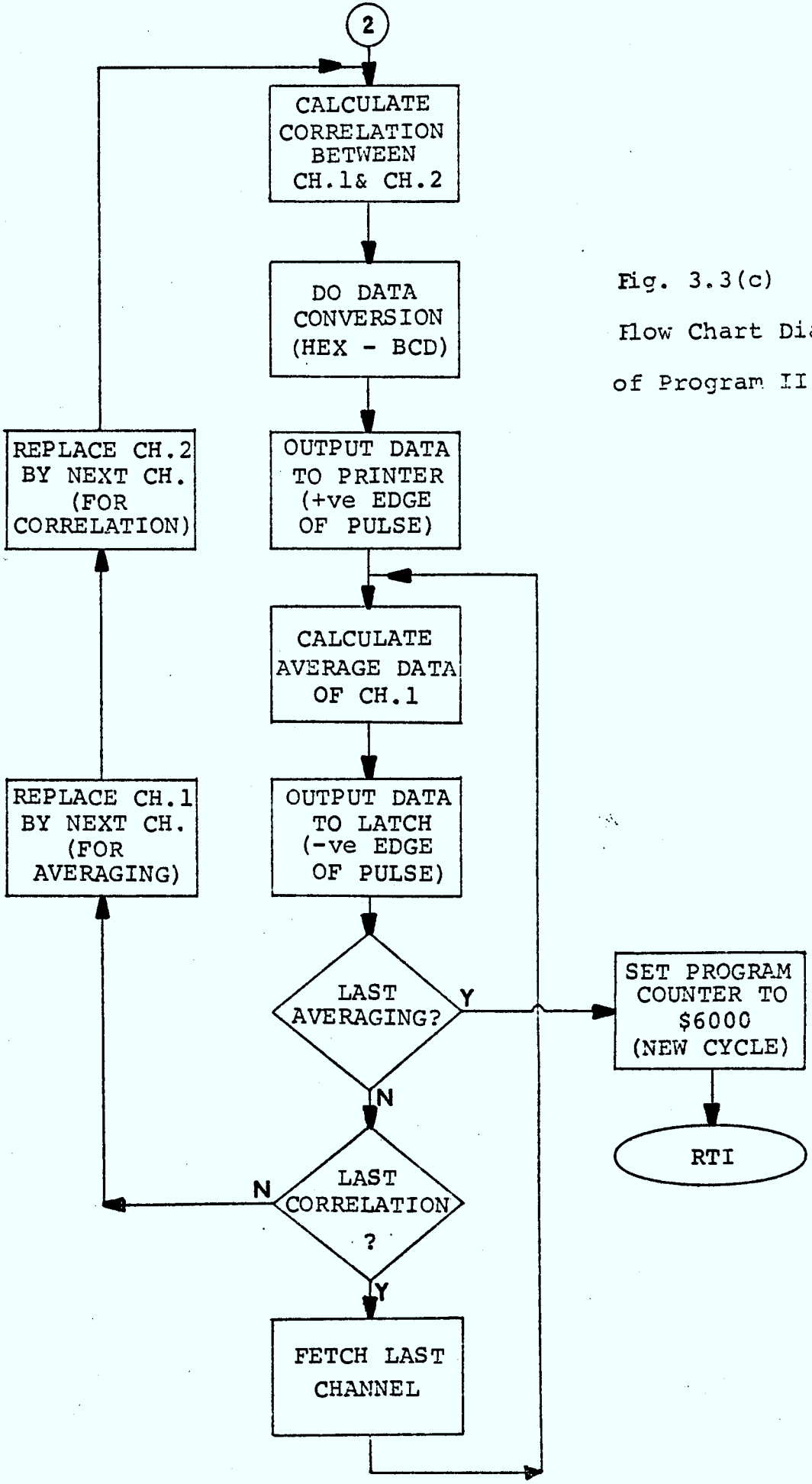

Fig. 3.3(c)

Flow Chart Diagram

of Program II

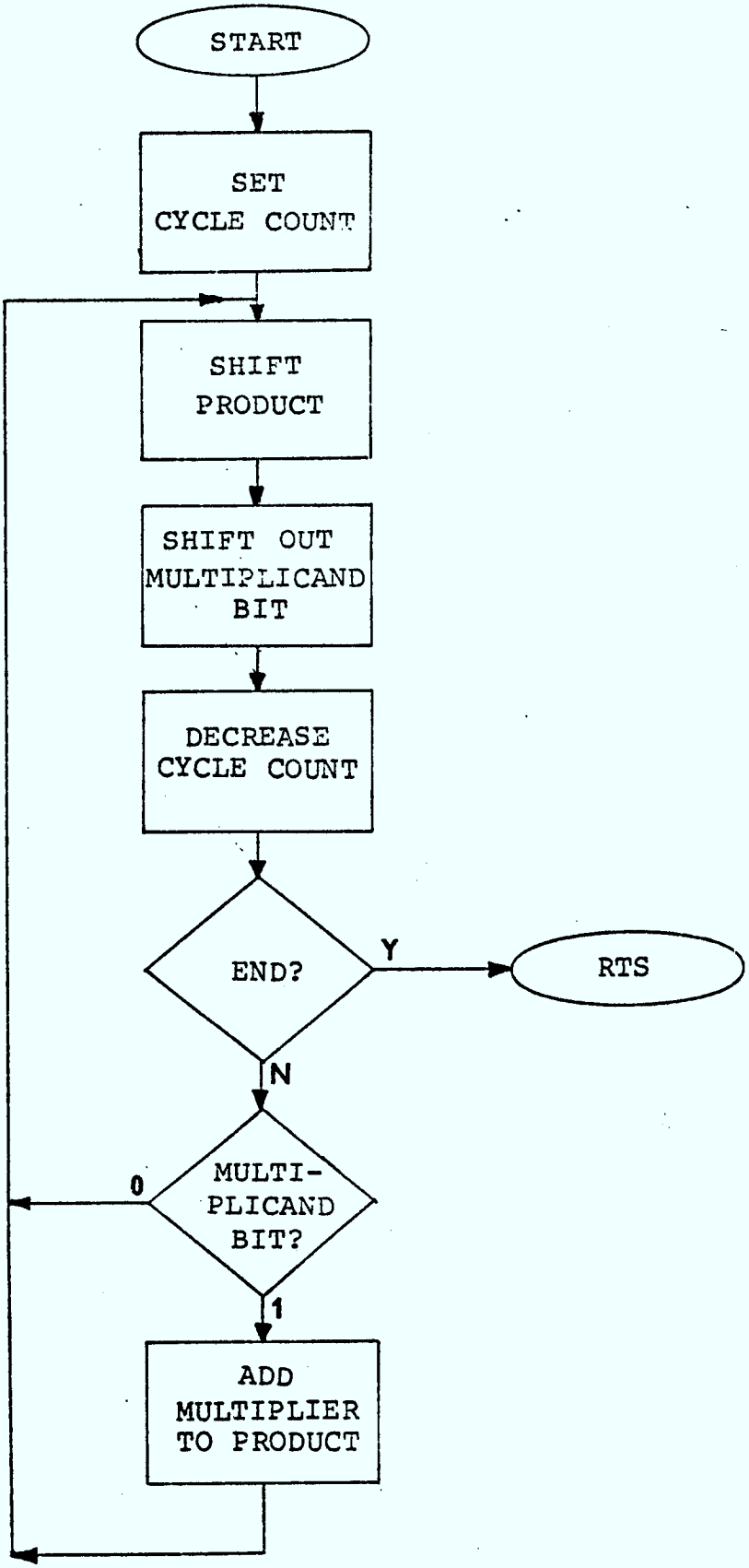

Fig. 3.4 Flow Chart Diagram of Multiply Subroutine

product. This action shifts the current sum of partial products and puts the next bit of the multiplier into the carry bit position. If the carry bit is one, the multiplier is added to the upper four bytes of product, otherwise the next iteration is executed

3.4.2 Division Subroutine.

This unsigned division routine would accept an 8-byte dividend and 4-byte divisor and generate a 4-byte quotient. Thirty-three iterations are required to form the quotient while another iteration is used to position it properly. After division, the quotient is in the low four bytes of dividend and the remainder is in the high four bytes. Figure 3.5 shows the flow chart diagram.

The first iteration starts by comparing the upper four bytes of dividend to the divisor. If the result is equal or positive, subtraction is performed and the result is copied into the upper dividend and simultaneously a quotient bit is produced. If otherwise, the quotient bit is set to zero. Following this the entire dividend is shifted left and the quotient bit which is contained in the carry bit is shifted in. When all iteration are completed the quotient fills the lower half of the dividend and the remainder is in the upper half.

For the correlation coefficient calculation the answer is always less than unity and remainder division must be performed. The division procedure is the same as before except for the number of iterations. For an 8-bit answer the number of iterations is increased to 41; that is, eight more iterations are required.

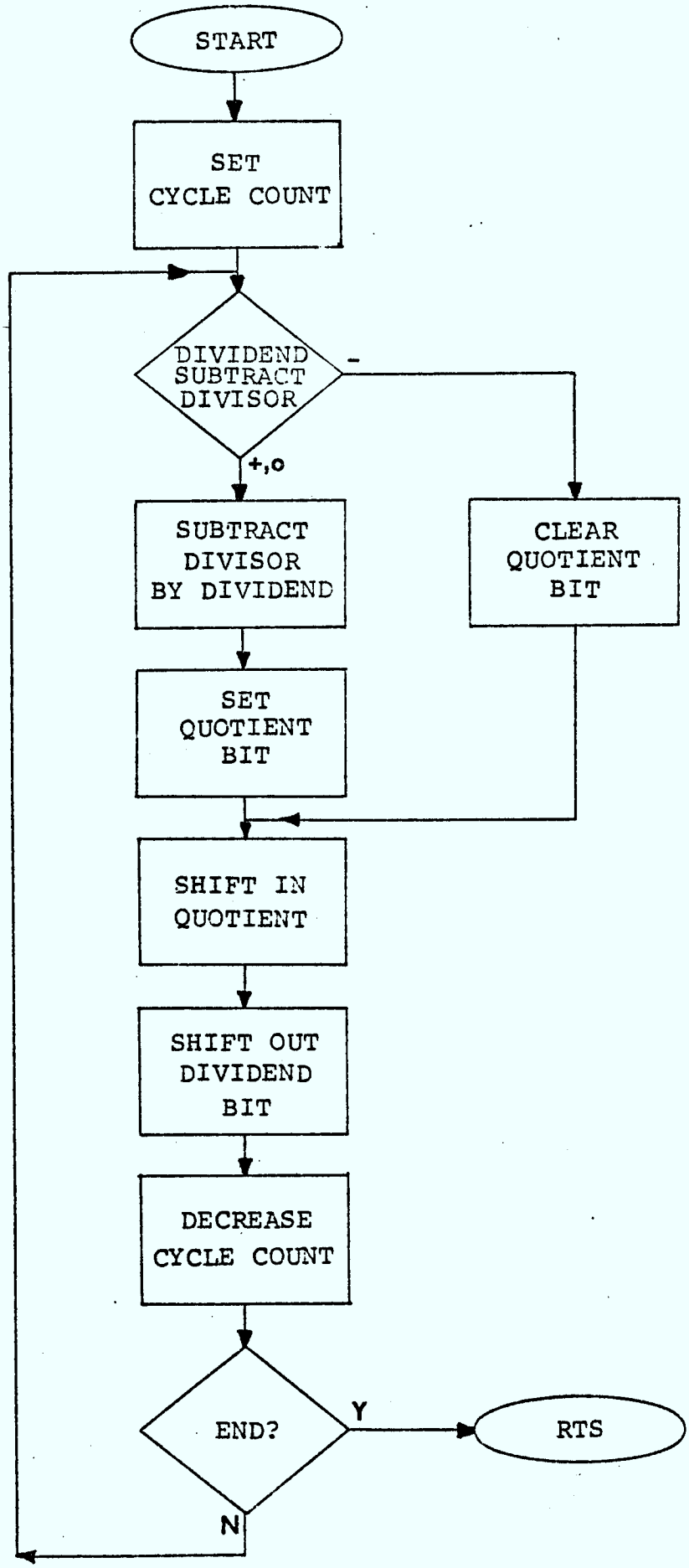

Fig. 3.5 Flow Chart Diagram of Divide Subroutine

After division the quotient is in the lowest byte of the dividend.

3.4.3 Clearing Subroutine

This subroutine is used to clear any memory data before executing any calculation. The clearing location is stored in 2-byte of memory and clearing length is stored in accumulator B. The flow chart diagram is shown in Figure 3.6.

3.4.4 Square Root Subroutine.

This program accepts an 8-byte data and produces a 4-byte answer using the Newton-Raphson method. This method is very straightforward and the expression is:

$$X_{n+1} = \frac{1}{2} \left(X_n + \frac{N}{X_n}\right)$$

where N is the data

X_{n+1} is the new root

X_n is the old root

The percentage accuracy depends on the number of iterations. as well as the initial root value. This program starts with an initial root of four bytes = 4xFF and 32 iterations. The flow chart diagram is shown in Figure 3.7.

3.4.5 Data Conversion Subroutine.

This subroutine converts the decimal HEX as a result of correlation calculation, to decimal BCD. It consists of two parts. Part one is used to convert decimal HEX to HEX while part two is used to convert HEX to BCD. The equation used for converting decimal

HEX to HEX is:

$$HEX = \frac{(\text{Decimal HEX}) \times (\$64)}{\$100}$$

To convert HEX to BCD the following method is used. The last four bits of data is compared to 5; if it is greater or equal, 3 is added to the data. Then, the first four bits is compared to $50; if it is greater or equal, $30 is added to the data. An iteration of eight for 8-bit data is used. Figure 3.8 shows the flow chart diagram.

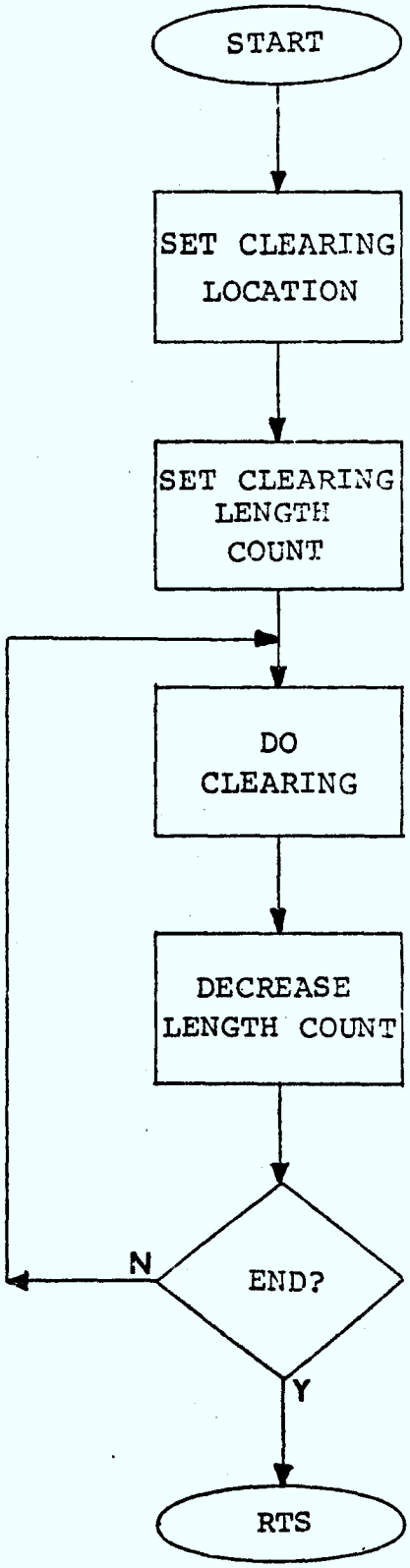

Fig 3.6 Flow Chart Diagram of Clearing Subroutine

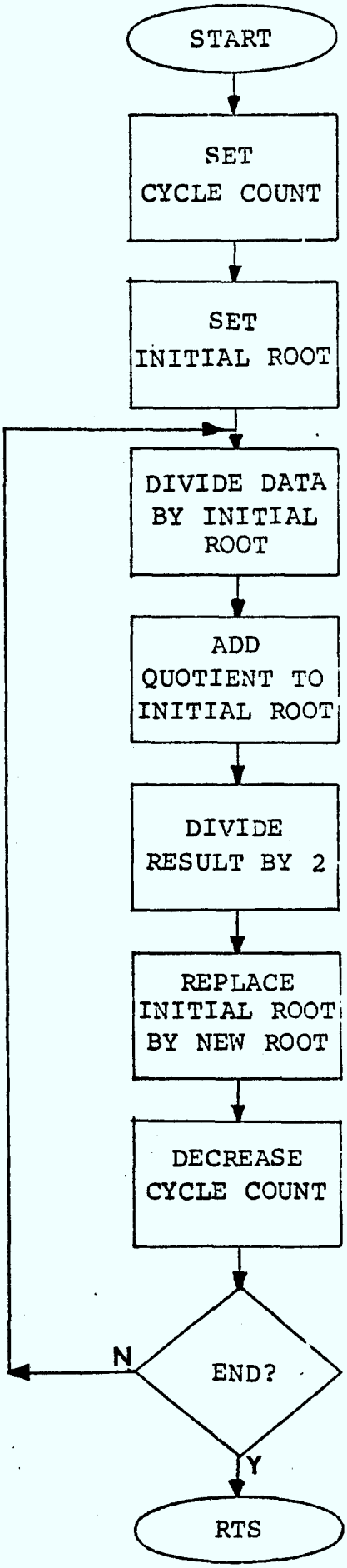

Fig. 3.7 Flow Chart Diagram of Square Root Subroutine

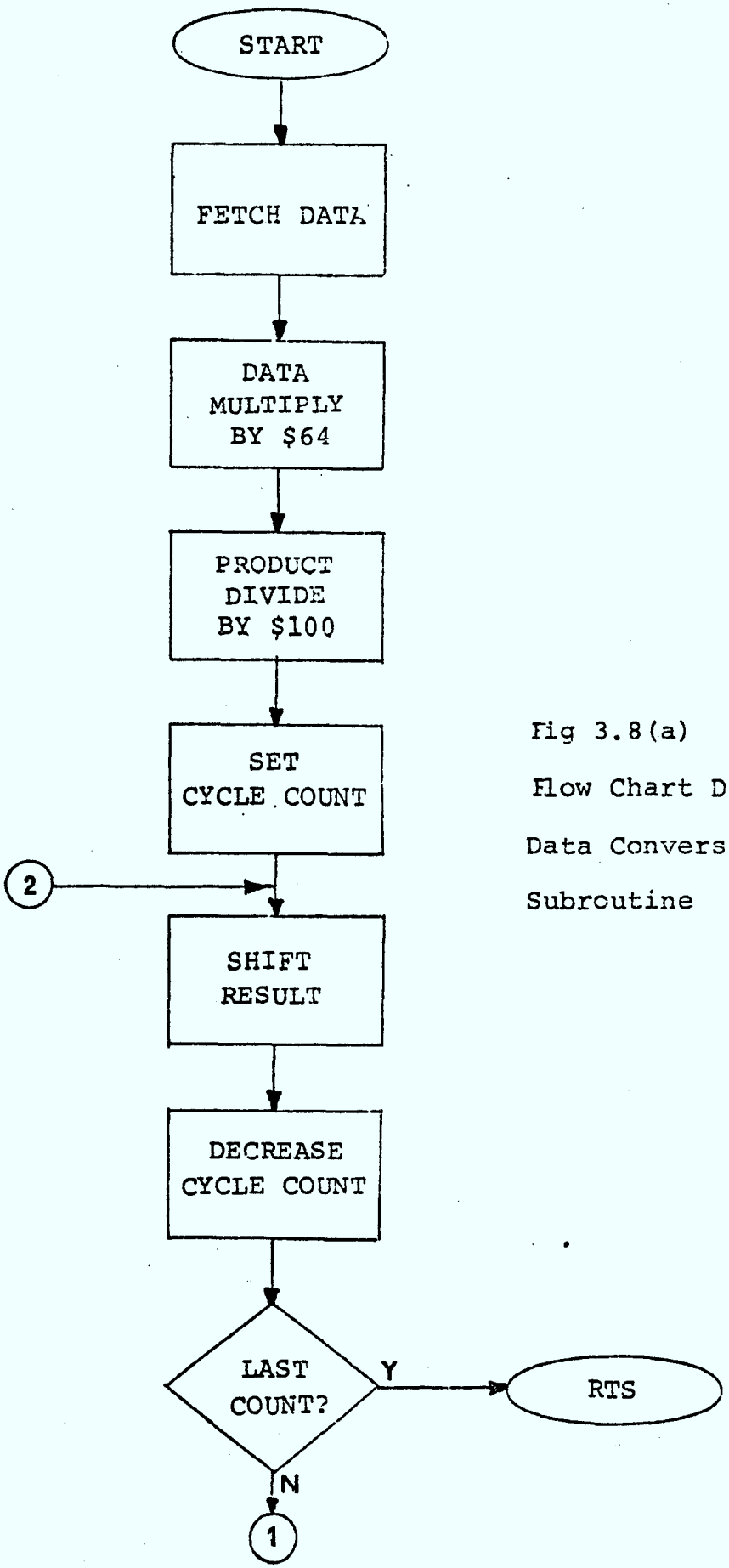

Fig 3.8(a)

Flow Chart Diagram of Data Conversion Subroutine

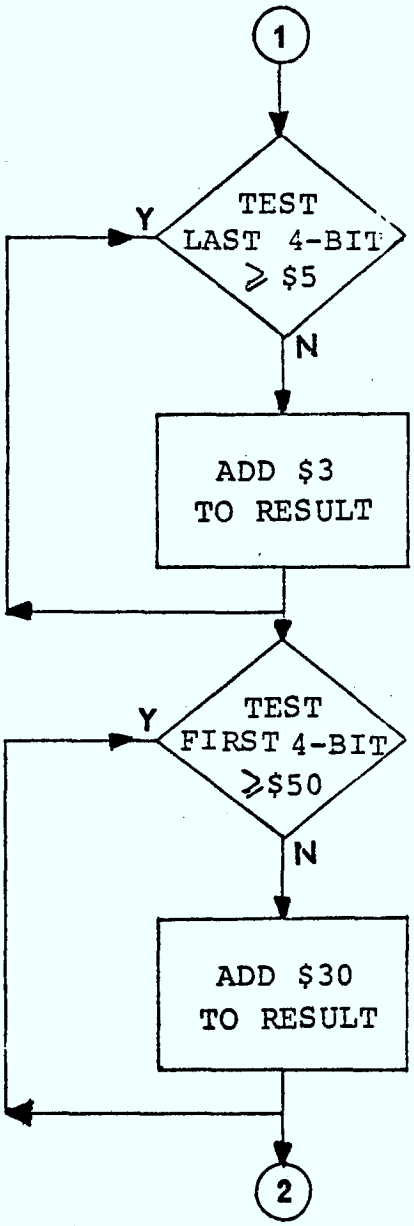

Fig 3.8(b) Flow Chart Diagram of Data Conversion Subroutine

Chapter 4. Data Analysis

The equipment has been in full operation since February 1979 and data has been recorded since then. Relative signal strength for Channel 2, Channel 3, Channel 4, with Channel 1 (top antenna) as reference plotted in Figure 4.1, 4.2, 4.3 respectively and each point in the figures refers to twenty-minute sampling. These show that relative signal strength is proportional to the height of the antenna. Higher height of the antenna results in higher signal gain. For each graph, a linear regression curve is contructed and these linear curves are shown in Figure 4.4. They appear to have almost the same slope. By using the data obtained from these curves a height-gain graph is derived, as shown in Figure 4.5. It gives three curves with Channel 1 (-85, -90, -95 dBm) as reference. It is not clearly shown what overall shape these curves have from this sample but a straight-line fit is used. (The height-gain is found to be about 3dB per doubling of height.) If these curves are extended they will intersect at a height of 120 meters with the signal level of -37dBm.

Furthermore, if some assumption are made, a height-gain curve up to the height of free-space can be constructed. For the ray path as shown in Figure 2.2 the line-of-sight propagation would give a calculated signal strength, on Channel 24 at London, of -30dBm (±10dBm) at 180 meters. Using this signal strength as the free-space signal level a height-gain curve is constructed and shown in Figure 4.6. This figure indicates that the signal strengths must fall-off with height at an approximately constant rate up to about 100 meters. This is much a greater height than that shown in Figure 1.9.

Cross correlations of signal fluctuation on the four antennas were computed every twenty minutes. The histograms for these correlation coefficients between Channel 1,2, 1,3 and 1,4 are shown in Figure 4.7, 4.8, 4.9 respectively. Higher correlation coefficient value is obtained between the uppermost antennas. Figure 4.10 shows the three smooth histograms. Note the rapid decrease of correlation as the antennas are separated. The vertical structure size to give a correlation of 0.5 is only about 25 feet. This interesting result is currently being studied in more detail.

Fig.4.1 Relative Signal Strength
(Channel 2 versus Channel 1)

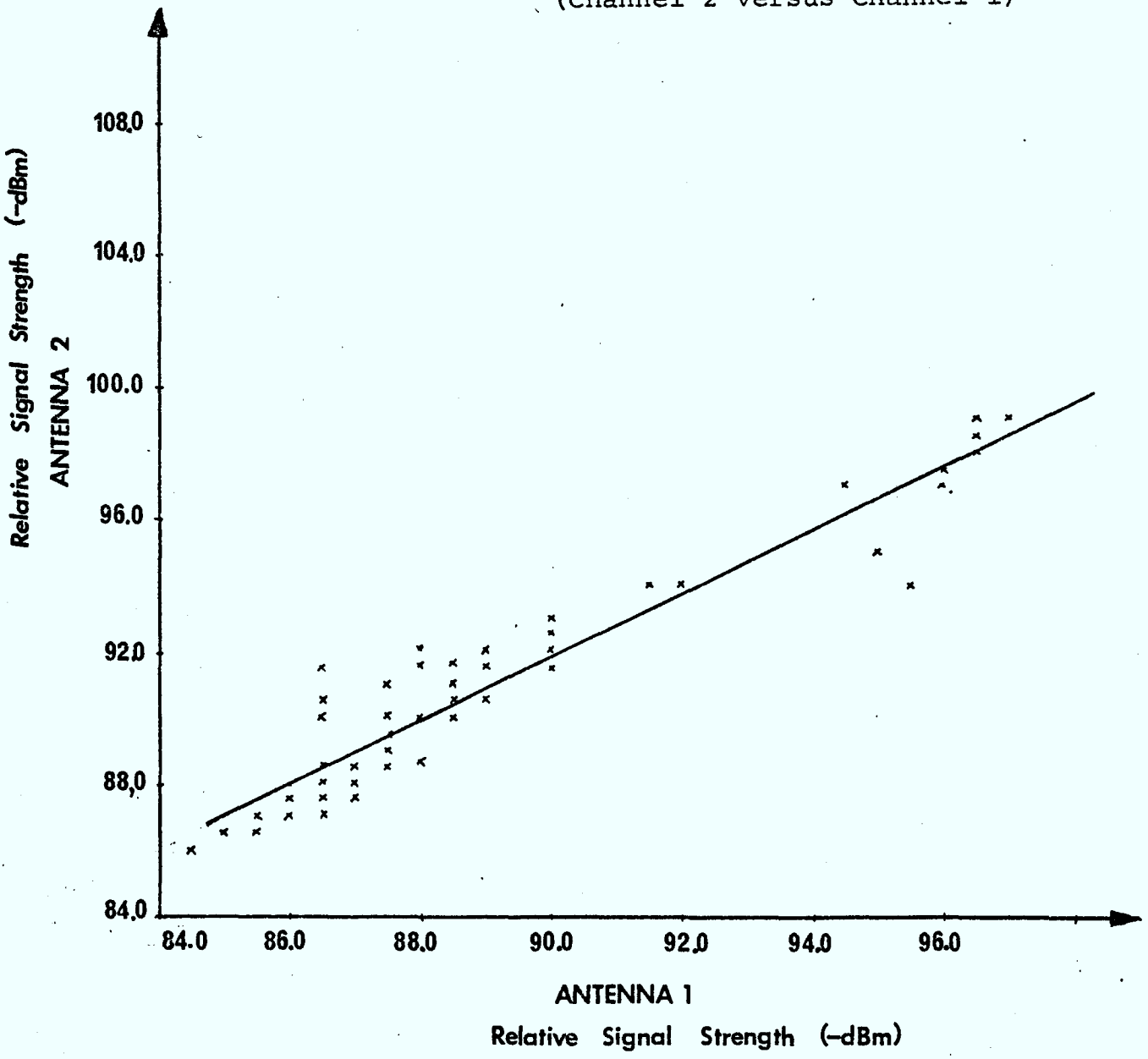

Fig 4.2 Relative Signal Strength

(Channel 3 versus Channel 1)

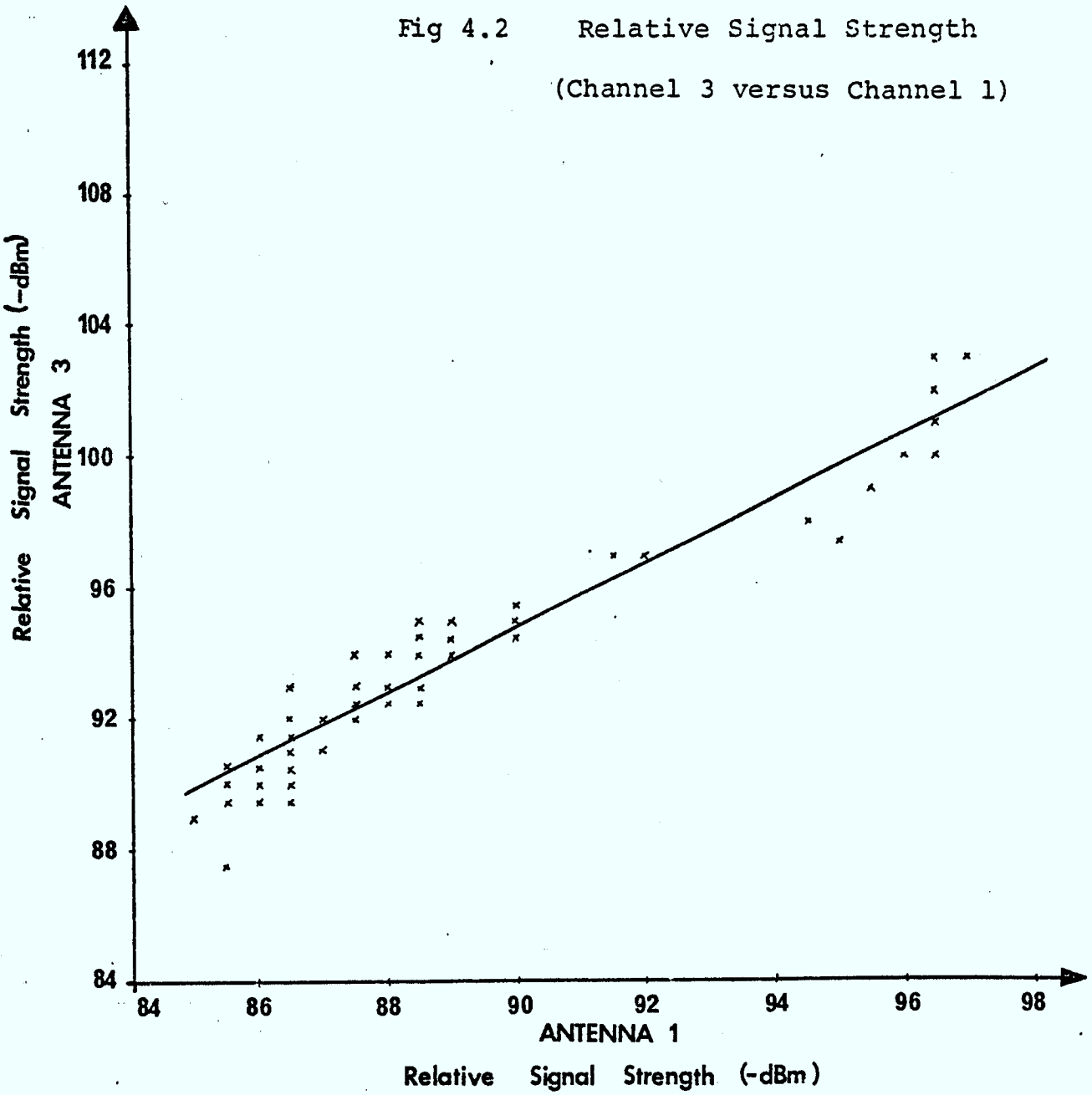

Fig 4.3 Relative Signal Strength
(Channel 4 versus Channel 1)

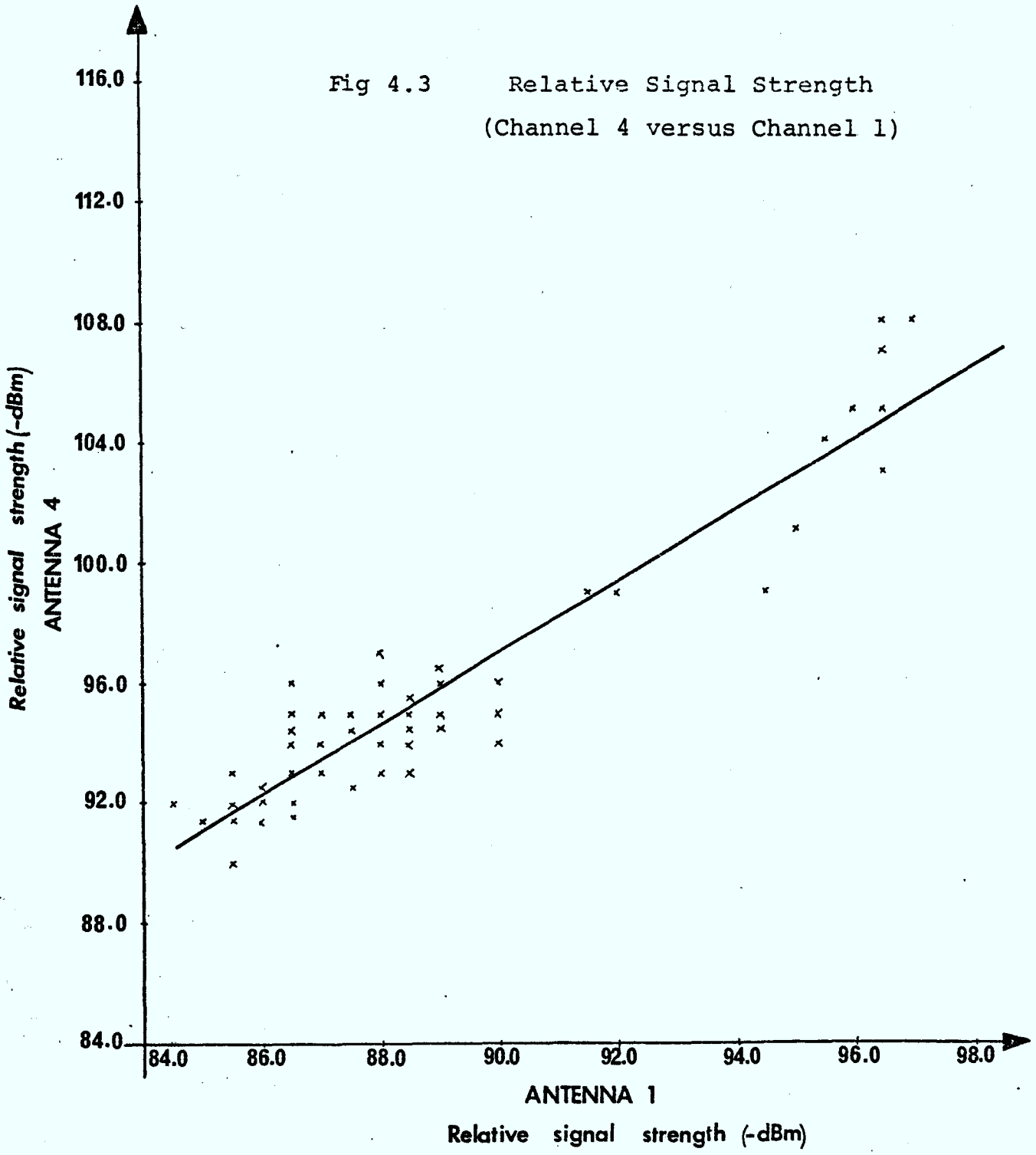

Fig 4.3 Relative Signal Strength
(Channel 4 versus Channel 1)

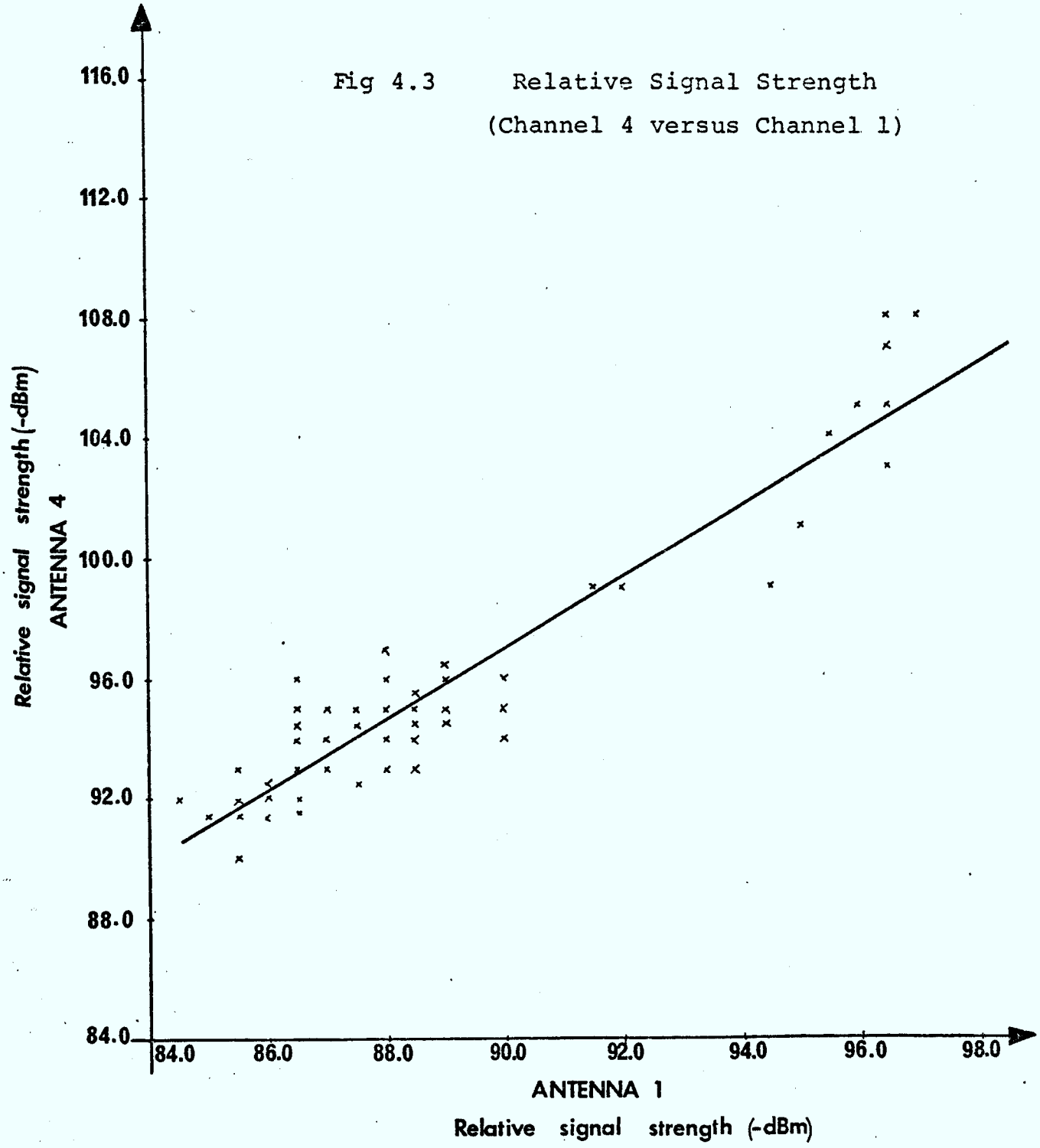

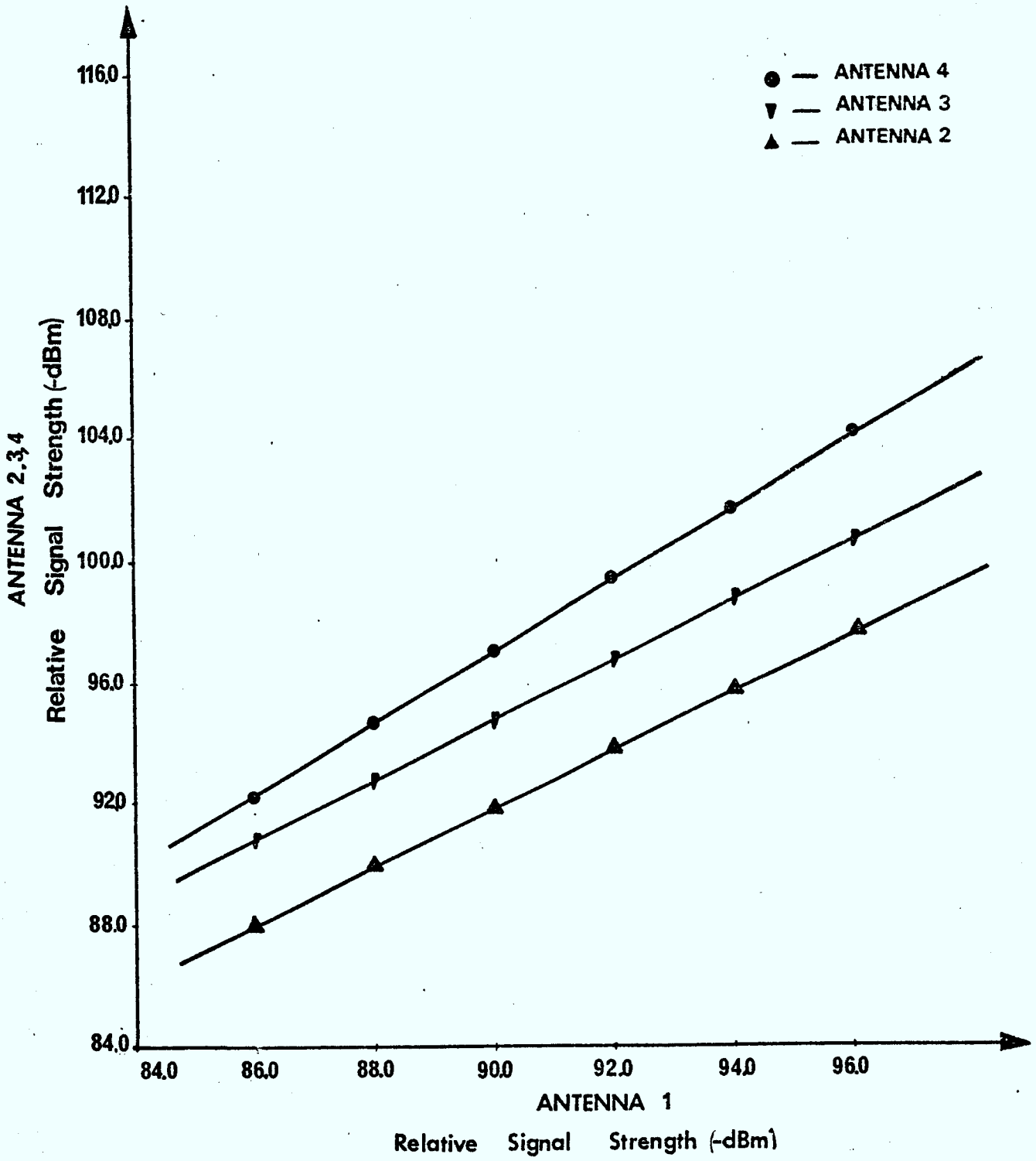

Fig 4.4 Relative Signal Strength

(Channel 2,3,4 versus Channel 1)

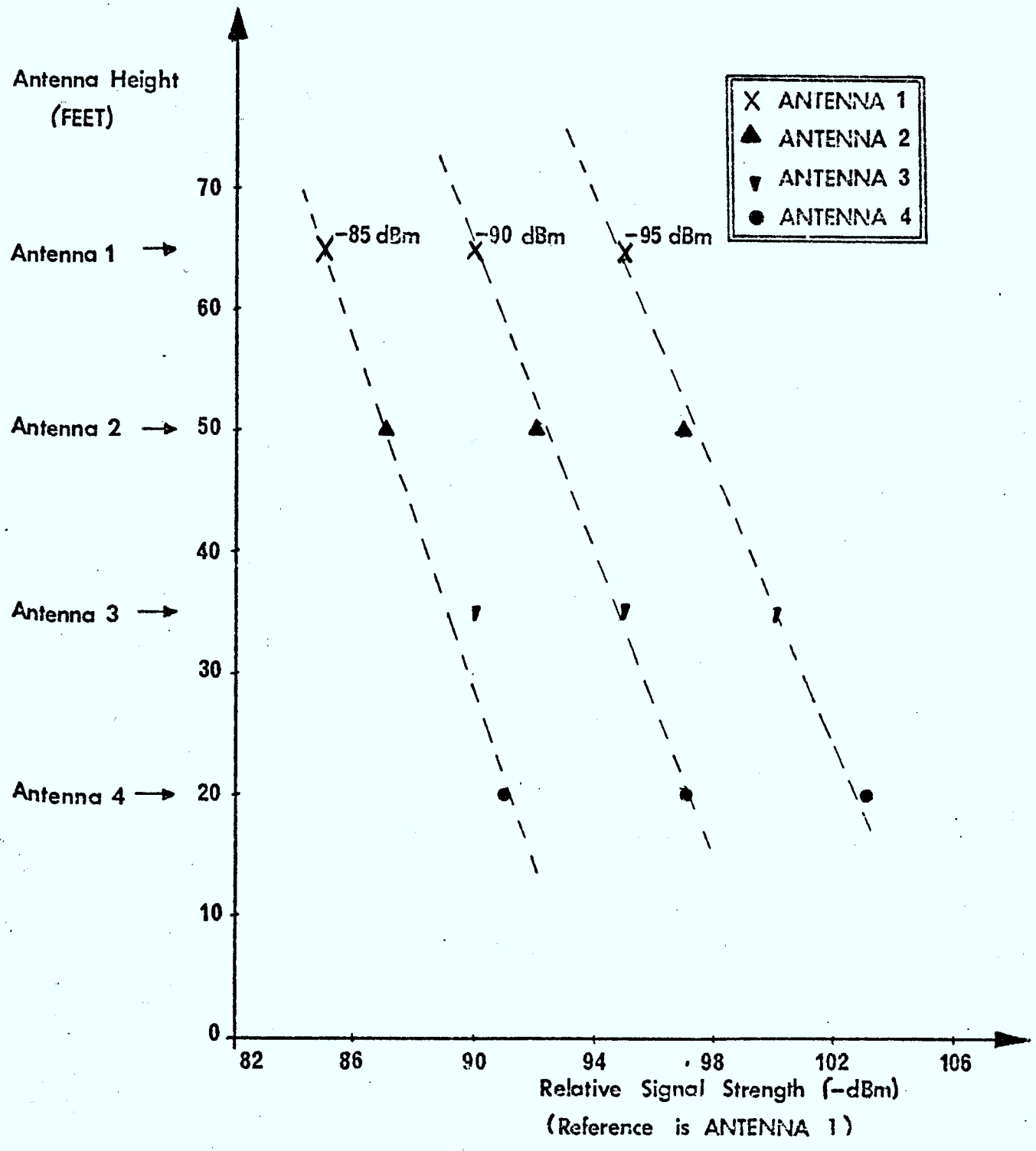

Fig. 4.5 Height Gain Measurement

(Channel 1 as reference)

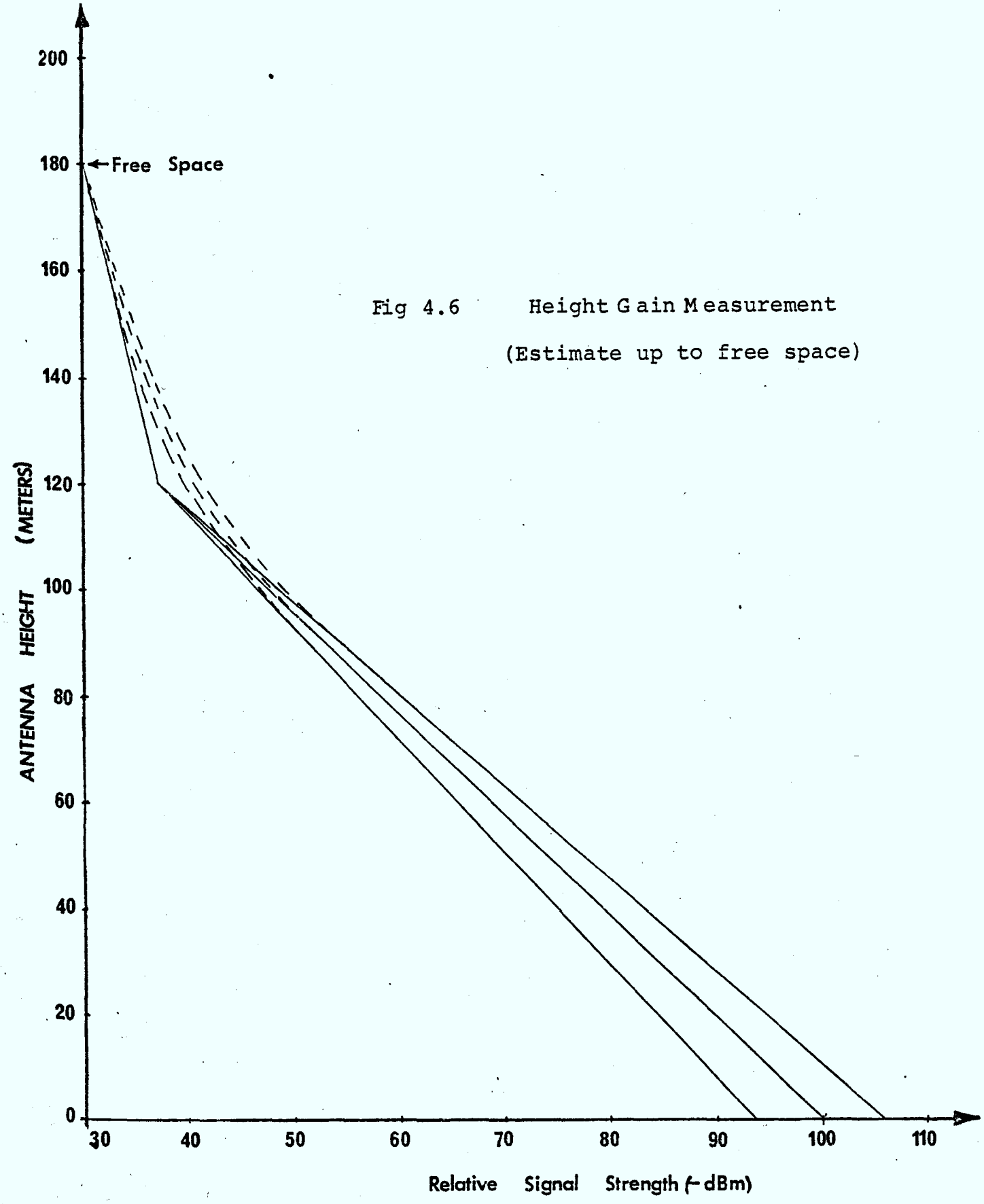

Fig 4.6 Height Gain Measurement

(Estimate up to free space)

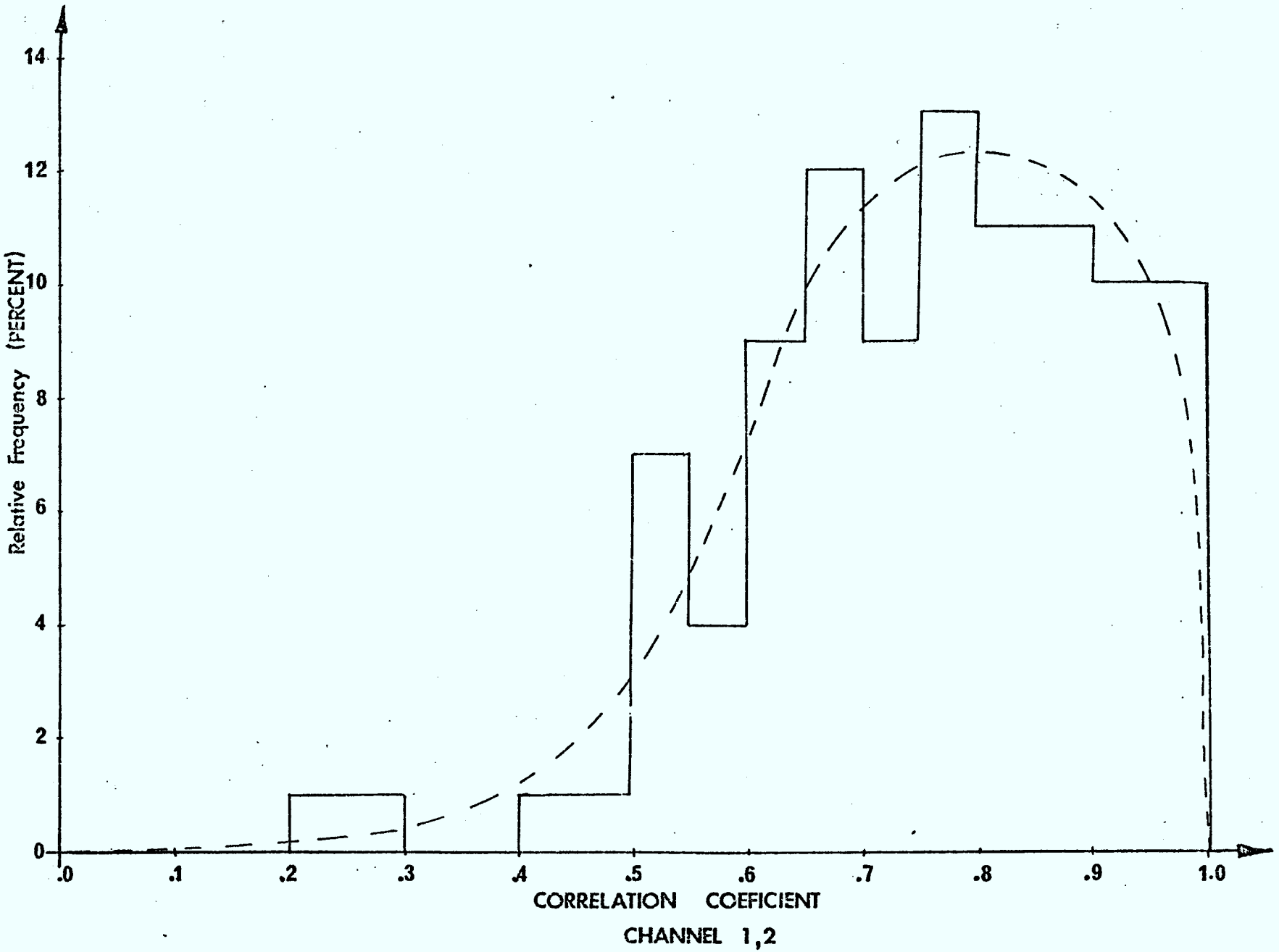

Fig. 4.7 Histogram of Correlation Coeifficient between Channel 1,2

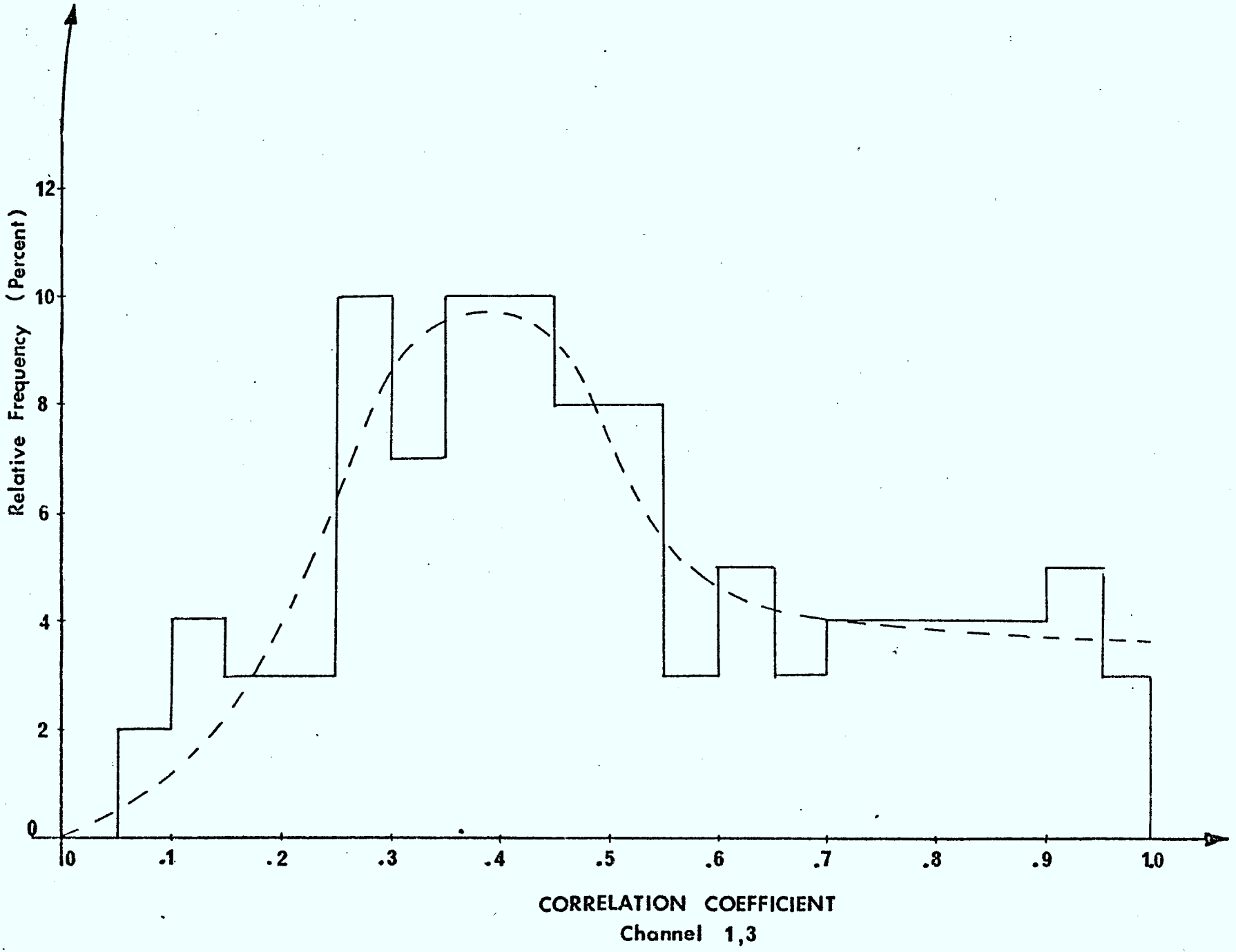

Fig 4.8 Histogram of Correlation Coefficient between Channel 1,3

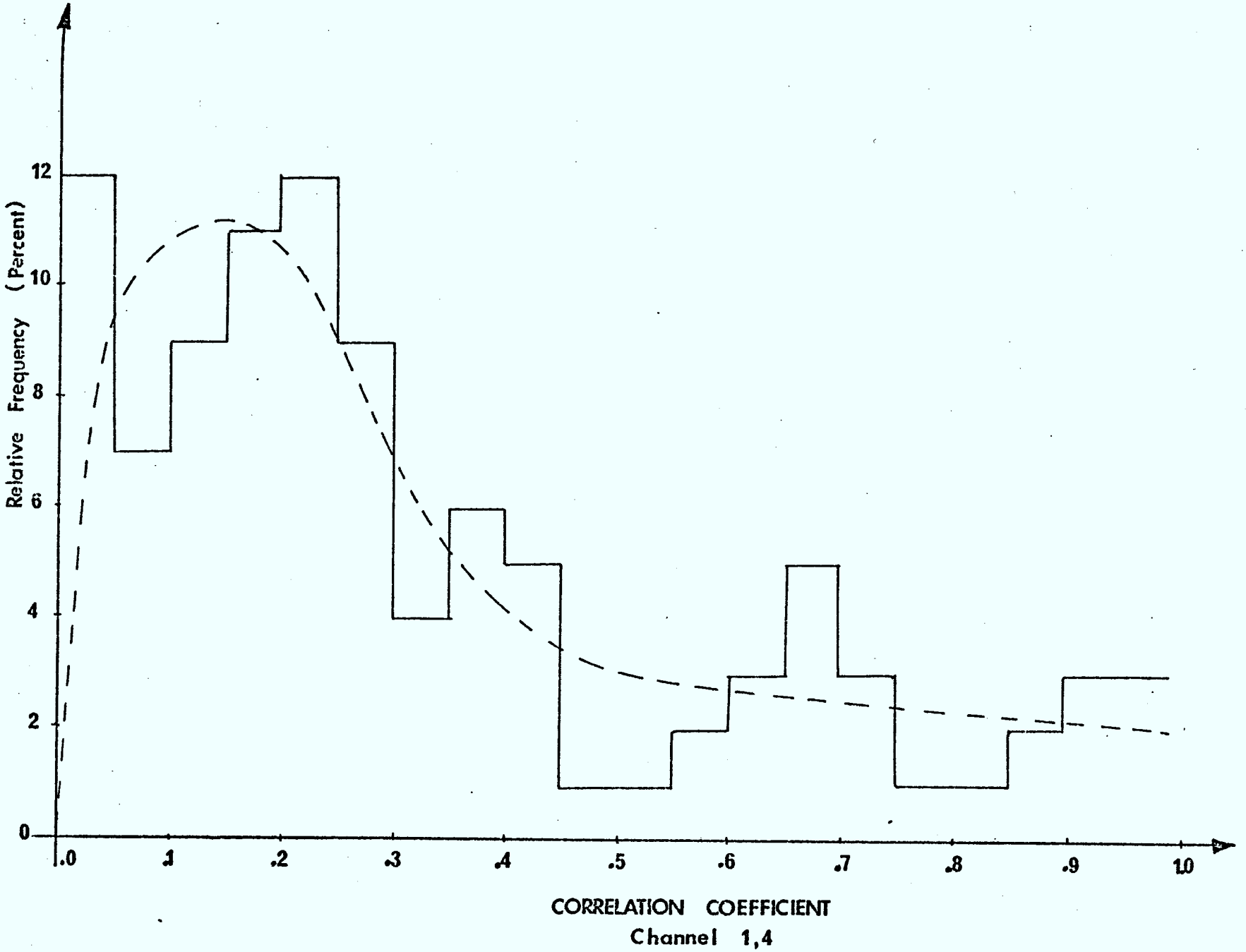

Fig. 4.9 Histogram of Correlation Coefficient between Channel 1,4

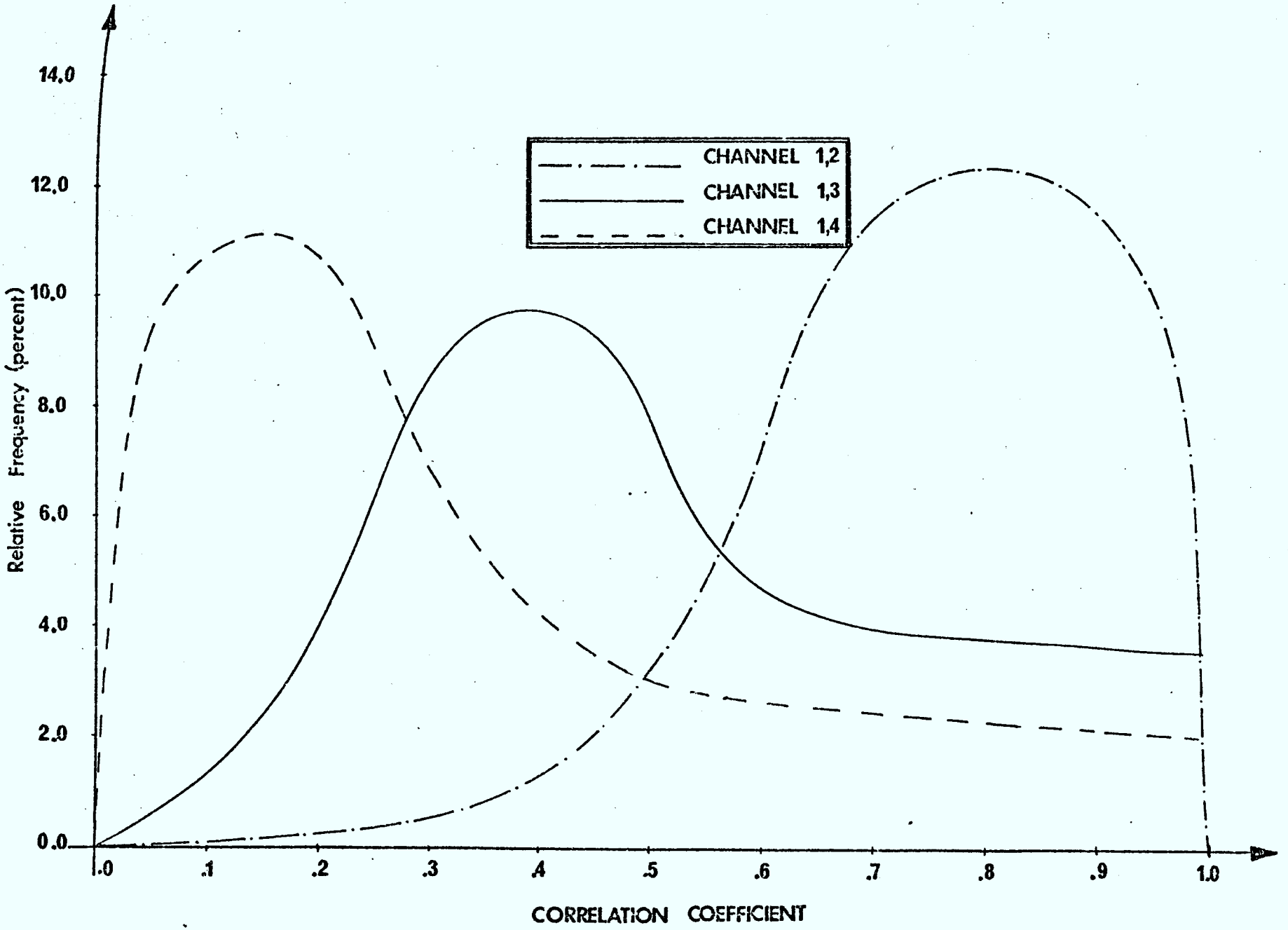

Fig 4.10 Smooth histograms of Correlation Coefficient between Channel 1,2, 1,3 and 1,4

APPENDICES.

Appendix 1.

Derivation of phase difference between the direct and reflected wave.

If a radio wave is transmitted from the transmitter T with antenna height h_t to the receiver R, with antenna height h_r separated by a distance d as shown in Figure A.1.

The phase difference between the direct and reflected path is

$$\Delta = \frac{2\pi}{\lambda}(L_1 - L_2)$$

$$= \frac{2\pi}{\lambda}\left[\left(\frac{h_t + h_r}{d}\right)^2 + 1\right]^{1/2} - \frac{2\pi d}{\lambda}\left[\left(\frac{h_t - h_r}{d}\right)^2 + 1\right]^{1/2}$$

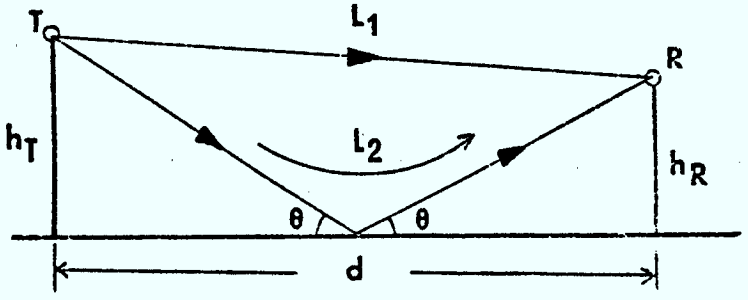

h_t - height of transmitting antenna

h_r - height of receiving antenna

d - distance between antennas

θ - angle of incidence

L_1 - line-of-sight path length between transmitting and receiving antennas

L_2 - direct and reflected path length between transmitting and receiving antennas

Fig. A.1 Geometry for Derivation of Phase Difference

Appendix 2.

Derivation of the radius of curvature of the ray path.

Consider a ray is incident upon the lower surface of a medium of refractive index n at an angle θ and refracted along the distance dh falling upon the upper surface at the angle $\theta + d\theta$ as shown in Figure A.2.

The radius of curvature p is given by:

$$p = \frac{AB}{d\theta}$$

and

$$AB = \frac{dh}{\cos(\theta+d\theta)}$$

$$= \frac{dh}{\cos\theta} \qquad \text{for } d\theta \approx 0$$

Hence

$$p = \frac{dh}{\cos\theta d\theta}$$

By Snell's Law,

$$n\sin\theta = (n+dn)\sin(\theta+d\theta)$$

Expanding the right-hand side and neglecting the second order infinitesimal, therefore;

$$n\sin\theta = n\sin\theta + n\cos\theta d\theta + \sin\theta dn$$

$$\cos\theta d\theta = -\frac{\sin\theta dn}{n}$$

and therefore;

$$p = \frac{n}{\sin\theta(-\frac{dn}{dh})}$$

For n = 1 as in the normal atmosphere, $\sin\theta = 1$ for small value of θ, therefore;

$$p = \frac{1}{-\frac{dn}{dh}}$$

$$= \frac{-1}{\frac{dn}{dh}}$$

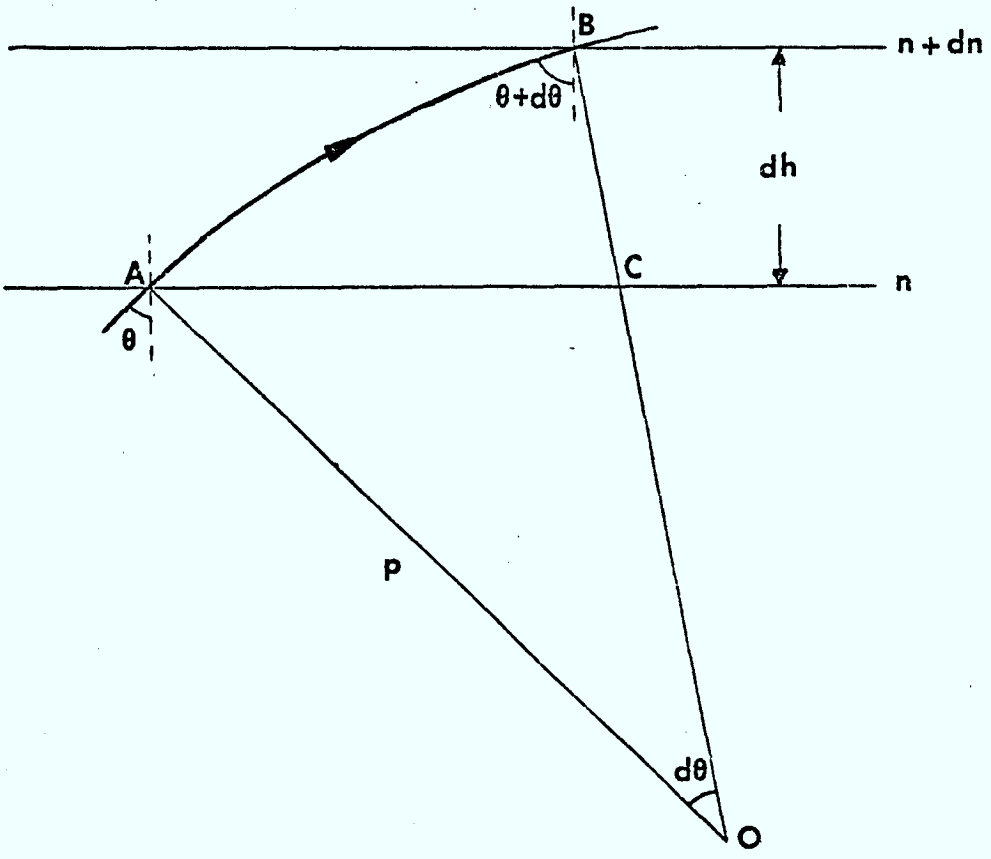

AB - ray path

n - refractive index

p - radius of curvature

θ - angle of incidence

dh - travel distance

dn - change in refractive index

Fig A.2 Geometry for Derivation of Radius of Curvature

Appendix 3.

Nomograph of signal attenuation over a smooth spherical earth.

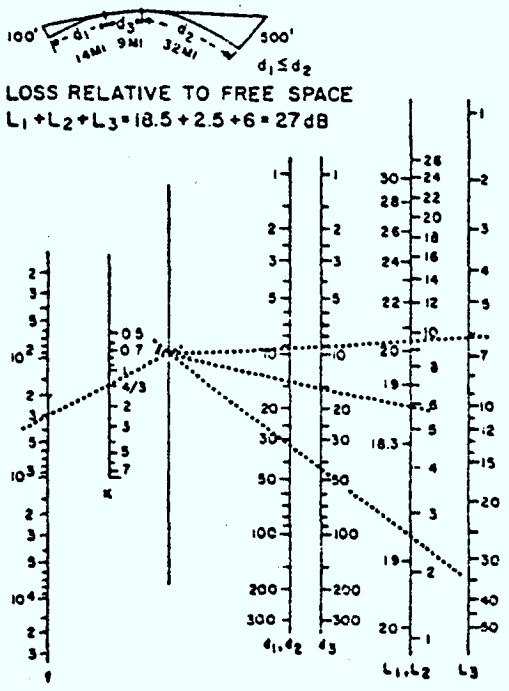

f = FREQUENCY IN MEGAHERTZ
K = RATIO OF EFFECTIVE EARTH'S RADIUS TO TRUE EARTH'S RADIUS
d = DISTANCE IN MILES
L = ATTENUATION IN dB

$$d_{1,2} = \sqrt{2\ ka\ \Delta h_{1,2}}$$

$d_{1,2}$ - are the distance to the horizon (see following page)

$\Delta h_{1,2}$ - are the antenna heights

ka - is the effective earth's radius

The derivation of $d_{1,2}$ can be shown using the Figure A.3.

From the figure,

$$ka + \Delta h_1 = \frac{ka}{Cos\theta}$$

and

$$\theta = \frac{d_1}{ka}$$

Since

$$Cos\theta = 1 - \left(\frac{\theta^2}{2!}\right) + \left(\frac{\theta^4}{4!}\right) + \cdots\cdots\cdots$$

when θ is very small, we may use only the first term, that is:

$$Cos\theta = 1 - \frac{\theta^2}{2!}$$

therefore,

$$Cos\left(\frac{d_1}{ka}\right) = 1 - \frac{1}{2}\left(\frac{d_1}{ka}\right)^2$$

and

$$\frac{ka}{Cos\left(\frac{d_1}{ka}\right)} = \frac{ka}{1 - \frac{1}{2}\left(\frac{d_1}{ka}\right)^2}$$

$$= ka + \frac{1}{2}\frac{d_1^2}{ka}$$

Since

$$ka + \Delta h_1 = \frac{ka}{Cos\theta}$$

therefore,

$$ka + \Delta h_1 = ka + \frac{1}{2}\frac{d_1^2}{ka}$$

$$\Delta h_1 = \frac{1}{2}\frac{d_1^2}{ka}$$

therefore,

$$d_1 = \sqrt{2\ ka\ \Delta h_1}$$

and similarly,

$$d_2 = \sqrt{2\ ka\ \Delta h_2}$$

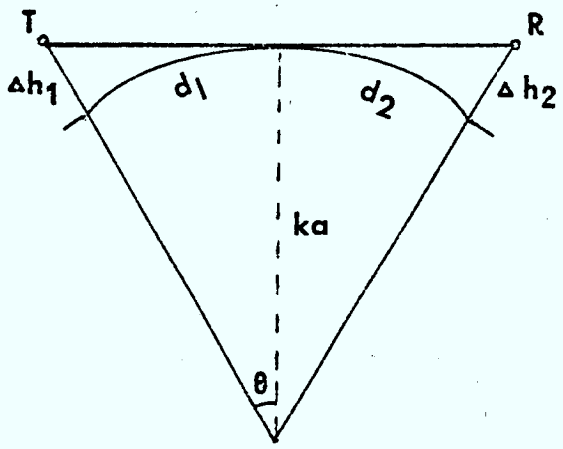

$d_{1,2}$ - are the distance to the horizon

Δh_1 - height of transmitting antenna

Δh_2 - height of receiving antenna

ka - effective earth's radius

Fig. A.3 Geometry for Derivation of Distance to Horizon

Appendix 4.

Nomograph of attenuation loss due to knife-edge-diffraction.

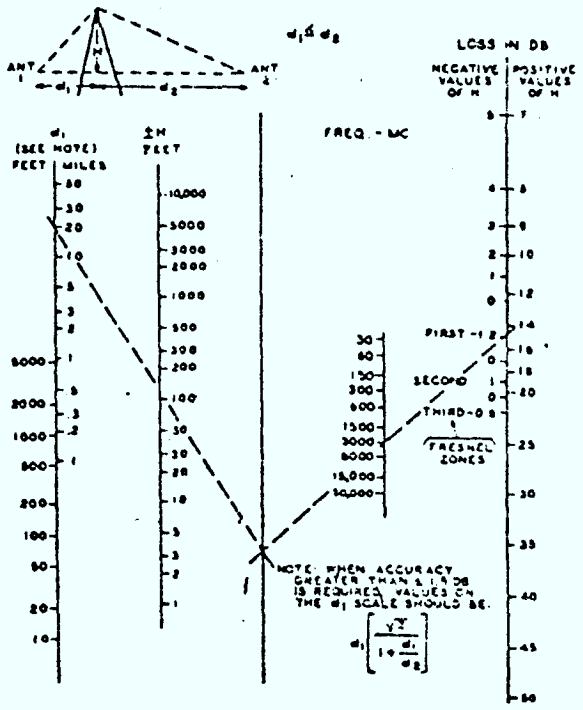

$d_{1,2}$ - are the distance to the obstruction

h - is the height of the obstruction

Appendix 5.

Specifications of the Converter.

This unit features two RF amplifiers and a mosfet mixer which together give high sensitivity and low cross-modulation characteristics.

Input frequency: 531.25 MHz

Typical gain: 30dB

Maximum noise figure: 3.8dB

IF output: 30 MHz

Power requirements: 12 volts $\pm$ 25% at 35mA

Appendix 6.

Specifications of the Receiver.

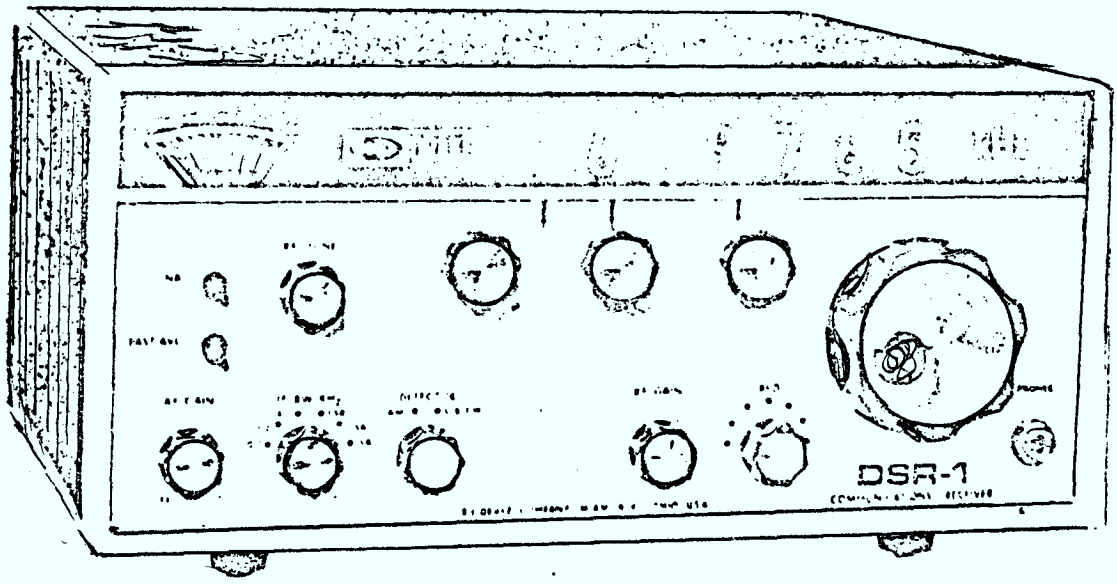

SPECIFICATIONS

Frequency Range:	10 kHz to 30 MHz continuous coverage.
Modes of Operation:	USB, LSB, CW, RTTY, AM, ISB.
Frequency Readout:	Complete to 100 Hz on six Nixie tubes.
Frequency Selection:	10 MHz, 1 MHz, 0.1 MHz steps switch selected. 0 to 0.1 MHz continuously variable.
Frequency Stability:	Frequency drift does not exceed 200 Hz in any 8 hour period at constant ambient temperature between 0° and 40°C and ± 10% variation from nominal line voltage after 1/2 hour warm up.
Sensitivity:	0.01–0.5 MHz: Less than 4 microvolts for 10 dB SINAD at 2.4 kHz SSB mode. Less than 25 microvolts for 10 dB SINAD at 6 kHz AM mode with 30% modulation. 0.5–30 MHz: Less than 0.3 microvolts for 10 dB SINAD at 2.4 kHz SSB mode. Less than 2 microvolts for 10 dB SINAD at 6 kHz AM mode with 30% modulation.
Image Rejection:	Greater than 60 dB relative to 1 microvolt below 10 MHz. Greater than 50 dB relative to 1 microvolt above 10 MHz.
IF Rejection:	Greater than 60 dB relative to 1 microvolt except in range of 4.5 to 5.5 MHz.

Appendix 7.

Specifications of the Printer.

GENERAL CHARACTERISTICS

COLUMN CAPACITY
Model 511A: 21 columns (19 data, 2 symbol)
Model 512A: 10 columns (8 data, 2 symbol)
COLUMN POSITION: Incoming data can be directed to any column position by internal cross-patching.
DECIMAL POSITION: A decimal point can be remotely programmed to print in any of the data columns.
ZERO SUPPRESSION: Automatic suppression of all non-significant zero figures to the left of a decimal point.
PRINT CHARACTERS: Refer to Table 1-2.
PRINT MODES: Automatic or Manual/Single
PRINT FORMAT
Horizontal: 7 characters per inch
Vertical: 5 lines per inch
PRINTING SPEED: Approximately 3 lines/second for black imprint plus additional 50 milliseconds for red imprint.
COLOR SELECTION: Manual or remote
RIBBON COLOR: Red/Black
RIBBON LENGTH: 19.7 feet (6 metters)
RIBBON WIDTH: 0.5 inch (13 mm)
PAPER TYPE: Fan-fold, 3½ inches wide, 5½ inches per sheet; total length 225 feet.

DATA AND SYMBOL INPUTS

FORMAT: 8-4-2-1 parallel-entry BCD
LOGIC: Positive True
LOGIC 1 LEVEL: +2.5 to +30 volts
LOGIC 0 LEVEL: +0.5 to −30 volts
INPUT IMPEDANCE: 12 Kilohms
CONNECTIONS: Refer to Tables 1-3 and 1-4

DECIMAL POINT INPUTS (J3-1 thru 19)

PRINT LEVEL: +2.5 to +30 volts
NON-PRINT LEVEL: +0.5 to −30 volts or open ckt.
INPUT IMPEDANCE: 12 Kilohms
MAXIMUM CAPACITY: 19 decimal points per single print line (Model 511A) or 8 decimal points per single print line (Model 512A).

REMOTE COLOR INPUT (J1-20)

COLOR switch must be at REM position.
RED PRINT LEVEL: +2.5 to +30 volts
BLACK PRINT LEVEL: 0.5 to −30 volts or open ckt.
INPUT IMPEDANCE: Greater than 15 Kilohms

PRINT COMMAND INPUT (J1-23 and 48)

PRINT LEVEL: +2.5 to +30 volts
QUIESCENT LEVEL: +0.5 to −30 volts
INPUT IMPEDANCE: 12 Kilohms
INPUT COUPLING: DC
WAVEFORM: Positive pulse with minimum duration of 1 millisecond risetime not critical.

INHIBIT OUTPUT (J1-22)

INHIBIT LEVEL: +5 volts
QUIESCENT LEVEL: +0.25 volt or less
OUTPUT IMPEDANCE: Less than 700 ohms
DURATION: equal to period of print cycle

+5 VOLT REFERENCE OUTPUT (J2-25)

Supplies 5 volts at any output impedance of 100 ohms for use with external circuitry

POWER REQUIREMENTS

VOLTAGE: 115 or 230 volts ±10%
FREQUENCY: 50 to 400 Hz
POWER: 16 watts maximum

TEMPERATURE RANGE

OPERATIONAL: +5°C to +40°C
STORAGE: −50°C to +55°C

PHYSICAL CHARACTERISTICS

HEIGHT: 4¼ inches
WIDTH: 7½ inches
DEPTH: 15½ inches
WEIGHT: 17 pounds (7.8 kg)

REFERENCES.

1. K. A. Norton, "The Propagation of Radio Waves Over the Surface of the Earth in the Upper Atmosphere," Part 1, Proc. IRE 24, October 1936, page 1367.

   K. A. Norton, "The Propagation of Radio Waves Over the Surface of the Earth in the Upper Atmosphere," Part 2, Proc. IRE, 25, September 1937, page 1203.

   K. A. Norton, "The Calculation of Ground Wave Field Intensity Over a Finely Conducting Spherical Earth," Proc. IRE 29, December 1941, page 63.

2. K. Bullington, "Radio Propagation at Frequencies Above 30 megacycles," Proc. IRE 35, October 1947, page 1122.
   K. Bullington, "Radio Propagation Fundamentals," Bell System Tech. J. 36, May 1957, page 593.

3. L. J. Anderson and L. G. Trolese, "Simplified Method for Computing Knife Edge Diffraction in the Shadow Region," IRE Trans. Ant. Prop., 6, July 1958, page 281.

4. W. Rae Young, Jr., "Comparison of Mobile Radio Transmission at 150, 450, 900, and 3700 MC," Bell System Tech. J. 31, November 1952, page 1068.

5. D. M. Black and D. O. Reudink, "Some Characteristics of Radio Propagation at 800 MHz in the Philadelphia Area," IEEE Trans. Veh. Tech. 21, May 1972, pp 45-51.

6. Y. Okumura, E. Ohmori, T. Kawano, and K. Fukuda, "Field Strength and its Variability in VHF and UHF Land Mobile Service," Rev. Elec. Comm. Lab., 16, September-October 1968, page 825.

7. J. H. Chisholm, W. E. Morrow, D. Nichols, J. Roche, A. Teachman, "Properties of 400 Maps Long-Distance Tropospheric Circuits," Proc. IRE, 50, December 1962, page 2464.

Appendix 8.

Specifications of the Chart Recorder.

FREQUENCY RESPONSE.	
(-3db Point)	
Full Scale	dc to 45 Hz
10 mm P-P	dc to 100 Hz
LINEARITY:	1% of full scale
SENSITIVITY:	10, 20, 50, 100, 200, 500, and 1000 mv/mm

Option 01:
Sensitivity: 1, 2, 5, 10, 20, 50, 100, 200, 500, 1000 mv/mm
Input Circuit: 1 Meg Differential
Cal: 20 mv

INPUT CIRCUIT:	Single ended, floating. — Option 01: Differential
INPUT IMPEDANCE:	100 k ohms — Option 01: 1 Meg.
STABILITY:	100 uv/°c (refer to input).
NOISE:	Less than .1mm
NUMBER OF CHANNELS:	Specified number of analog, 1 event marker, and 1 timer/event marker (driven by internal 1 second timer.) Single Channel 1 timer/event.
ANALOG CHANNEL WIDTH:	1-6 Channel: 5cm (50 divisions) | 8 Channel: 4cm (40 divisions)
LIMITING:	Electro/magnetic: approximately ½ mm beyond printed co-ordinates.
CHART SPEEDS:	Four speeds of 1, 5, 25, and 50 mm/sec. Electrically switchable from front panel, other speeds available on special order.
CALIBRATION:	200 mv internal calibration. — Option 01: 20mv
PAPER:	200 foot nominal roll (one roll supplied with recorder) See Installation Section for paper types.
POWER:	117 volts ± 10%, 60 Hz 117 or 230 volts ± 10%, 50 Hz. (Specify) See Installation Section for power requirements.

PART B

MIDPATH MONITORING AND ACOUSTIC SOUNDER STUDIES

Chapter B1.

The Port Burwell Midpath Monitoring Study (Introduction)

It was proposed that among the several activities associated with this contract would be midpoint measurements on one or more of the paths. There were several reasons for choosing the Erie path for this activity:

(1) It was the most central path among the group being studied.

(2) There were four channels (12, 24, 35, 54) which could be used. (Only Detroit had more available channels).

(3) About half the path was over water and half over land which made it an interesting path.

(4) Erie had already been chosen for the height-gain measurements.

The measurements which were made at the midpath site were acoustic sounder recordings to look for temperature inversions, etc., and monitoring of Erie channels 12 and 24. Acoustic sounding recordings began on July 9 and monitoring studies began on August 18. The midpath station was closed down on November 29.

Originally it was hoped that some comprehensive refractometer measurements would be carried out in conjunction with this study but these could not be arranged. Also it was planned to shift the midpath monitor to a second midpath but it was too late in the year before a good data sampling had been obtained from the Erie midpath.

The data on the Erie path adapted from several of the reports associated with this study are given in Appendix B1 (following). The obvious point for the midpath station may be seen to be 40-50 Km from London and close to the Lake Erie shoreline. A suitable location was found at a recording site operated by the Canada Centre for Inland Waters, atop the cliff overlooking Lake Erie. The C.C.I.W. were generous in allowing us to use their site and to put our recording equipment in their trailer. The photos on the following page show the trailer and the monitoring antennas, the acoustic sounder 'antenna' surrounded by bales of straw, (the sounder will be described in the next chapter) and the relative location of sounder and trailer. Lake Erie may be seen through a gully beyond the acoustic sounder 'antenna' in the middle photo.

A map showing the relative locations of the various stations is given in Figure B1-1. As may be seen from this map, the midpath monitoring site which was approximately 2 Km East of Port Burwell was located very closely under the paths between the Erie stations and the receiving site at the University of Western Ontario. At U.W.O. the receiving antennas were located on the roof of the Physical Sciences Building, at a height of 54 feet above ground.

The acoustic sounding equipment will be briefly described in the next chapter (chapter B2). Results of the midpath channels 12 and 24 measurements will be presented and discussed in chapter B3, and results using combined acoustic sounder and VHF/UHF monitoring records will be presented in chapter B4.

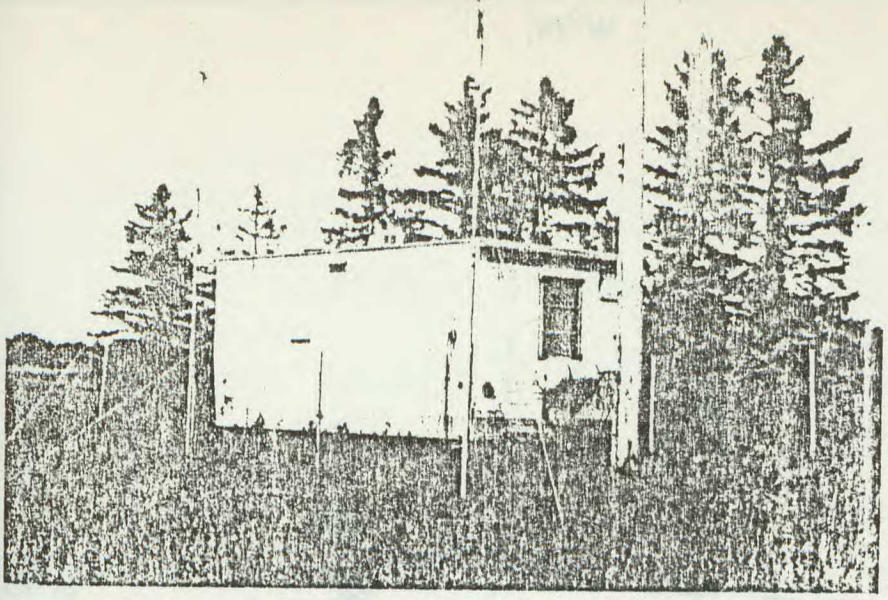

PHOTO B1-1

THE CANADA CENTRE FOR INLAND WATERS TRAILER AT PORT BURWELL WITH THE CHANNELS 12AND 24 ANTENNAS.

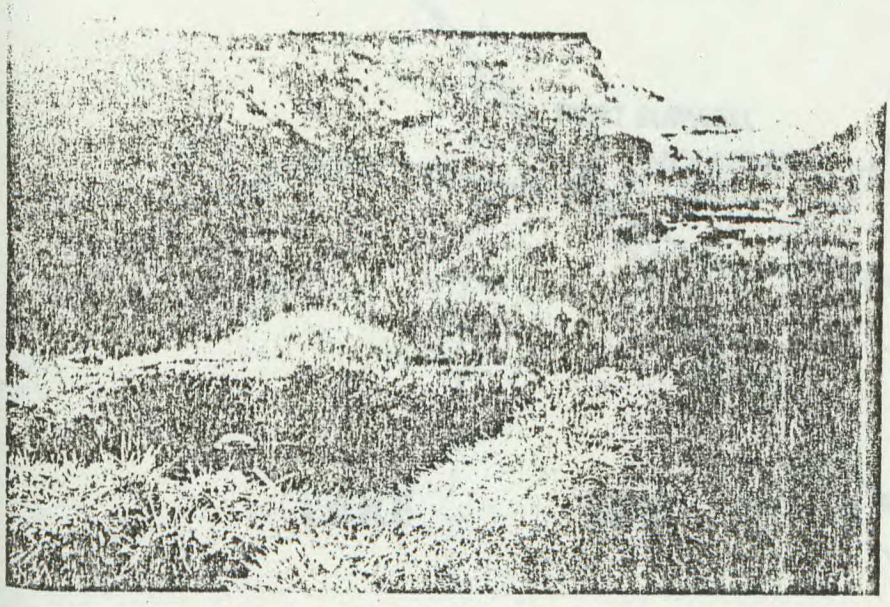

PHOTO B1-2

THE ACOUSTIC SOUNDER 'ANTENNA' SURROUNDED BY BALES OF STRAW IN THE FOREGROUND WITH LAKE ERIE IN THE BACKGROUND.

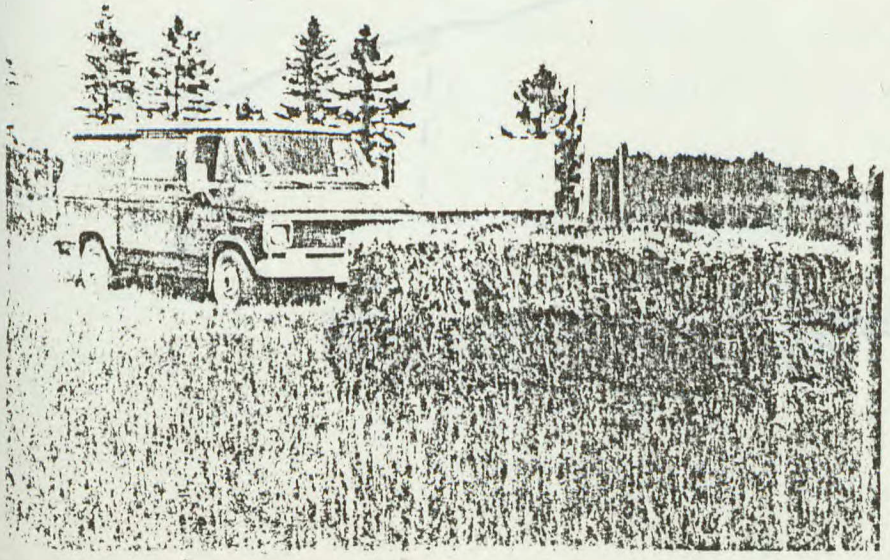

PHOTO B1-3

THE RELATIVE LOCATIONS OF ACOUSTIC SOUNDER 'ANTENNA' (FOREGROUND) AND RECORDING TRAILER.

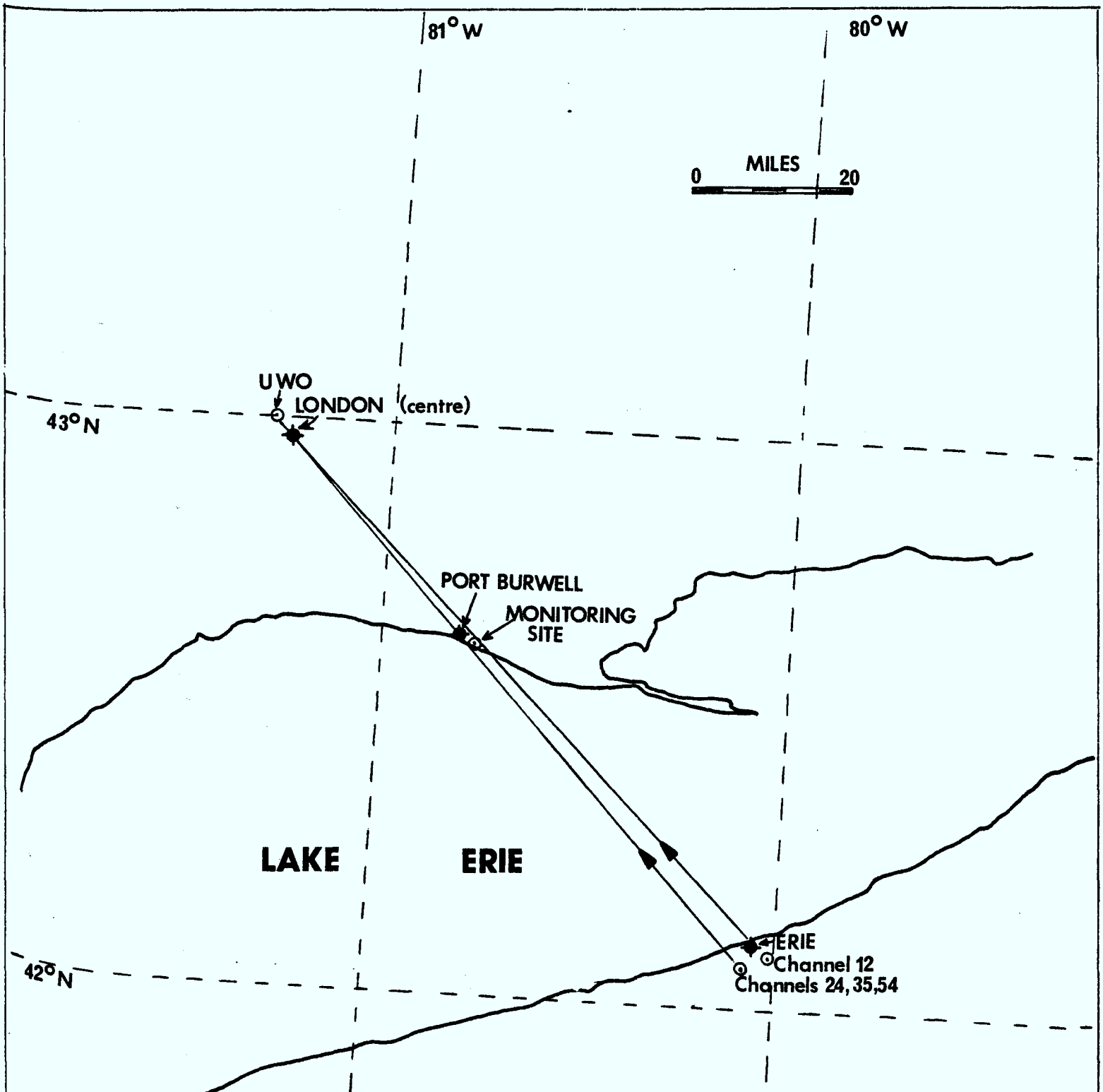

Fig. B1-1

Map Showing Location of Transmitters and Receivers for Midpath Study

APPENDIX B1.

Table B1-1. Details of the Erie channels.

Erie	Channel 24	Channel 35	Channel 54	Channel 12
Freq. Pict.Carr.	531.25	597.25	711.25	205.25
Call	WJET	WSEE	WQLN	WICU
Lat(N)	42.04	42.04	42.04	42.06
Long(W)	80.07	80.06	80.07	80.01
Bearing (deg)	136.7	136.4	136.7	134.7
Distance (Mi)	90.3	90.7	90.3	91.4
Eff. Ht (Ft)	740	960	880	1,000
Actual Ht. (Ft)	600	760	714	789
ERP	1.10 MW (0.66 MW)	2.00 MW (0.60 MW)	0.91 MW (0.22 MW)	316 KW

London monitor location : 43.00°N, 81.28°W

Port Burwell monitor location : 42.62°N, 80.78°W

The following pages give information and plots for the paths from London to Erie (copied from the 'Work Plan for VHF/UHF Propagation Measurements', March 1977, by Barrington, Palmer and McCormick).

In the following tables B1-2 and B1-3 D(Km) is the distance from the receiving site in kilometers, H,(M) is the terrain height above sea level in meters, as scaled from 1:250,000 topographic maps, and H_2(M) is the relative terrain height in meters after

correction for the earth's curvature, using the 4/3 rule. The correction is taken to be zero at the centre of the path. H_2 plus an arbitrary constant is plotted in Figures B1-2 and B1-3 for the two Erie paths. Also shown are the Port Burwell locations. The calculated positions do not quite agree with the known Port Burwell monitor position, as shown in Figure B1-2.

TABLE B1-2

LONDON

TO

WQLN, WSEE, WJET (Erie channels 54, 24, 35)

D(KM)	H_1(M)	H_2(M)	D(KM)	H_1(M)	H_2(M)	D(KM)	H_1(M)	H_2(M)
0.0	244	-67	26.2	259	132	134.2	174	-48
2.6	244	-45	27.6	244	124	134.4	183	-41
3.5	244	-38	28.0	244	126	134.5	198	-27
4.2	244	-32	34.4	229	147	135.2	214	-16
5.8	259	-4	35.8	229	149	136.9	229	-13
6.7	275	19	36.4	229	151	138.3	244	-9
7.2	275	23	40.0	229	166	138.5	259	4
8.0	275	29	47.2	214	176	138.9	275	17
8.8	275	35	53.0	198	175	139.4	290	28
13.4	275	68	53.2	183	161	140.2	290	22
15.2	275	81	53.4	174	152	140.8	290	17
18.4	259	86	60.0	174	165	141.5	290	12
20.2	244	82	70.0	174	174	142.2	305	21
20.6	244	84	80.0	174	171	142.7	336	48
22.0	259	108	90.0	174	156	143.0	351	60
24.6	259	123	100.0	174	130	143.5	366	71
25.0	244	110	110.0	174	92	144.0	381	82
25.4	244	112	120.0	174	42	145.0	397	90
25.8	259	130	130.0	174	-19	145.4	412	101

Antennas

0.0	275	-36	London
145.3	614	303	WQLN (Channel 54)
145.3	583	272	WJET (Channel 24)
145.9	641	330	WSEE (Channel 35)

FIGURE B1-2

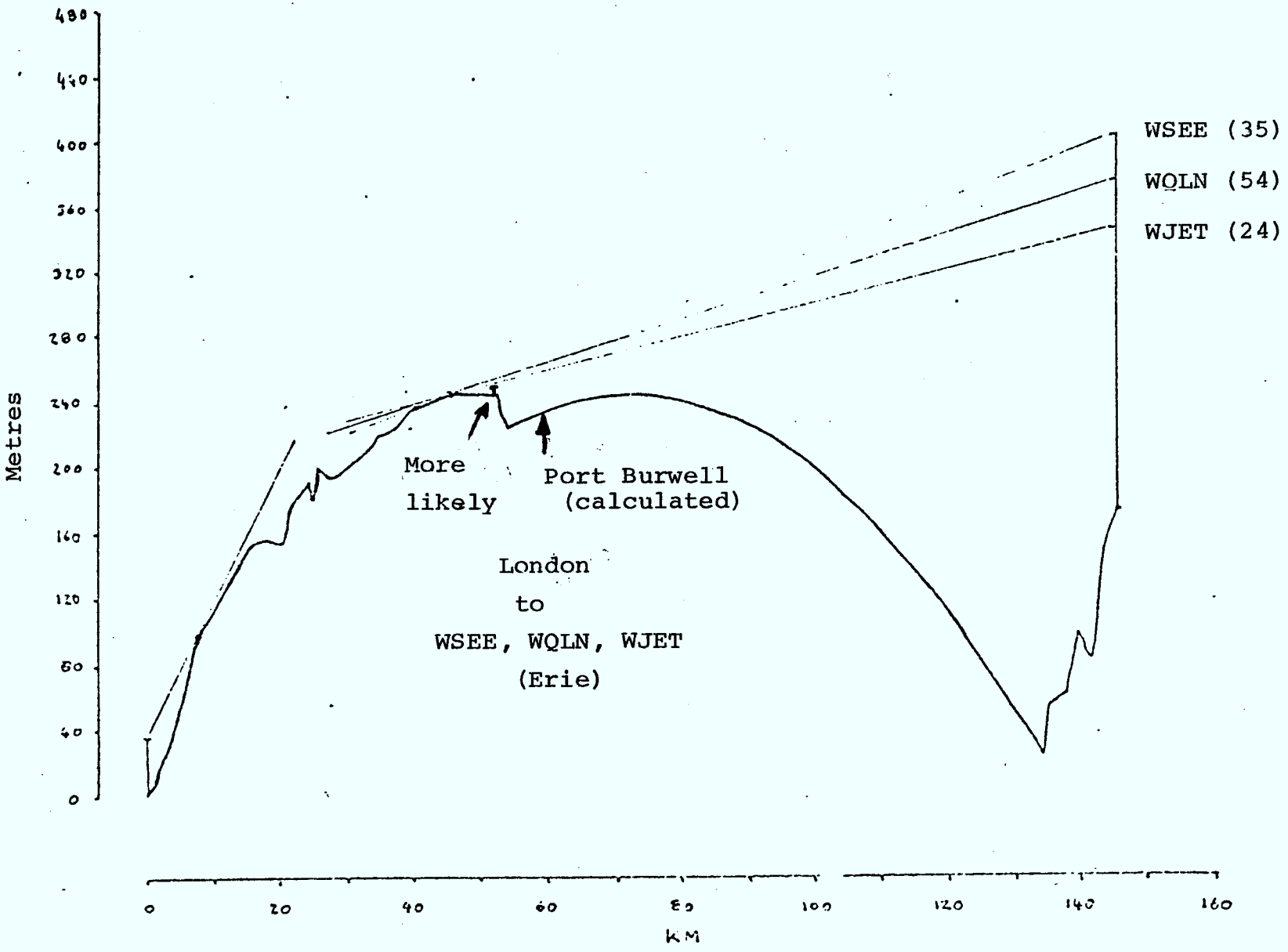
Metres
480
440
400
360
320
280
240
200
160
120
80
40
0
0
20
40
60
80
100
120
140
160
KM
WSEE (35)
WQLN (54)
WJET (24)
More likely
Port Burwell (calculated)
London
to
WSEE, WQLN, WJET
(Erie)

TABLE B1-3

LONDON

to

WICU (Erie channel 12)

D(KM)	H_1(M)	H_2(M)	D(KM)	H_1(M)	H_2(M)	D(KM)	H_1(M)	H_2(M)
0.0	244	-76	27.4	244	117	134.6	214	-3
2.6	244	-54	33.6	229	134	136.6	229	-3
3.5	244	-47	33.9	229	135	137.5	244	5
4.3	244	-40	35.1	229	141	137.8	259	18
5.8	244	-28	36.7	229	148	138.4	275	30
6.8	244	-20	40.1	229	162	139.2	290	38
7.3	244	-16	45.4	214	167	139.8	290	34
7.8	275	19	45.8	214	168	140.4	290	29
8.8	275	26	47.4	214	173	140.6	290	28
13.1	275	58	52.0	198	170	141.0	305	39
15.2	275	73	60	174	163	141.3	305	37
17.3	259	71	70	174	173	142.6	351	73
20.5	244	77	80	174	172	143.8	366	78
21.1	244	81	90	174	159	144.1	381	90
22.1	259	102	100	174	134	145.0	381	83
22.8	259	106	110	174	97	146.5	381	70
23.1	259	108	120	174	48	147.2	381	64
24.8	259	118	130	174	-12	147.6	381	61
25.4	244	106	134.2	183	-32	147.6	420	100
26.6	244	113	134.4	198	-18			

Antennas

0.0	275	-45	London
147.1	420	100	WICU

FIGURE B1-3

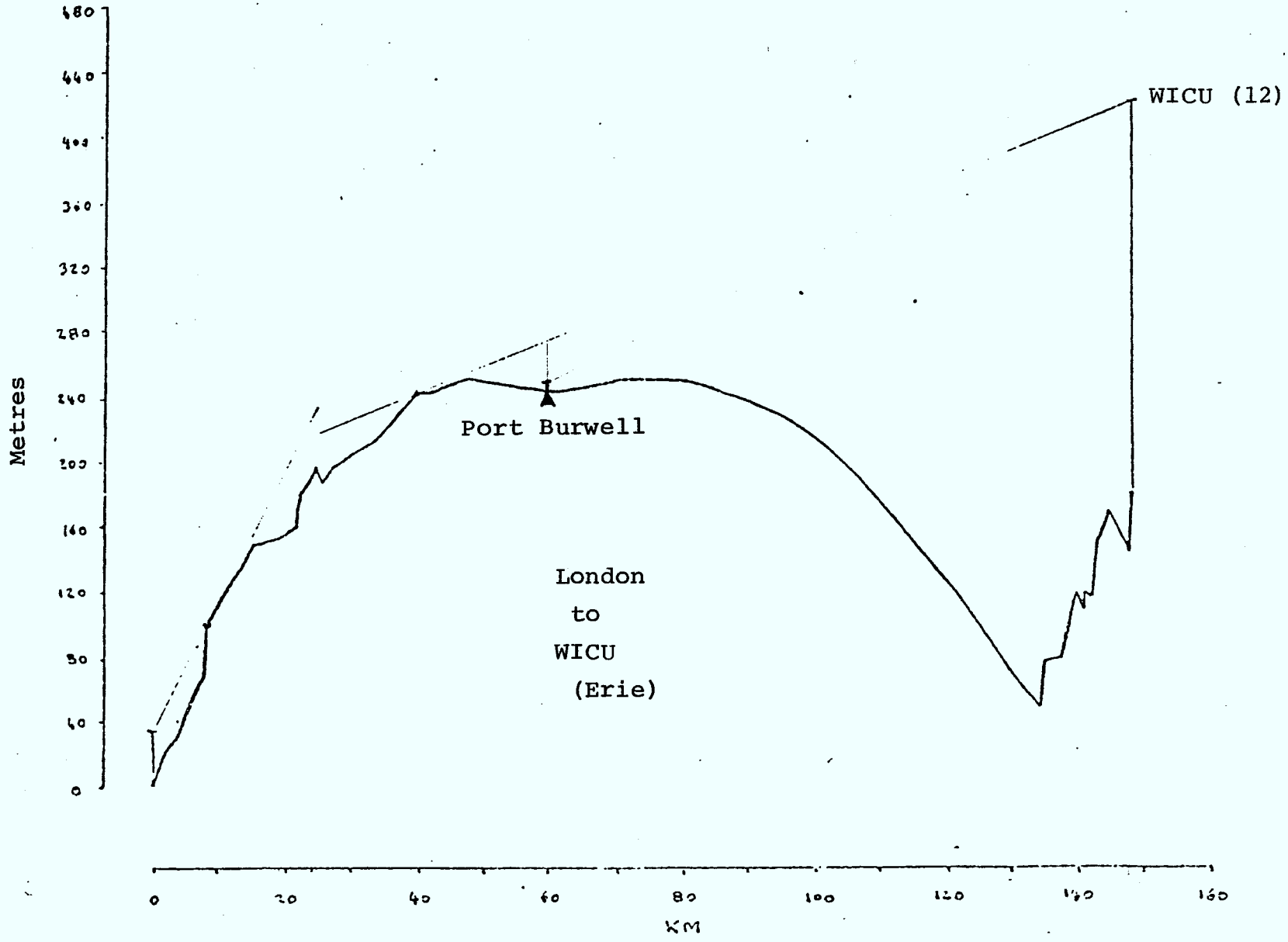
480
440
400
360
320
280
240
200
160
120
80
40
0
Metres
WICU (12)
Port Burwell
London
to
WICU
(Erie)
0
20
40
60
80
100
120
140
160
KM

Chapter B-2

ACOUSTIC RADAR EXPERIMENT

The acoustic radar used in this experiment is a device developed and manufactured by the Communications Research Centre. It consists of three parts:

1.) a parabolic disk with a driver

2.) preamplifier

3.) power amplifier and the signal processing electronics

During the experiment, the disk antenna and the preamplifier have been located about 30m from the trailer which was used to shelter the electronics. A photograph of the experimental site is enclosed (Fig. B1-1, B1-2, B1-3).

The antenna has been equipped with a straw cuff (see Fig. B1-2, B1-3) as suggested by Strand (1971). The purpose of the cuff is to decrease the formation of sidelobes. The radiation pattern of the antenna-cuff combination is similar to the one described by Hall; the half power beam width is expected to be narrower than 10°.

The acoustic radar has been operated with about 30W of electrical power available at the terminals of the acoustic driver. The carrier frequency was 2 KHz, and the pulse duration 100ms. The repetition rate was 90s. The receiver was adjusted to the range of 500m. (about 3s per one recorder sweep.) The analogue multiplier ramp waveform used for the linear programming of the receiver to achieve the range correction was adjusted to about $k=0.2s^{-1}$. This setting results in the increase of the gain of the receiver which can be described by the linear relation.

$$G = k.t$$

It was found that a steeper increase of gain resulted in the overload of the receiver at the end of the three-second receiving period.

A facsimile recorder was used for the display of the results. No attempt was made to acquire any other record of the acoustic radar data.

$$P_r = P_t\, \sigma(\theta) \frac{c\,\delta}{2} \frac{A}{\ell^2}\, \tau^2 G$$

where P_r and P_t are the transmitted and received power, respectively, $\sigma(\theta)$ is the scattering function, δ duration of the acoustic pulse and A is the collecting area of the antenna. The distance between the scattering volume and the antenna is ℓ, τ is the transmission of the atmosphere, and G the antenna gain.

The usual assumption is to consider that the atmosphere generates the Kolmogorov spectrum of turbulence. The scattering function then becomes

$$\sigma(\theta) = 0.055\lambda^{1/3}\cos^2\theta\left[\frac{C_v^2}{c}\cos^2\frac{\theta}{2} + 0.13\frac{C_r^2}{T^2}\right] \quad (\sin\frac{\theta}{2})^{-11/3}$$

The velocity structure parameter C_v^2 and the temperature structure parameter Cr^2 do not depend on the direction of the velocity or the temperature gradient.

$$C_v^2 = \left\langle \left[\frac{u(x) - u(x+r)}{r^{1/3}}\right]^2 \right\rangle$$

$$C_r^2 = \left\langle \left[\frac{T(x) - T(x+r)}{r^{1/3}}\right]^2 \right\rangle$$

Here, the wind speed is u at point x and r is measured along the x axis. The direct backscatter ($\theta=\pi$) depends only on temperature term.

The reflection from uniform temperature gradients of a stable atmosphere is of the specular type. The reflectivity in this case can be calculated as

$$R = \frac{T_1 + T_2 - 2\sqrt{T_1 T_2}}{4T_0}$$

Temperature T_0 is the reference temperature for unity index of refraction. The above expression is valid for an abrupt change of absolute temperature from T_1 to T_2 in a distance smaller than the acoustic wavelength.

One can therefore conclude for a monostatic system:

- only temperature fluctuations contribute to backscatter.
- uniform temperature gradients contribute to the detected signal.

CONVECTIVE PLUMES

The thermal plume structure is typical for the unstable atmosphere. It can be seen in Fig. B4-9. The thermal plume structure indicates the rise of heated and thermally nonuniform air parcels from the ground due to surface heating from solar radiation. The facsimile record shows the vertical structure of the convective plumes. Unstable atmospheric conditions and the formation of plumes is usual from 9a.m. till late afternoon.

TEMPERATURE INVERSIONS

When thermal radiation from the earth surface cools the earth surface sufficiently, cold layer of air forms just above the solid surface. This is typical at night. The depth of this cold layer increases progressively after sunset. A typical facsimile presentation of this situation can be seen on Fig.B4-11.

The last of the convective plumes disappear usually about 5p.m. and the formation of the temperature inversion becomes detectable.

A second type of temperature inversion is caused by large scale downward motion called subsidence in the troposphere. The fast descent of air causes adiabatic heating. At the time the subsidence reaches the range of our instrument (500m), the temperature of the descending layer is greater than the temperature of the cold air trapped underneath.

OTHER PHENOMENA

The facsimile records provide a wealth of information about a number of meteorological conditions. One can detect precipitation (Fig.B4-6). It is also possible to estimate wind direction from the records. On virtually all of the charts, one can detect topographic reflections, which show as darker areas near the origin of the vertical scale. From the intensity of these reflections one can estimate the wind direction and velocity.

STRAND,O.N. (1971): Numerical study of the gain pattern of a shielded acoustic antenna, J.Acoust. Soc. Am. 49 1698-1703.

HALL JR.,F.F. (1972): Temperature and wind structure studies by acoustic echo-sounding, Remote Sensing of the Troposphere, edit.V.E.Derr,U.S. Government Printing Office, 18-2-18-25.

LITTLE,C.G. (1969): Acoustic Methods for remote probing of the lower atmosphere, Proc. IEEE 57 , 571-578.

Chapter B3.

The Port Burwell Midpath Monitoring Study.

Erie channels 12 and 24 were monitored at Port Burwell from 18 August to 29 November, 1978. The receiving antenna on channel 12 was a Jerrold J105-12 with a stated gain of 10.5dB. The antenna on channel 24 was a Delhi 'super para 5' with a stated gain of about 18 dB (although measured gains at C.R.C. were about 10 dB for this antenna). Both antennas were at a height of 20 ft. above ground and may be seen in photo B1-1.

As may be seen in Figure B1-2 and B1-3, the Port Burwell location is in the 'line-of-sight' region for both Erie stations. (These figures use the standard 4/3 rule for earth curvature and thus show ray paths as straight lines).

The Port Burwell monitoring study was therefore essentially a very different study from the monitoring at London since:

(a) London is beyond line-of-sight whereas Port Burwell is line-of-sight for the Erie stations.

(b) The signals received at London will be very much affected by atmospheric ducting, trapping, guiding, etc, whereas the important parameters at Port Burwell will probably be interference between direct and reflected ray paths.

(c) The Erie to Port Burwell path was almost entirely over water whereas a study of Figures B1-2 and B1-3 indicates that probably the critical regions for the Erie-London path are over land.

For the above reasons correlation of interesting activity at the London monitor and the Port Burwell monitor was not expected. This was borne out by the results of the experiment since, of the intervals which were chosen as being of interest for detailed study at each monitor, only one interval was common to both. This interval was November 10-11 and is discussed later in this chapter and in chapter B4.

Both channels 12 and 24 antennas at Port Burwell had a clear view over Lake Erie to the Erie transmitters (see the photos in chapter B1). It was therefore expected that rather interesting and strong fluctuation effects would be seen on the records due to interference between the ray reflected from the lake surface and the direct ray. In general this was not observed. The usual records were monotonously flat. In the entire three month monitoring study there were only about twenty intervals, each usually of a few hours duration, when significant variations of signal strength were observed. Two of these intervals will be discussed later.

The initial question in interpreting the results was whether one could normally consider the lake surface as giving a specular reflection or whether even small waves would degrade this component. There are a large number of studies of this problem (see for instance Fessenden (1974) and references therein). Somehow, none of the references consulted give a very clear answer to this question. It was shown both theoretically and experimentally that a perfectly smooth lake will give an almost perfect specular reflection (Kerr, 1951, pp 403 and 423, 427). Lake Erie is seldom perfectly smooth.

The Rayleigh criteria for a surface to be considered smooth (Kerr, 1951, p.411) is $h\sin\psi < \lambda/8$ where h is the peak-to-peak height of the perturbations of the surface, ψ is the grazing angle and λ is the wavelength being used. For the geometry of this experiment ψ is of the order of .04° and λ is of the order of 1m. Therefore in order to be not smooth the surface perturbations would have to have a peak-to-peak amplitude greater than 177 meters! If however there are waves on the lake of wavelength comparable to the radio wavelength, as would very often be the case here, this conclusion that the lake is always smooth is no longer altogether valid and a more complex analysis, such as Fessenden (1974) would be needed. For an idealized case of sinusoidal water waves, amplitude fluctuations of the received signal should be seen associated with the propagation of the water wave pattern. Since this was not observed in this experiment it is concluded that the sinusoidal model is not very useful for small grazing angles and an extended lake surface. This is as expected because an extended set of water waves while having a relatively constant wavelength does not maintain the necessary phase coherency to fit well to a sinusoidal model. The sinusoidal model applied to small waves of the lake surface does indicate however that there will be some scattering of radio waves from the lake waves if the wavelengths are comparable. Therefore it is concluded that there should be a specularly reflected ray from the Lake Erie surface but on rough days this ray may be somewhat weaker.

The received signal strength for the combination of a direct ray and a specularly reflected ray is given by (Bolgiano, 1968)

$$E = 2E_o \left| \sin \left(\frac{2\pi h_T h_R}{\lambda d}\right) \right| , \qquad \text{(Equation B1)}$$

where E_o is the free space amplitude, h_T and h_R are the effective transmitting and receiving antenna heights and d is the effective distance between receiver and transmitter. For the geometry in this experiment h_T and h_R are obtained by drawing in the tangent plane for the reflected ray in Figure B1-2 and measuring the antenna heights above this plane. The sine term in the above equation (B1) has a magnitude 0.14 for channel 24 and 0.11 for channel 12 for Erie-Port Burwell. These small magnitudes are due to the direct ray and the reflected ray, which has undergone a 180° phase change at reflection, almost cancelling one another. The grazing angle is so small (see above) that the path lengths for the direct and reflected rays are almost exactly the same. This result assumes that the reflection coefficient is exactly -1 and that the reflecting surface is a plane.

This result also assumes that the direct ray is propagating clearly through free space. In the present geometry the direct ray travels only a few tens of meters above the lake surface (see Figure B1-2) and since the Fresnel zone size $\sqrt{\lambda d}$ is here of the order of a few hundred meters, the ray is clearly not travelling through free space for most of its path. This is even more true of the ray path close to the receivers when the path is parallel for a short distance (about 200 meters) to the flat 'plateau' above the lake cliffs. Therefore to perform a meaningful computation of the

theoretical signal strength to compare with observed values it would be necessary to use a much more complex model. It is hoped that some of this modeling may be done in the future.

In the present analysis therefore there are no meaningful theoretical values with which to compare the received signal strengths. The crude estimate using formula B1 for the signal strengths gave about -42 dbm for both channels 12 and 24. The transmitter antenna gain and fraction of total transmitter power in the receiver bandwidth were jointly taken at 0dB in this estimate. Figure B3-1 indicates that at least the correct order of magnitude has been obtained.

Average signal strengths in the various months are shown in Figure B3-1. Two phenomena are of interest here:

(1) The average signal strength received varied in a systematic way, increasing by about 15dB (!) from August to November on channel 24 but by only about 4½dB on channel 12.

(2) The form of daily variation on both channels changes from being a pronounced enhancement during daytime in August to being a slight depression during daytime during September-October. The November diurnal variation is insignificant. The daily variation is more pronounced on channel 24 than it is on channel 12.

It is assumed that the explanation of these two phenomena has to do with changes in the refractivity profile. A change in the refractivity profile which would increase the clearance between the direct ray and the lake surface might be expected to cause a significant increase in the received signal strength.

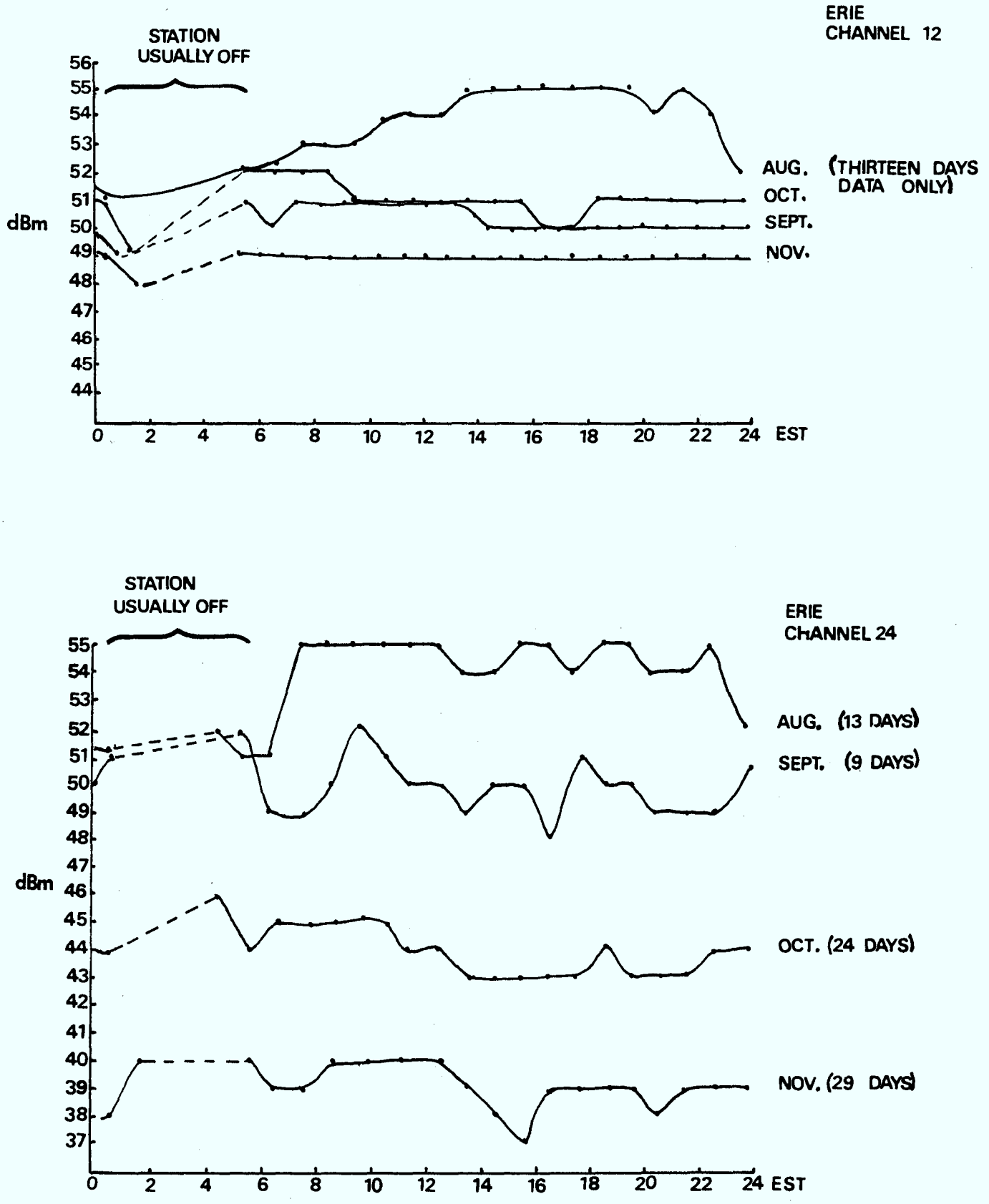

FIG. B3-1 RELATIVE SIGNAL STRENGTHS RECORDED AT PORT BURWELL MIDPATH STATION

The important parameter in the refractivity profile is

$$\frac{dN}{dZ} \simeq -.33\frac{P}{H} - 1.4\frac{dT}{dZ} + 8.2\frac{dq}{dz} \qquad \text{(Equation B2)}$$

where Z is the height in meters, N is called the 'refractivity'=10^6x (index of refraction -1), P is the atmospheric pressure in millibars, H is the scale height of the atmosphere in meters, T is the temperature in °K, and q is the water vapour mixing ratio in g/Kg. The upward curvature of the ray (away from the earth) is $10^6 dN/dZ$.

The 'normal' atmospheric conditions are dT/dZ = -6.5°C/Km and dq/dz + -1g/Kgm (see Bolgiano, 1968) giving $dN/dZ \sim -.04m^{-1}$. To obtain the increased clearance between the ray and the lake it is required to make dN/dZ more -ve. This can obviously be achieved by (from Equation B2), (a) increasing P (b) decreasing H (c) increasing (making more positive) dT/dZ (d) decreasing (making more -ve) dq/dz. These separate possibilities will now be discussed.

(a) Increasing the pressure P. The maximum changes in pressure were only about 1½% during this study and there was no seasonal variation of average pressure. Therefore pressure variations obviously play a negligible role here.

(b) Decreasing the scale height H. Since H=KT/mg (K is Boltzmann's constant, m is the molecular mass and g is the acceleration due to gravity). Since T is the only variable here, $d(\frac{1}{H})=\frac{-1}{H}\frac{dT}{T}$. The percentage variation then in $d(\frac{1}{H})/\frac{1}{H} = \frac{-dT}{T}$ is of the order of 7% which would cause approximately a change in $\frac{dN}{dZ}$ of -.02 between August and November. There will also be smaller but

significant daily variations due to the temperature effect. In general, better propagation would be expected at night when the temperature is cooler.

(c) Making dT/dZ more positive. As mentioned above, the average lapse rate is taken to be -6.5°C per Km. Dry air will normally have about twice the lapse rate of moist air. (This would represent a change of dN/dT of about $.01m^{-1}$). Therefore moist air over the lake might be expected to give improved propagation. A measured temperature profile is necessary to accurately evaluate the effects of dT/dZ.

(d) Decreasing dq/dz. The mixing ration q also varies with height in an irregular manner, which requires measurement. Only approximate predictions can be made from ground based data. In general, one might expect that over the lake dq/dz would be higher than normal (more moisture near the lake surface). This would give poorer propagation over the lake. The variations in dN/dT caused by the parameter are also of the order of .01 m^{-1}.

It is thus seen that the variations in refractivity due to changes in T and due to changes in dT/dZ plus dq/dz are approximately of the same order of magnitude.

In Figure B3-2 observed midday values of Erie 24 signal strength are shown along with the temperatures at London. The trend of the two curves is similar, presumably showing the effects of T on the propagation. The details of the two curves do not agree however. Therefore on any given day the form of the temperature and humidity profiles

ERIE 24

B3 - 2

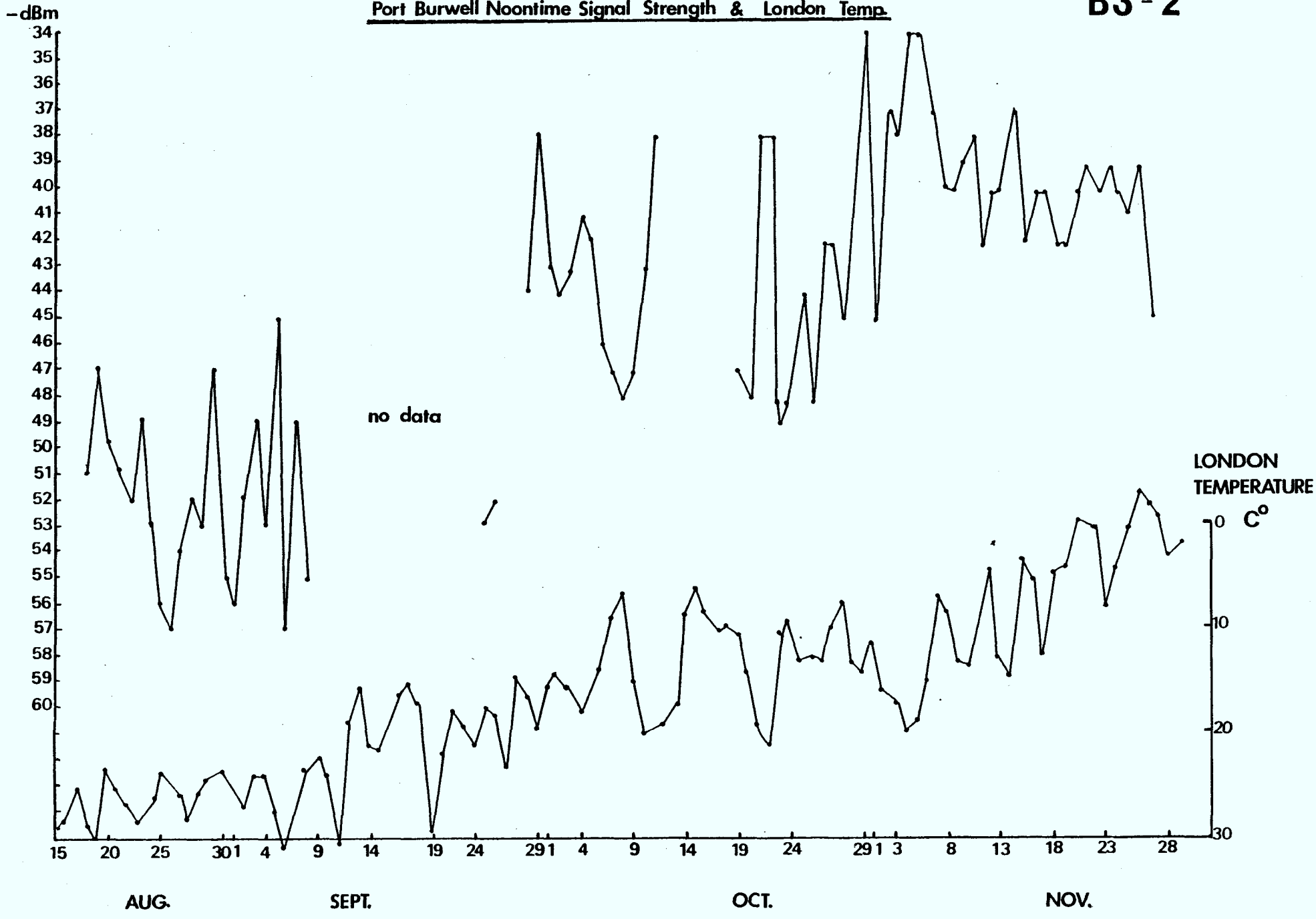
Port Burwell Noontime Signal Strength & London Temp.
-dBm
34
35
36
37
38
39
40
41
42
43
44
45
46
47
48
49
50
51
52
53
54
55
56
57
58
59
60
no data
LONDON
TEMPERATURE
C°
0
10
20
30
15
20
25
30
1
4
9
14
19
24
29
1
4
9
14
19
24
29
1
3
8
13
18
23
28
AUG.
SEPT.
OCT.
NOV.

would need to be known in order to do a more exact analysis. It is speculated that the form of day-night variation shown in Figure B3-1 is due to the lake being cooler than the daytime air in August, giving enhanced daytime propagation, but that in September-October the opposite effect may be occurring.

Fluctuations in Signals at the Midpath Monitors.

About twenty intervals, of a few hours each, had noticeable fluctuations of signal levels on one or both of the Port Burwell channels 12 and 24. Two examples of such events are shown in Figures B3-3 and B3-4 along with the associated acoustic sounder records.

In Figure B3-3 three intervals of signal fluctuations are presented. There is no obvious correlation between the fluctuations on the two channels. The acoustic sounder records show evidence of some form of inversion activity during this period (this period will also be discussed again in the next chapter). In general, the intervals of signal fluctuations at midpath did not appear to associate with noticeable events on the London monitors. It is impossible for this interval, and for most of the intervals of signal fluctuation, to say anything definite about what might be happening based on the acoustic sounder records alone.

Figure B3-4 shows a somewhat more pronounced record of signal fluctuations. The acoustic sounder records show strong evidence of cloud and a possible sibsidence. This interval coincided with very warm, humid weather with light wind. It is conjectured that over

Echo Sounder

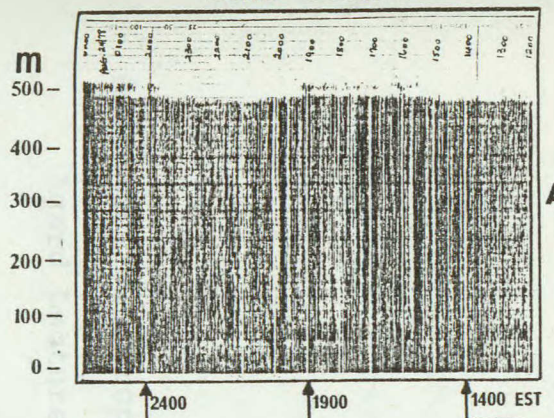

AUG. 23 1978

P.B. Erie 12

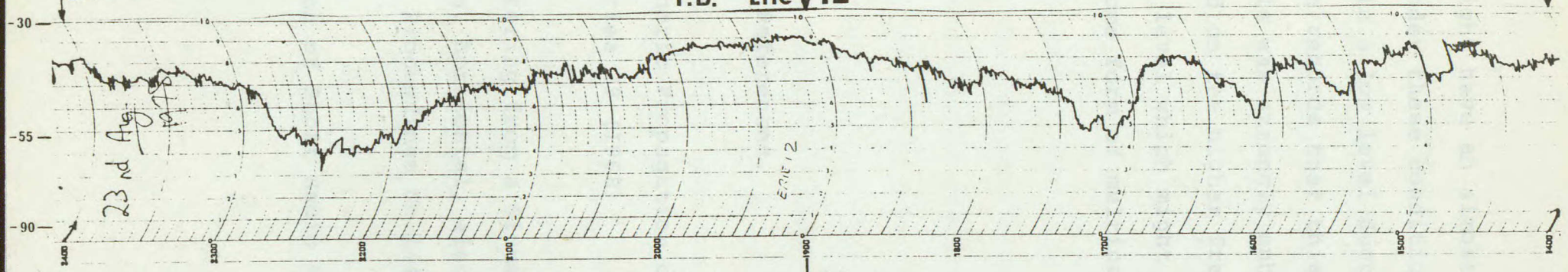

dBm)

P.B. Erie 24

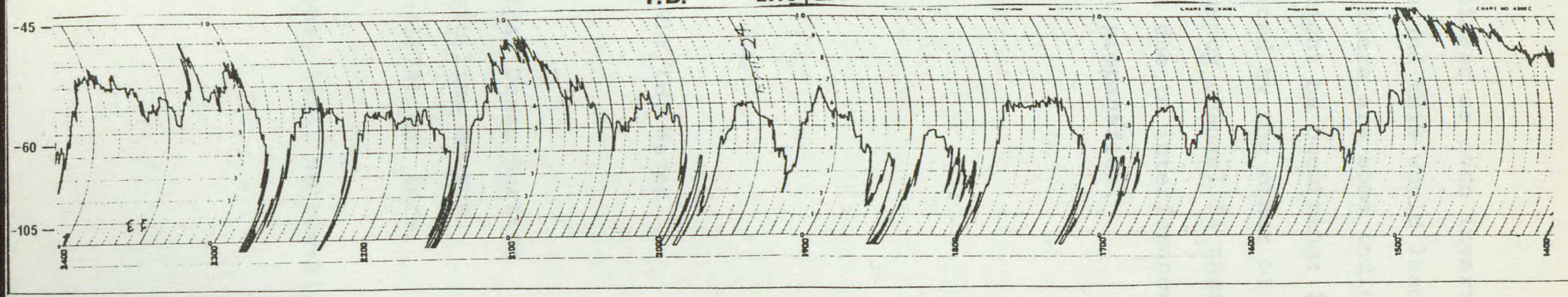

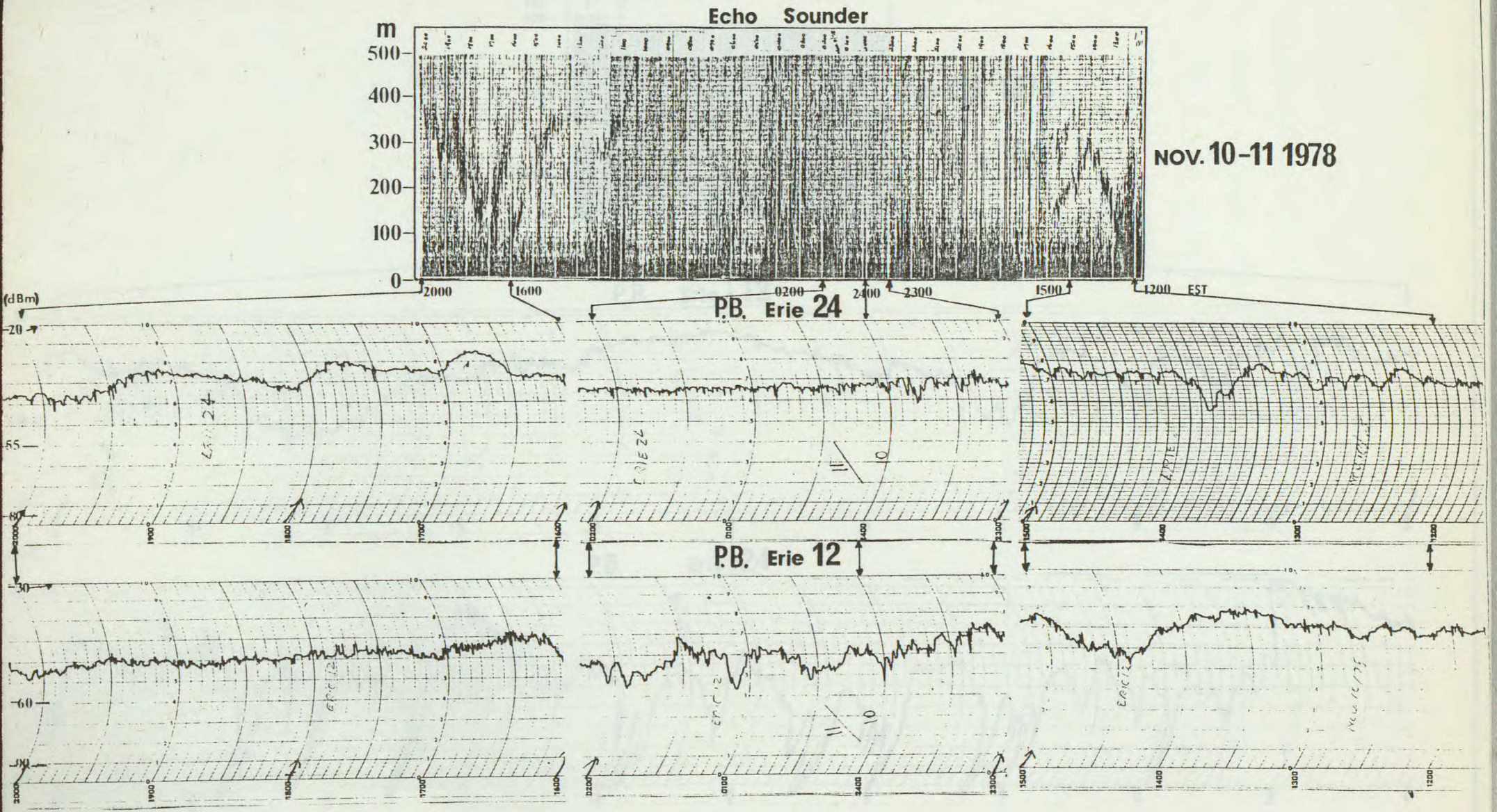
Echo Sounder
m
500
400
300
200
100
0
2000
1600
0200
2400
2300
1500
1200 EST
NOV. 10-11 1978
(dBm)
-20
-55
-80
P.B. Erie 24
P.B. Erie 12
-30
-60
-90

the cooler lake one might have an almost linear or even inverted temperature profile under these conditions and this would lead to enhanced propagation in a low level duct. There are some indications on the signal strength records that this might be occurring: The signal on both channels was strongly enhanced by the order of 10dB during this period and on the higher frequency channel 24 there are sharp drops in signal level which might be due to interference effects, indicating some form of multipath propagation.

References.

Bolgiano, R., Tropospheric Propagation of VHF/UHF Waves. Agard Lecture Series 29 (1968)

Fessenden, D.E., Scattering from a Sinusoidal Ocean Surface excited by a long, horizontal, electric line source. Agard Conference Proceedings No.144, (1974) ed. Ince.

Kerr, D.E., Propagation of Short Radio Waves, 1951, McGraw-Hill.

Chapter B4.

Comparison of Acoustic Sounder and London Monitoring Records.

In experiments on propagation at VHF/UHF it is necessary to have data on the atmospheric temperature and humidity profiles in order to attempt any detailed study of the propagation. This atmospheric data would normally be obtained by radiosonde measurements. In this experiment these measurements were not available. (It was hoped that a comprehensive set of refractivity profiles would be measured over Lake Erie during this project, by another agency.) For atmospheric information, therefore, the only data which was available was from standard weather maps which were kindly supplied by Atmospheric Environment Services at London Airport, via Professor Hay at the Physics Department, U.W.O., and also an acoustic sounder was operated at the Port Burwell midpath site from July 9 to November 29, 1978.

The acoustic sounder system used here was described in Chapter B3. In general, the acoustic sounder records show enhanced reflections from regions having sharp variations in the temperature profile, (see review by Hopper, 1978). Therefore, while it did not give any quantitative measurements, it was hoped that the acoustic sounder records would give some indication of the form of the temperature profile. For UHF propagation the important features of the profiles are those which give the refractivity profiles shown in Figure B4-1, (from Kerr, 1951).

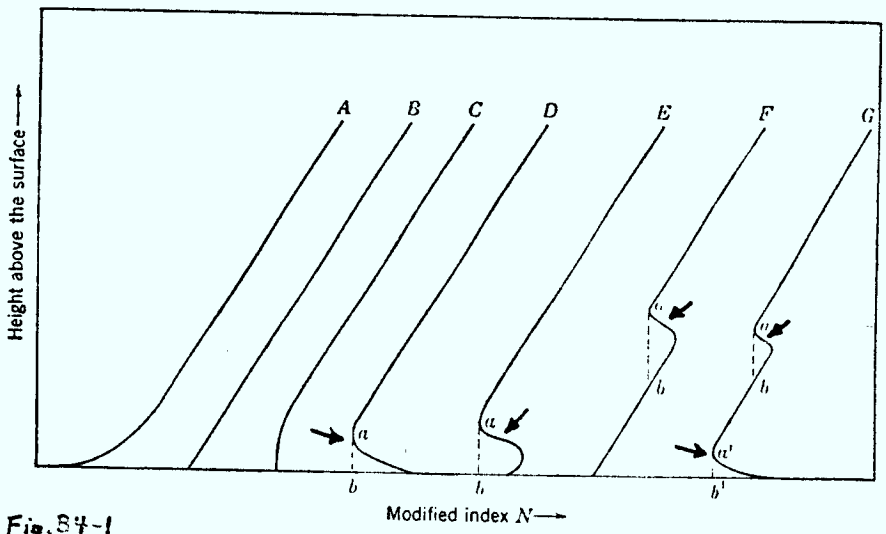

Fig. 84-1 —Idealized modified index profiles: (*A*) Substandard surface layer; (*B*) profile for standard refraction; (*C*) superstandard surface layer; (*D*) superstandard surface layer with surface duct; (*E*) elevated superstandard layer with surface duct; (*F*) elevated superstandard layer with elevated duct; (*G*) surface and elevated superstandard layers with both surface and elevated ducts. In all cases the duct extends from *a* to *b* and from *a'* to *b'*.

This figure is a plot of various types of modified refractive index N (see Chapter 3), and these curves would be more or less the negative of the temperature profile curves. The features marked by arrows should show up on the acoustic sounder records. Unfortunately, the curves are also affected by the humidity profiles and the effect of humidity on acoustic sounder records is not clear.

A further problem with this sounder was the limited height coverage. More powerful acoustic sounders can obtain good records up to several kilometers. The present apparatus is much more limited. It often appeared, when studying the data, that the features which could be associated with signal enhancements were just out of view above the 500 meter maximum height on the sounder records.

In the remaining part of the chapter a number of samples of data are shown. These were chosen because they either showed interesting enhancements (or lack of) on the signal strength records or they showed interesting features on the acoustic sounder records. These are presented in chronological order.

For each sample there is a discussion of the weather conditions, etc. It will be seen that no single type of weather condition is responsible for all enhancements. For each enhancement there is generally a complex pattern of weather conditions. Also, enhancements usually have a pattern of smaller scale events which also need to be explained.

One original question was whether the enhancements would be different for the over-water (Erie) path versus the over-land paths, (Toronto and Detroit). A study of the following figures will show that the Toronto and Detroit enhancements look more similar to one another than they do to the Erie enhancement. Therefore, there are probably some systematic differences between over-water and over-land paths but this problem still requires further study.

Kerr, D.E., Propagation of Short Radio Waves, 1951, McGraw-Hill.

Hopper, V.D., Acoustic Sounding of the Atmosphere, 1978, Endeavour, pp.121-126.

Figure B4-2, July 18-19, 1978

This example was interesting in that it showed signal enhancements which were very similar in appearance and almost simultaneous in time on Toronto and Detroit. On the Erie channel the enhancements were not so strikingly similar in appearance to those on the other two stations and there is an indication that the Erie enhancements took place an hour or so earlier.

The weather map for this period showed a strong northward flow of warm air behind an almost stationary frontal system. The signal enhancements might then coincide with bursts of northward moving warm moist air which would cause changes in the refractivity profiles. At night one might expect warm air movement to take place most strongly above the cooler surface layer so it is uncertain whether any indication of the movement of the warm air masses would be seen on the echo sounder records.

The echo sounder shows dark patches near zero height associated with strong ground cooling which took place during afternoon and evening on July 18 up till about 0500 on July 19, a drop of about 18°C and then strong warming from 0500 to 1000, a rise of about 20°C. The sounder records also show some darkening at upper heights during late evening of July 18 and morning of July 19. Darkening of this sort usually correlates with enhanced propagation. The darkening is probably associated with features at a greater height than this sounder reaches.

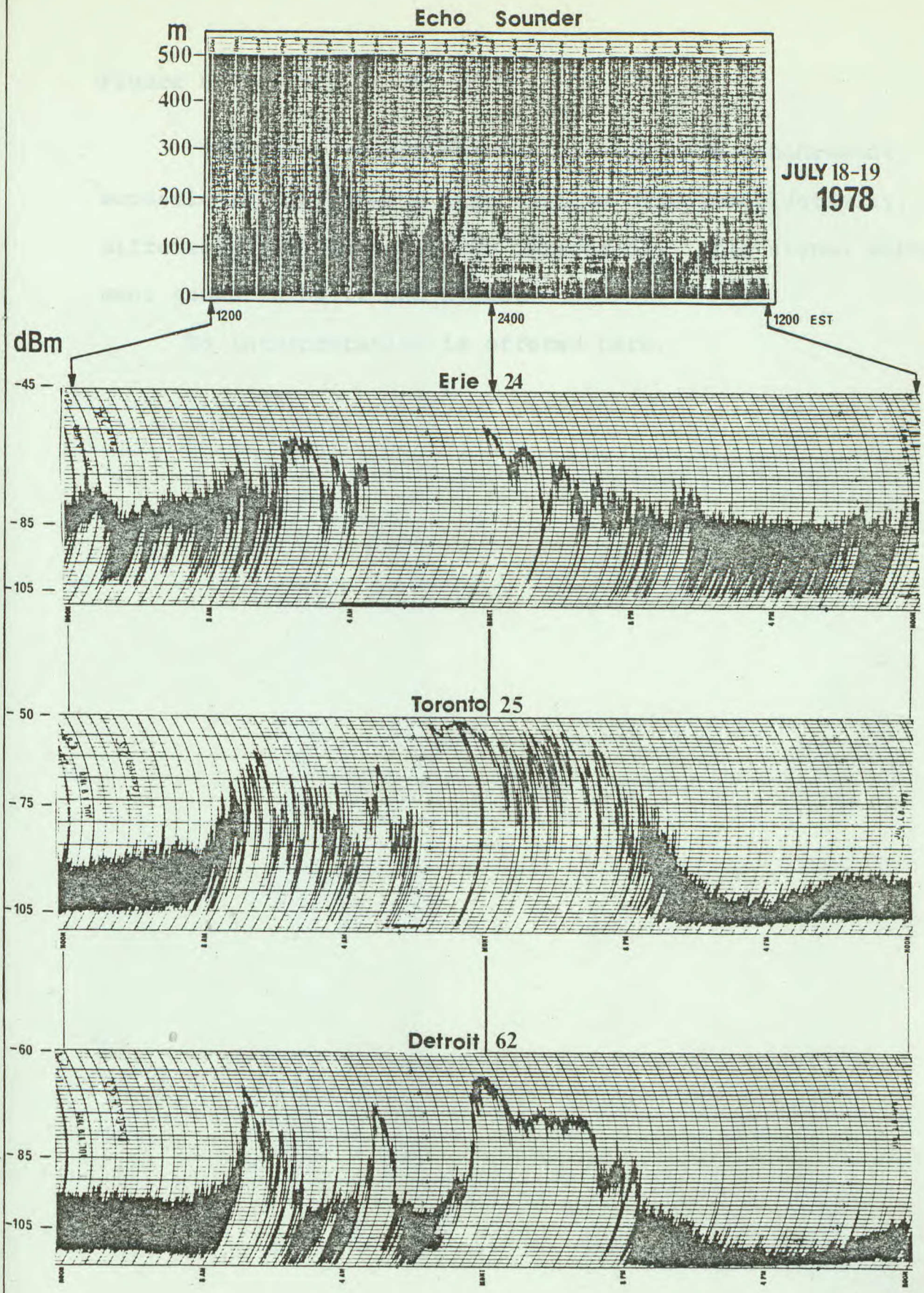
Echo Sounder
m
500
400
300
200
100
0
JULY 18-19
1978
1200
2400
1200 EST
dBm
-45
-85
-105
Erie 24
-50
-75
-105
Toronto 25
-60
-85
-105
Detroit 62

Figure B4-3, July 27-29, 1978

This is a record showing no nighttime enhancement. The acoustic record shows a vast variety of weather activity, quite different from the other two periods of little signal enhancement shown in B4-12 and B4-13.

No interpretation is offered here.

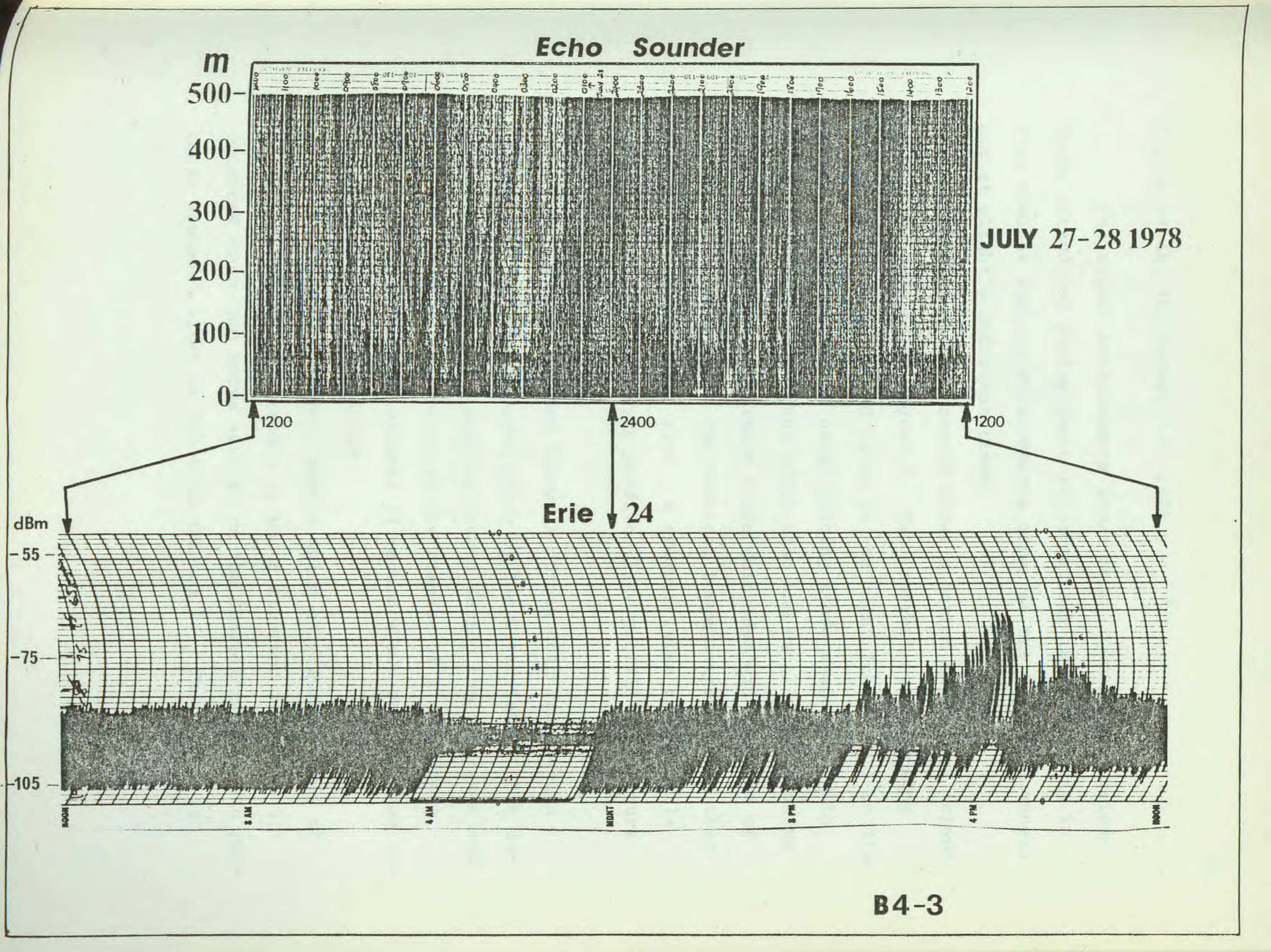
Echo Sounder
m
500
400
300
200
100
0
1200
2400
1200
JULY 27-28 1978
Erie 24
dBm
-55
-75
-105
NOON
8 AM
4 AM
MIDNT
8 PM
4 PM
NOON

B4-3

Figure B4-4A, 4B, August 3-4, 1978

The signal enhancements shown here (ignore the spurious blobs introduced during photo-reproduction) is interesting in that similar looking enhancements occur on the various channels but at slightly different times.

The echo sounder record shows a period of rain or 'cloud' during the evening of August 3. Two interesting downcoming hill-like traces occurred later in the night (these will be discussed below). At 0800 the usual upgoing trace associated with ground warming appeared and after that the usual daytime plume activity. The ground warming trace coincides with the end of signal enhancement since the vertical temperature profile then acquires a steeper lapse rate. A steeper lapse rate profile gives a poorer refractivity profile (like profile A in Figure B4-1).

The weather pattern showed a strong cold front which passed over and then stopped south of the Great Lakes. The activity seen on the echo sounder record during the afternoon and evening of Aug. 3 is typical of the passage of a cold front. Note also that the Erie channel 24 record shows some daytime enhancement during this period.

The twin enhancement events which show most clearly on the Toronto channel 25 record at about 2100 and 2400 Aug. 3 occurred about two hours earlier on the Detroit records and probably somewhat later on the Erie channel 24. This event is

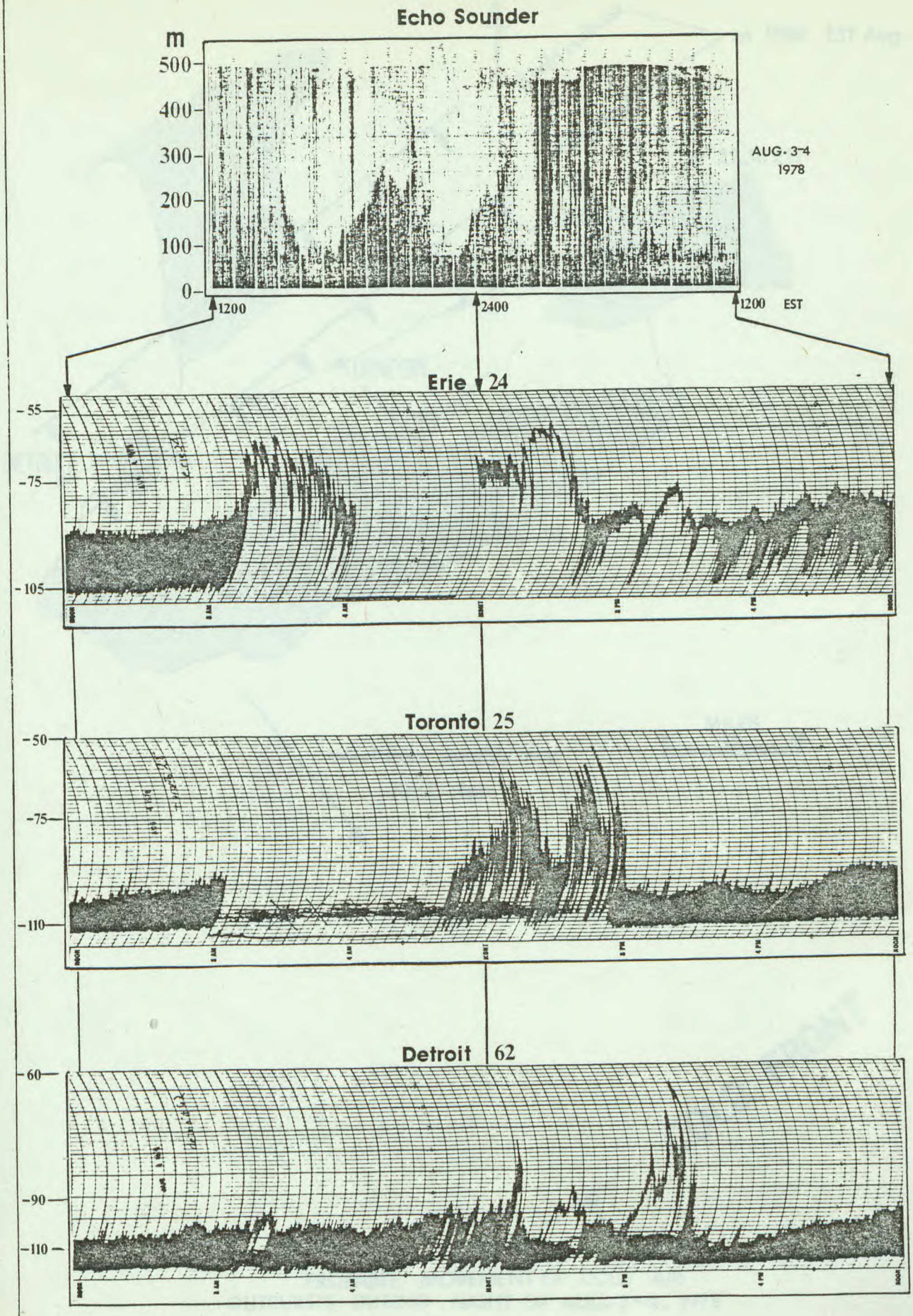
Echo Sounder
m
500
400
300
200
100
0
AUG. 3-4
1978
1200
2400
1200 EST
Erie 24
-55
-75
-105
Toronto 25
-50
-75
-110
Detroit 62
-60
-90
-110

B4-4A

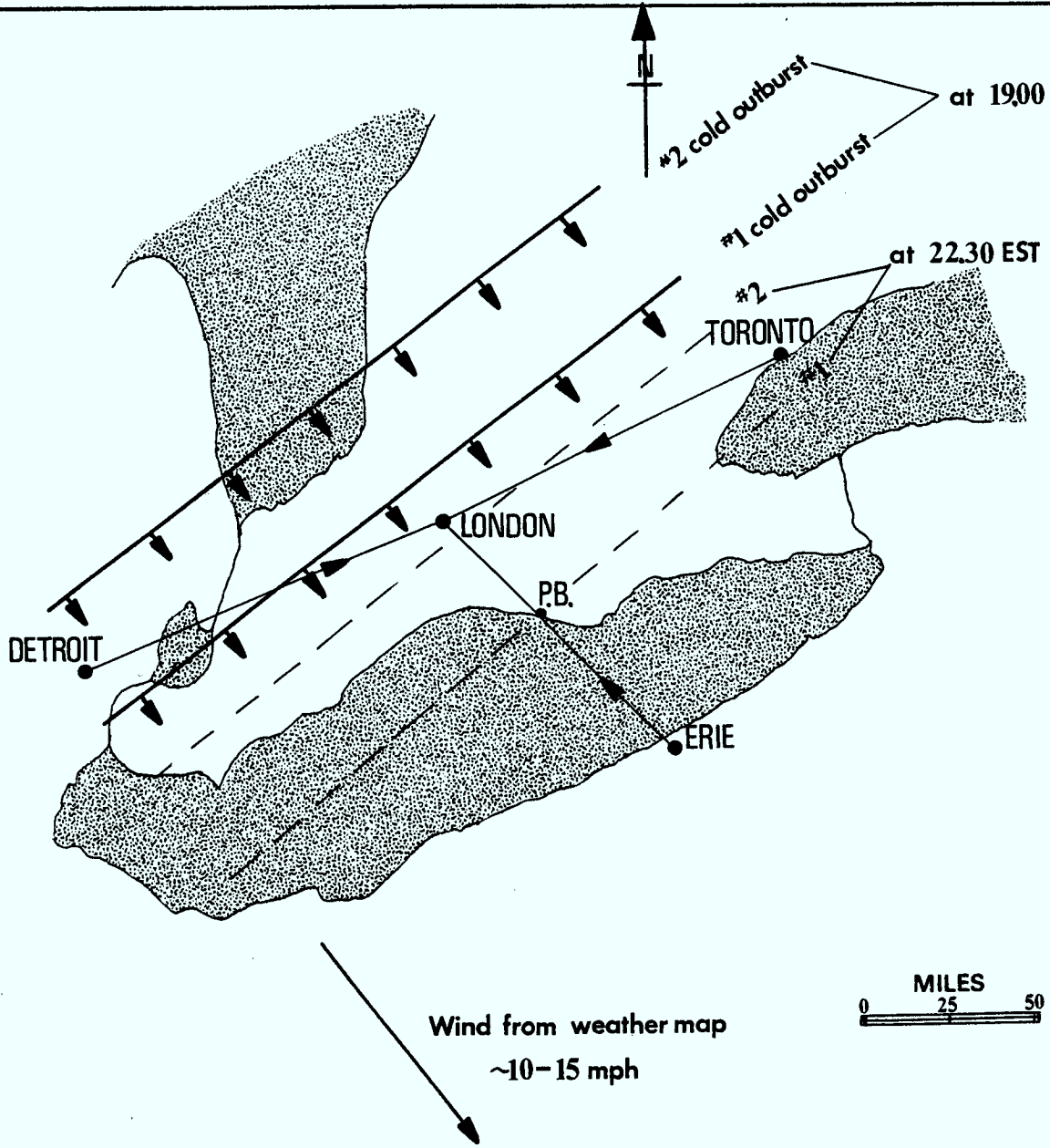

PROBABLE MOVEMENT OF COLD AIR
OUTBURSTS DURING NIGHT OF AUG. 3-4, 1978

B4-4B

assumed to be associated with the two downcoming hill-like features on the echo sounder record. A possible explanation which seems to fit both the weather records for this period and the records shown in Figure B4-4A is as follows: The twin enhancement event and the downgoing hills on the echo sounder are associated with the movement across the area of two outbursts of cold air. Figure B4-4B shows the position of these outbursts at 1900 EST and 2230 EST on Aug. 3. The observed time delays and movements are in agreement with the winds shown on the weather map for this period. The two 'hills' on the echo sounder records are probably caused by the colder outbursts moving in across the warmer ground layer and giving increased temperature gradients near the gound. There should also be features from these outbursts at greater heights than is shown on the sounder record.

Figure B4-5, August 5-6, 1978

The night preceeding the sample of Figure B4-4. Only Erie channel 24 is shown. There was a good enhancement on this channel during the night. This disappeared with ground warming in the morning at about 0900 (see the usual feature on the sounder record). The sounder record also hints at some form of activity, probably temperature inversions, during much of the night but these are not clearly defined and could be at greater heights than the 500 meter maximum for the sounder.

Weather records were incomplete for this period. The region was being influenced by a high pressure region and the appearance of events here is generally similar to those of Figures B4-7 (see comments for B4-7).

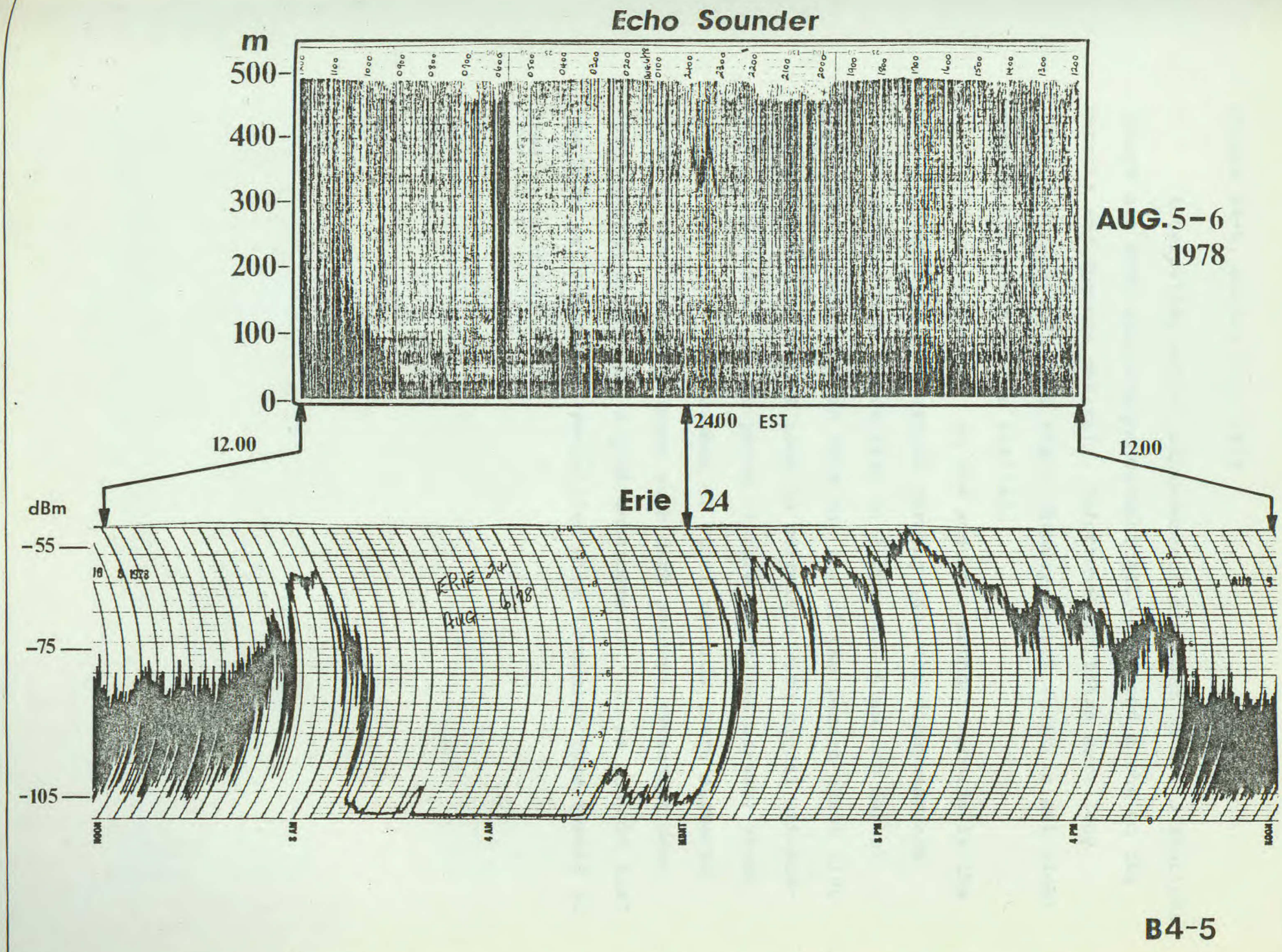
Echo Sounder
m
500
400
300
200
100
0
AUG. 5-6
1978
12.00
2400 EST
12.00
Erie 24
dBm
-55
-75
-105
MIDNIGHT
8 PM
4 PM
NOON

B4-5

Figure B4-6, August 6-7, 1978

Interesting signal enhancements are seen on all 3 stations (there are some spurious photographically-produced blobs on the Detroit and Toronto charts). Unfortunately there were long off-the-air periods this night (Sunday night) so it is not clear whether the patterns are similar.

The main feature on the acoustic sounder records is the "hill" associated with ground warming (and the disappearance of the enhancement) about 0900 on August 7. Also two darker regions which extend down from the top of the record about 2100 on Aug.6 and 0700 Aug. 8 seem to correlate with signal enhancements. (There is also a patch of rain (vertical streak) about 1145 on Aug. 7). On a number of other records there appeared to be an association between such dark patches extending down from maximum height and signal enhancements. It is thought that the dark patches may be associated with inversion type events at greater heights.

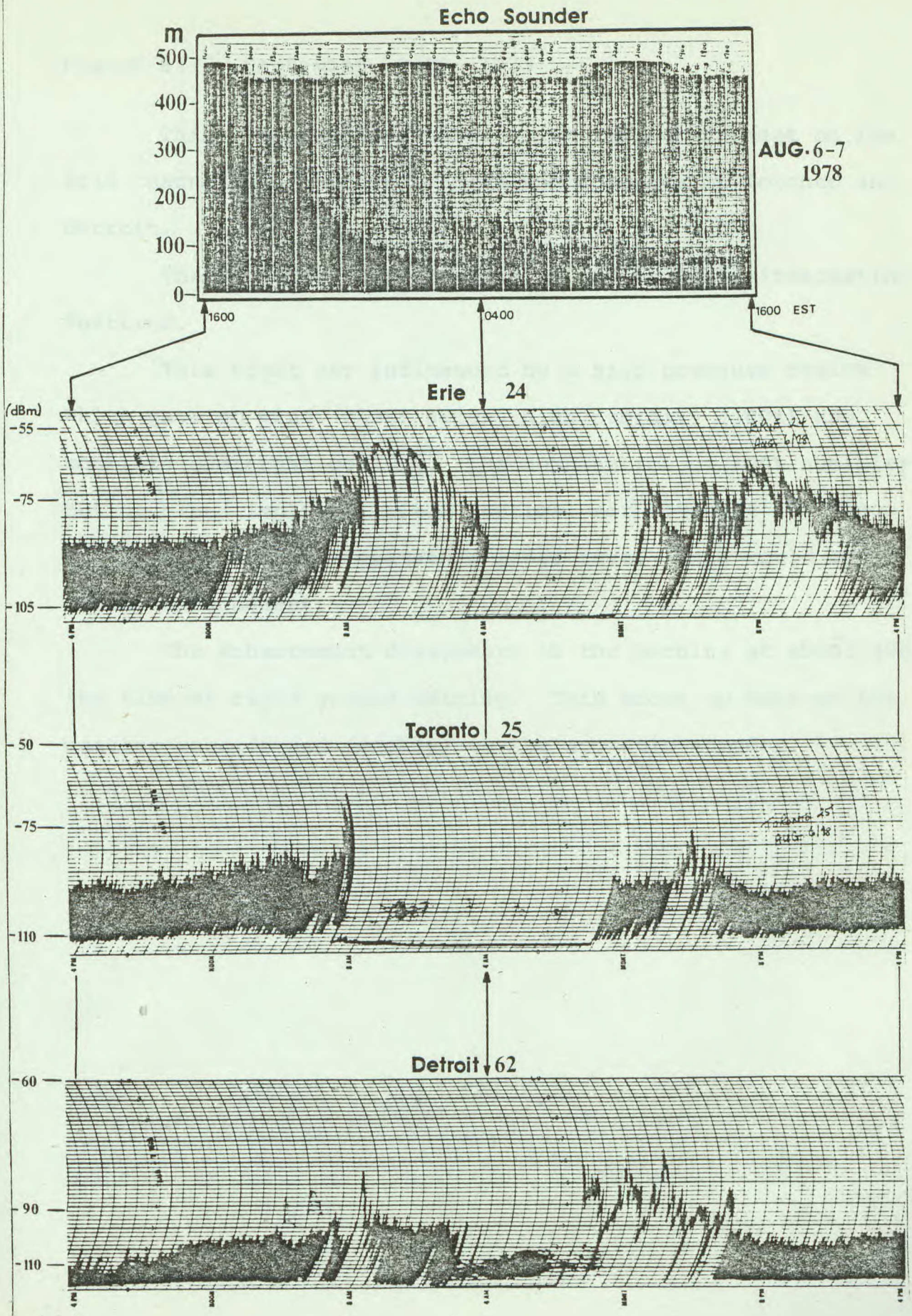
Echo Sounder
m
500
400
300
200
100
0
AUG. 6-7
1978
1600
0400
1600 EST
Erie 24
(dBm)
-55
-75
-105
Toronto 25
-50
-75
-110
Detroit 62
-60
-90
-110

Figure B4-7, September 28-29, 1978

This period shows a good nighttime enhancement on the Erie channel but less pronounced enhancements on Toronto and Detroit.

The acoustic sounder shows no particularly interesting features.

This night was influenced by a high pressure region which gave no wind, clear skies, high humidity (100%) and moderate overnight cooling. The combination of 100% humidity, but no cloud implies limited vertical air movement and hence a less than normal temperature lapse rate. This would cause signal enhancement.

The enhancement disappears in the morning at about 0900, the time of rapid ground warming. This shows up both on the weather records and (weakly) on the acoustic sounder.

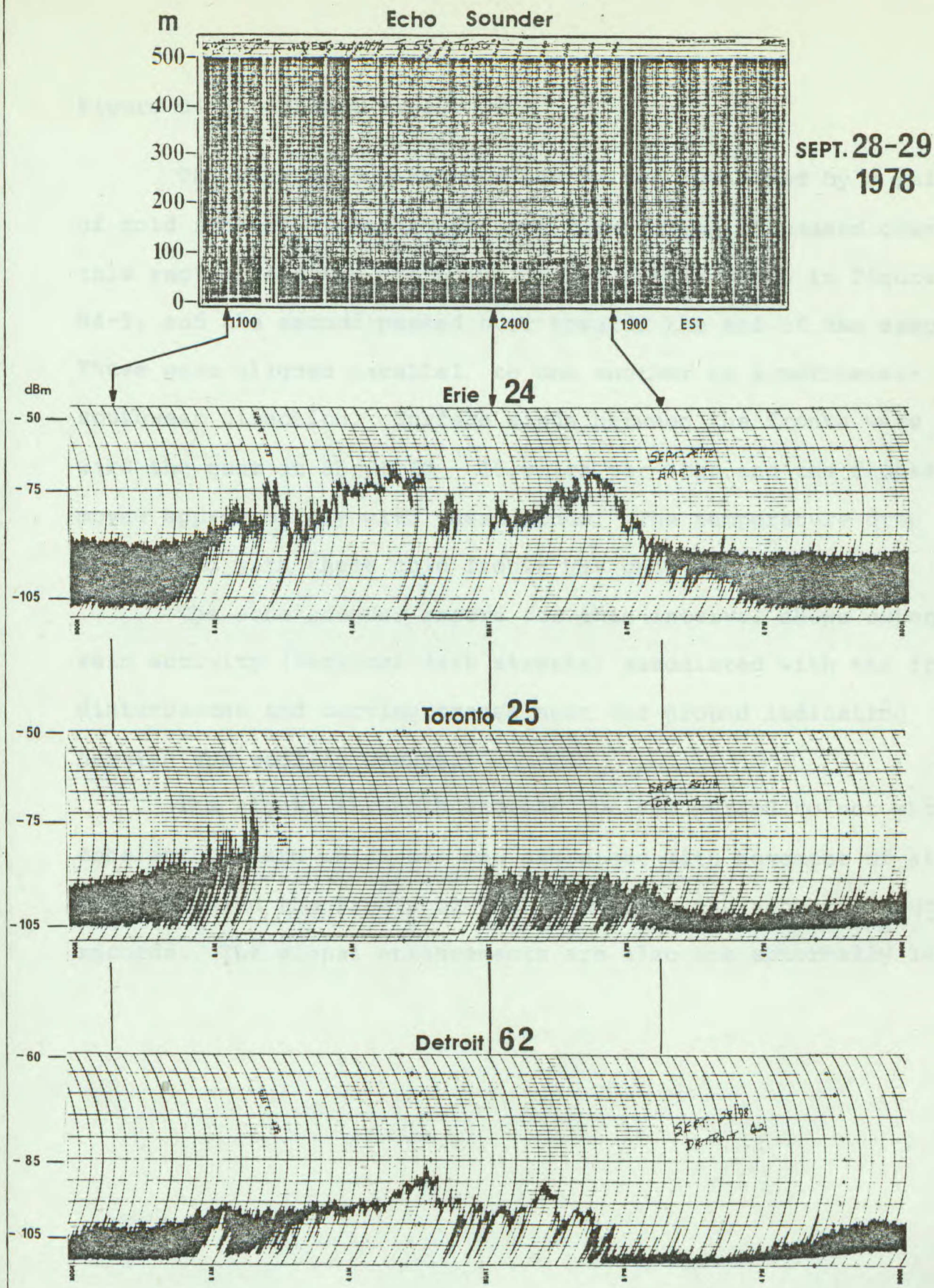
m
Echo Sounder
500
400
300
200
100
0
1100
2400
1900
EST
SEPT. 28-29
1978
dBm
Erie 24
- 50
- 75
-105
Toronto 25
- 50
- 75
-105
Detroit 62
- 60
- 85
- 105

Figure B4-8, October 12-13, 1978

The weather during this sample was dominated by a pair of cold frontal disturbances, the first of which passed over this region near the beginning of the sample shown in Figure B4-5, and the second passed over towards the end of the sample. These were aligned parallel to one another in a northeast-southwest direction. Surface winds between the fronts were toward the east at about 10 - 15 miles per hour and the fronts moved approximately with these winds. The temperature drop associated with these cold fronts was only about 6C°.

The echo sounder record for this interval shows extensive rain activity (vertical dark streaks) associated with the frontal disturbances and curving traces near the ground indicating heating and cooling events.

The signal strength records for the period to not show a coherent pattern which one can associate with movement of air masses behind the fronts or with events on the acoustic sounder records. The signal enhancements are also not abnormally large.

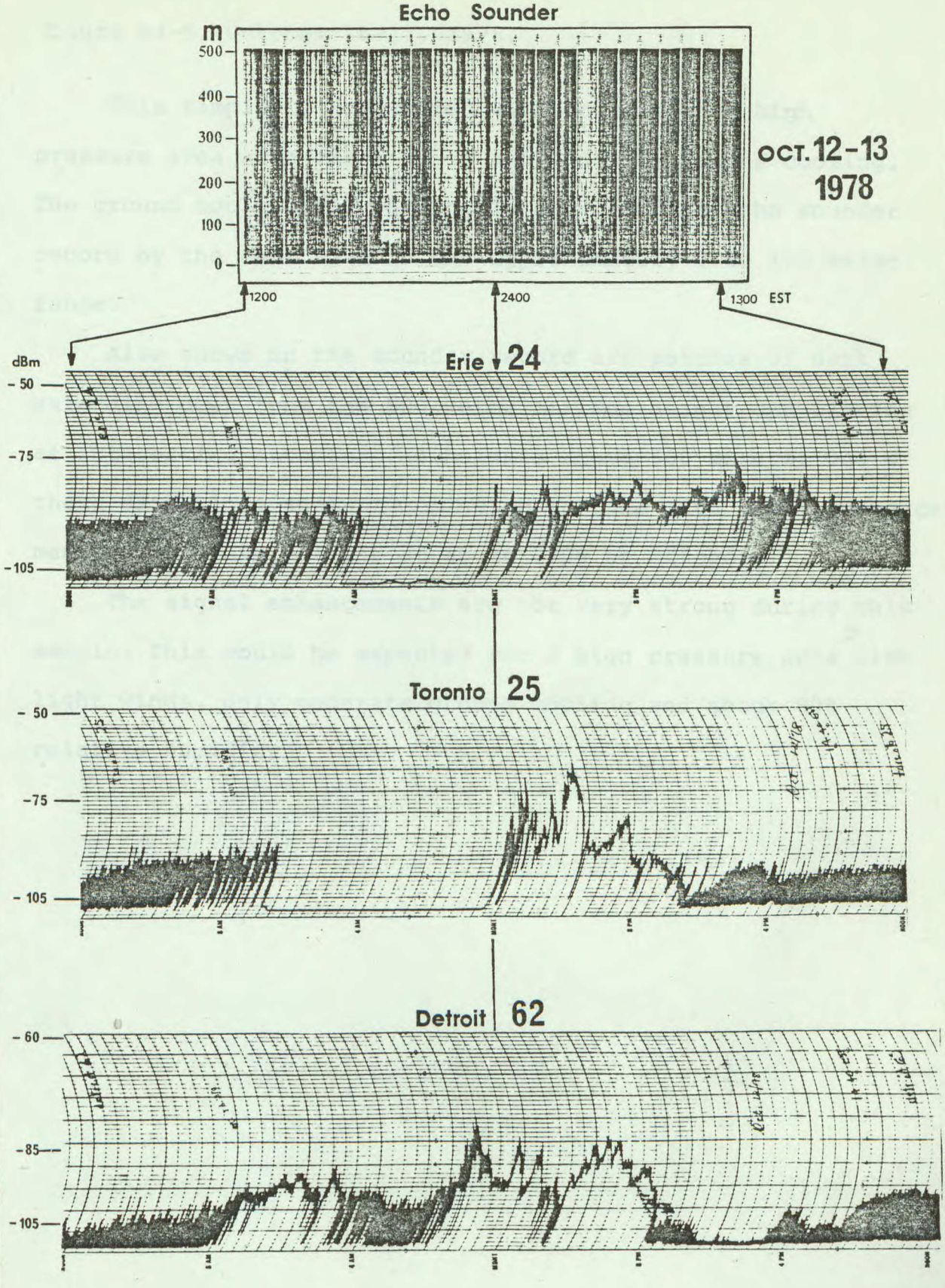
Echo Sounder
m
500
400
300
200
100
0
1200
2400
1300 EST
OCT. 12-13
1978
dBm
Erie 24
- 50
-75
-105
Toronto 25
- 50
-75
- 105
Detroit 62
- 60
-85
-105

Figure B4-9, October 16-17, 1978.

This sample is associated with an extensive high pressure area with clear skies and moderate ground cooling. The ground cooling and warming is shown on the echo sounder record by the dark band in the approximately 0 to 100 meter range.

Also shown on the sounder record are patches of dark extending down from the 500 meter maximum height and hinting at interesting structure at heights above 500 meters. One of these darkenings seems to coincide in time with signal enhancement on Erie and Detroit at about 0300 on October 17.

The signal enhancements are not very strong during this sample. This would be expected for a high pressure area with light winds, only moderate ground cooling and about 80% relative humidity.

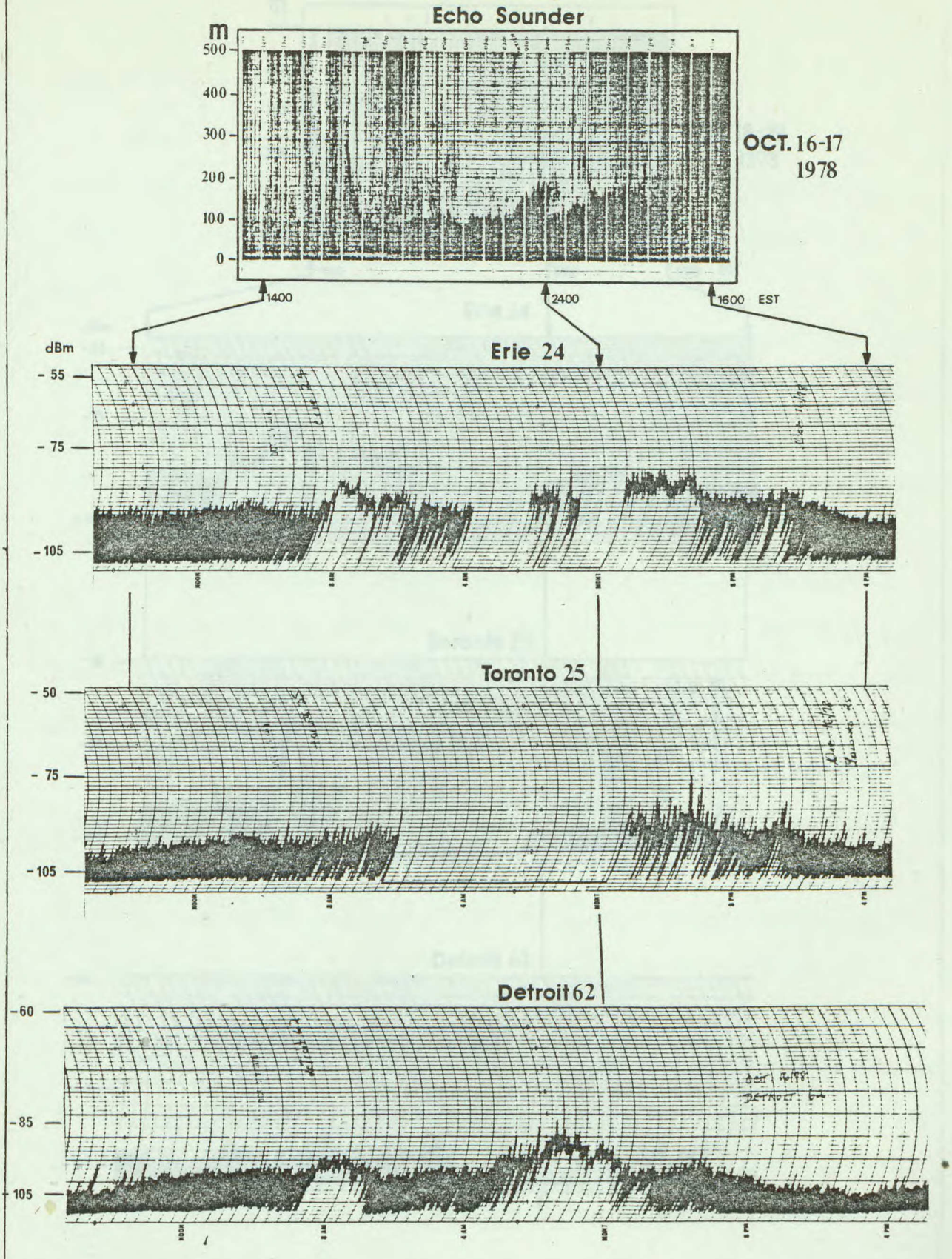
Echo Sounder
m
500
400
300
200
100
0
OCT. 16-17
1978
1400
2400
1600 EST
dBm
Erie 24
- 55
- 75
-105
Toronto 25
- 50
- 75
-105
Detroit 62
-60
-85
105

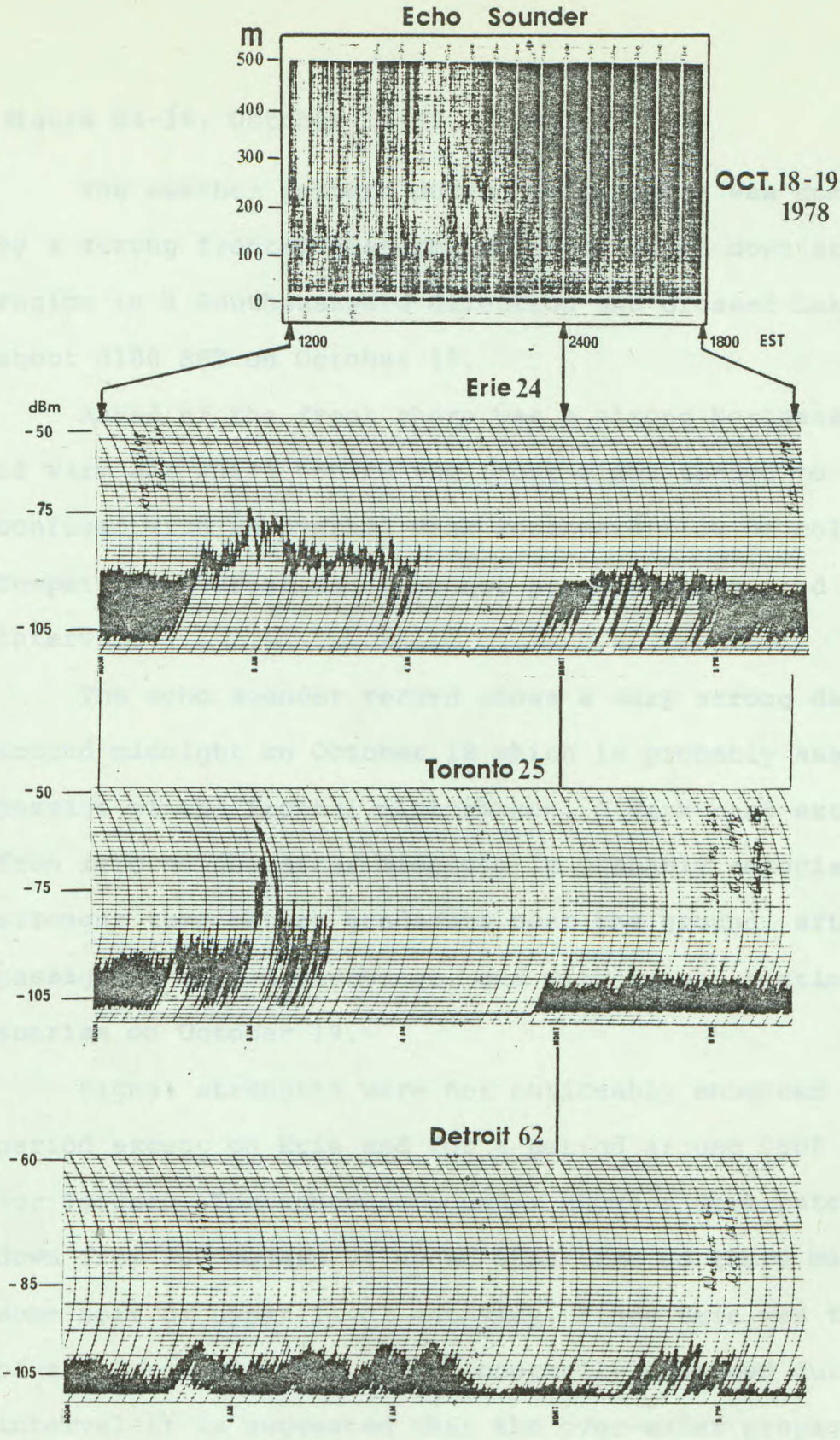
Echo Sounder
m
500
400
300
200
100
0
OCT. 18-19
1978
1200
2400
1800 EST
Erie 24
dBm
-50
-75
-105
Toronto 25
-50
-75
-105
Detroit 62
-60
-85
-105

Figure B4-10, October 18-19, 1978.

The weather pattern during this sample was dominated by a strong frontal disturbance which moved down across this region in a Southeastward direction and crossed Lake Erie at about 0100 EST on October 19.

Ahead of the front there was a strong Northeastward flow of warm air while behind the front winds tended to be light and confused with an overall weak Southward flow of cold air. Temperature variations were not notably pronounced during this interval.

The echo sounder record shows a very strong dark patch around midnight on October 18 which is probably associated with passage of the frontal disturbance. A dark band extending up from zero height after midnight is probably associated with stronger temperature gradients near the ground, after the passage of this disturbance, and with ground heating after sunrise on October 19.

Signal strengths were not noticeably enhanced during this period except on Erie and for a period around 0800 on October 19 for Toronto. The acoustic sounder shows a dark patch extending down from 500 meters at about this time so there may have been some sort of upper level activity. Since Erie was the only one of the three stations to be abnormally enhanced during this interval it is suggested that the over-water propagation is important here.

Figure B4-11, November 10-12, 1978.

This is a two day stretch of records which showed some interesting enhancements and some interesting activity on the acoustic sounder records. This period was also shown in Chapter B3 (Figure B3-3) as being a time when signal fluctuations were observed on the midpath monitors at Port Burwell. The times of midpath signal fluctuation do not obviously coincide with signal enhancements on the channels shown in Figure B4-11.

The weather records for this period show an occluded frontal system which moved slowly into the region in a Southward direction at around midnight on November 10 and then remained relatively stationary over the region throughout the remainder of the period. This system was accompanied by high humidity (fog was reported most of November 11), slowly falling temperatures, extensive cloud. Winds were light on November 11 and increased on November 12 to moderate speeds.

On the echo sounder charts there are some traces whose height varies in an irregular fashion. These may be inversions associated with the fog layers which were reported. Other traces of interest on the sounder chart is the 'grassy' echo extending from zero height, from evening of November 11 to morning of November 12. This will also be seen on Figures B4-12 and B4-13. In all three cases it coincides with a lack of nighttime signal enhancements. The only other feature on the sounder chart is the characteristic

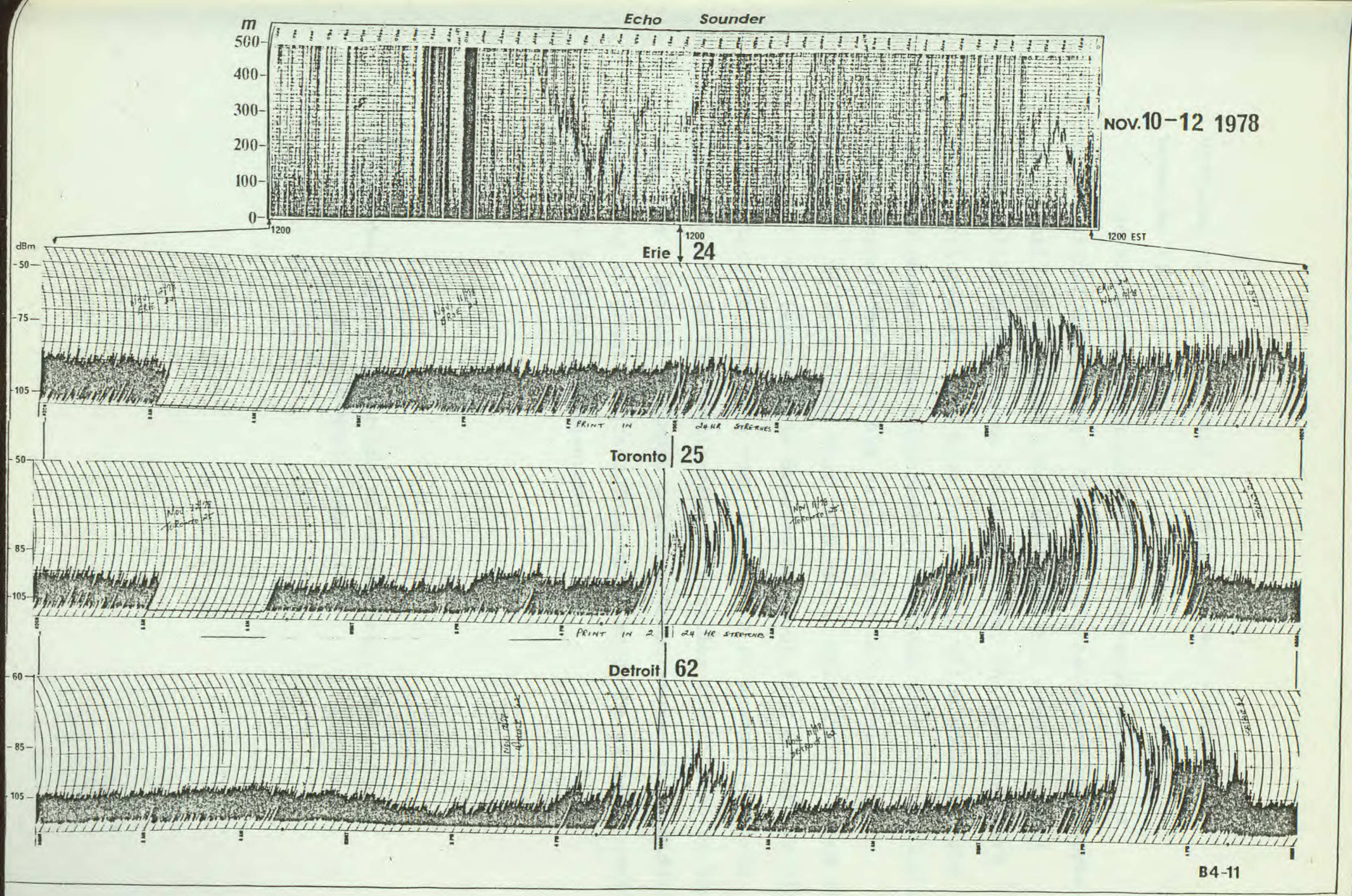
Echo Sounder
m
500
400
300
200
100
0
1200
1200 EST
NOV. 10–12 1978
1200
Erie 24
dBm
-50
-75
-105
PRINT IN 24 HR STRETCHES
Toronto 25
-50
-85
-105
PRINT IN 2
24 HR STRETCHES
Detroit 62
-60
-85
-105

vertical streaks from rain, from about 2400 - 0300 on November 12.

The signal strength records show several periods of strong signal enhancement. The mid-day enhancement on November 11 is unusual. It occurred simultaneously, but with different intensities, on all three channels shown. The sounder chart shows features at this time but nothing which would explain the enhancement. This enhancement coincided with the lifting of dense ground fog; (the sun was reported as occasionally visible). It is assumed that this was a radiation fog since the ground level temperatures dropped by about 12°C during the night. The pattern is therefore very similar to an example shown in Petterssen*. In his (Petterssen's) profiles the lifting of the fog gave a period of almost constant temperatures and humidities extending to great heights. This would be quite suitable conditions for propagation enhancements.

Petterssen S., Introduction to Meteorology, 1969, McGraw-Hill, page 141.

Figure B4-12, November 14-15, 1978.

This is a particularly good example of a night with little signal enhancement.

The most striking weather feature of this period was a noticeable decrease of temperatures, of about 12°C, from November 14 to November 15. The winds and humidity were moderate. The acoustic sounder record shows no notable features other than some periods of light rain (not confirmed by weather report) and the 'grassy' trace during most of the period. (See also B4-13.)

There does not seem to be any obvious explanation for the lack of enhancement on this night.

Echo Sounder

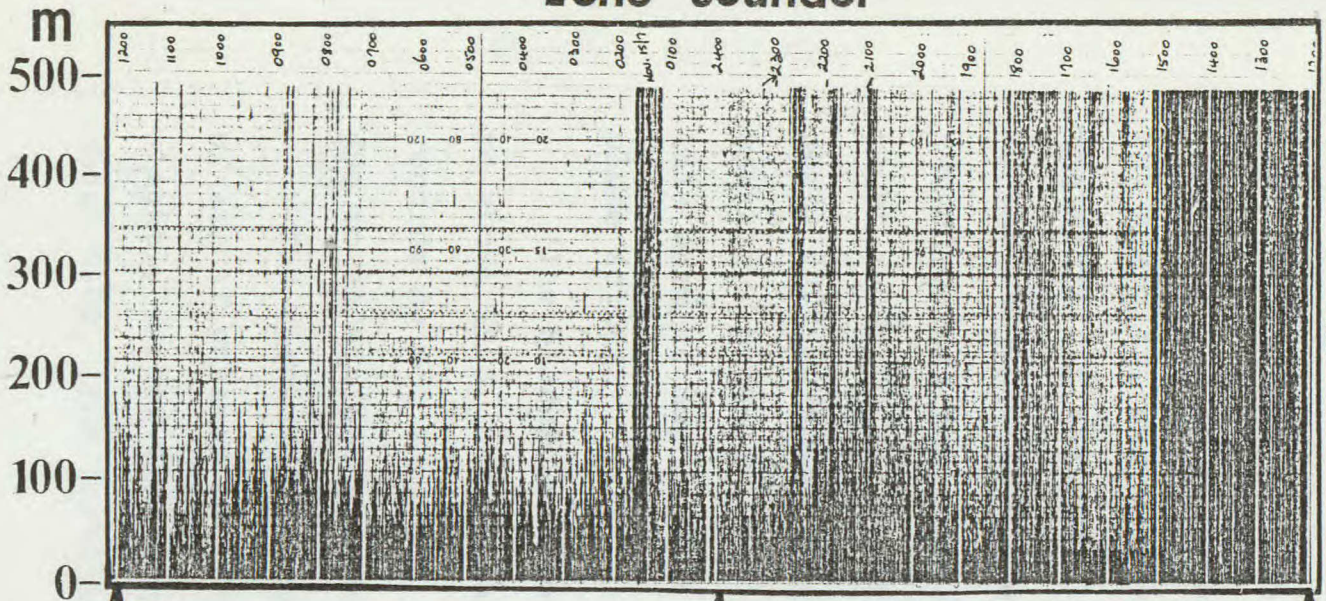

NOV. 14–15
1978

Erie 24

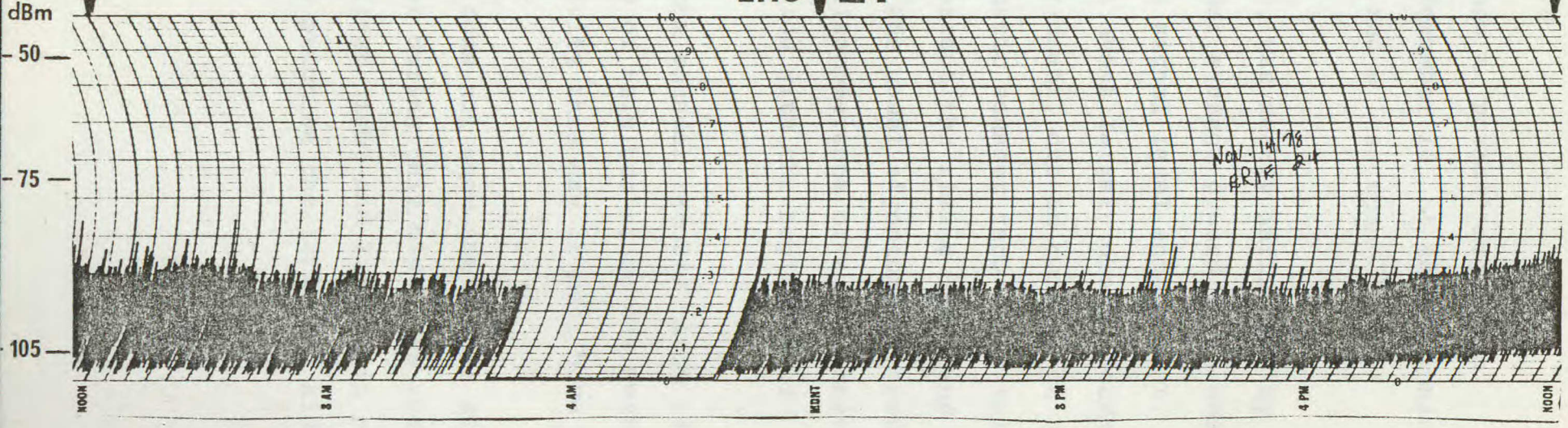

Figure B4-13, November 16-17, 1978.

This sample was chosen to show a 'normal' nighttime signal strength enhancement, on November 16, at the beginning (right hand side) of this sample and a less than 'normal' enhancement the following night.

The first night, November 16, was weakly influenced by a high pressure area but shows rather average ground level cooling, 80% humidity, and some cloud. The signal level enhancement, therefore, is the usual nighttime event largely due to decrease in the atmospheric temperature gradient, due to cooling of the ground during the night. The acoustic sounder record for this night shows no notable features except the rising dark band at about 0900 November 16, which is the usual signature of ground warming. (Note the simultaneous disappearance of enhancement). This warming may be seen to coincide with the beginning of plume activity.

(The blacked-out region on the sounder records, from 1400 to about 1900, has the appearance of rain but since the weather records do not show any rain activity this day it must have been due to an equipment defect).

The second nighttime period does not show the normal amount of signal enhancement. The weather during this night was very slightly warmer than during the first night and light rain began about 0600, (the vertical streaky patch on the left-hand side).

Echo Sounder

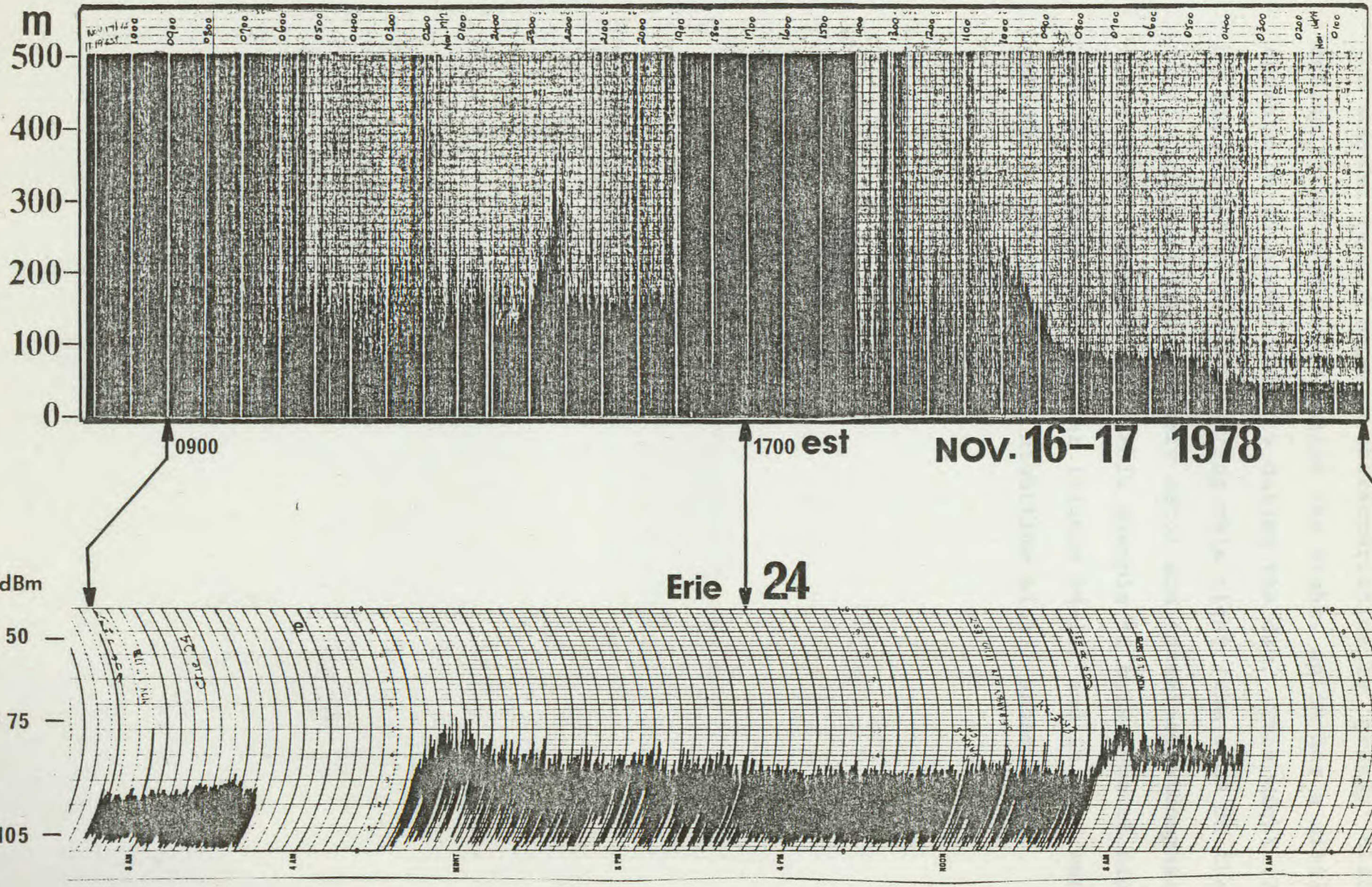

B4-13

The sounder record shows a characteristically 'grassy' trace, extending up from zero, during the night, which has a similar appearance to plume activity during the day. This might (?) be associated with winds during this night (the wind on the first night was approximately zero) and therefore atmospheric turbulence. Another noticeable example of this type of nighttime record has been seen earlier (Figure B4-12) and it also was a period of less than normal nighttime signal enhancement.

PART C

DATA PROCESSING PROGRAMS

Data Processing of the UHF-VHF TV Monitoring Project

I Introduction

The joint Canadian/U.S. project on the Great Lakes propagation measurements is the result of the proposal for an "Interim Technical Standard for Licensing 900 MHz Private Land Mobile Radio Stations in Border Zones" at the Washington meeting between Canadian Department of Communications and the U.S. Federal Communications Commission on September 8-9, 1976. The aim of the program is the acquisition of reliable statistics on the enhancement of signals beyond the radio horizon due to superrefraction and ducting To derive such statistics, signals from the existing VHF and UHF TV transmitters are recorded at several sites in the region. The TV channels and receiver sites were chosen so that data for several propagation paths, of which some are over water, would be available.

Although the major interest is in the UHF band, some VHF transmitters are included to facilitate the evaluation of the frequency dependent phenomena. To the extent feasible, all of the paths will be monitored for one full year at recording sites in London and Ottawa for the Canadian side. The signal strength output information is recorded on chart paper recorder and 5 minute signal strength probability distributions are recorded by the digital tape recorder controlled by a minicomputer (HP21MX).

A large number of measurements were made: Thus simplification of the data is required. The initial data processing is carried out in one month data blocks. The data for each station

is first stored in half hour intervals according to the time of day at which it was recorded. For each of these half hour data sets the median path loss is calculated as well as the path loss exceeded for 5, 10, 90, 95% - - etc., of the time. These path loss data are then plotted as a function of the time of the day. In the first stage of the data analysis a number of corrections to the path loss data have not been taken into consideration. For example, the antenna gain and cable loss have not been fully tested since it was not available, but the general shape of the path loss curves were given. Some plots have been used in the interim report in February, 1978. In the final stage of the data processing, the first stage data processing has been improved. The intermediate tapes which store two months' half hour cumulative distribution are created for further use.

The computer programs to process the data are developed in the Cyber 73 machine and finalized in the Xerox machine. In this way they can run both in The University of Western Ontario (London site) and Communications Research Centre (Ottawa site).

II Some remarks on the Experimental Data Tapes

The recording system was set up in May, 1977 at the London site. The system began to collect the data in 4 channels. After the end of August, 1977 it was fully operational. The data for 16 channels were recorded.

The data tapes store different types of data. It records the 5 minute signal strength distribution starting in every 5th

multiple minute; the time series data in the beginning of every hour and the calibration data once every few days (around 5 days).

Unfortunately, at the beginning of the operation of the recording system the distribution data were not recorded automatically starting at every 5th multiple minute. It was delayed until after the calibration since the recording of the signal is suspended during the calibration. This was later corrected.

In the period between February, 1978 and June, 1978, there were some difficulties in the recording system. Some numbers were scrambled. The heading information was checked and corrected. The data cannot be altogether corrected but the error is within a small percentage. Sometimes the recorded number of the distribution data in each 5 minutes exceeds the maximum number (3000) that it should be. The calibration data had been saved from the teletype. Therefore new tapes were created on which the distribution data with corrected heading were recorded **without** the correct calibration data.

Theoretically the data is collected continuously. In practice the recording system is off from time to time for different reasons. Commonly the recording is interrupted due to tape changing. The other reasons are power failure or the recording system is 'down' due to mechanical breakdown. Therefore there is no data during some short periods.

It is assumed that zero signal level will be received when the transmitting station is off the air. However the weak signals due to background noise will still be detected. It was initially

assumed that station log data giving transmitted power and on-off air times would be available. It is not always true. In cases where the station log data are not available a specific minimum value of noise level has to be chosen as a criterion for determining the on-off period of the station and it is then assumed that full power is transmitted for the on-air period.

There were some periods for which the data had not been recorded in all 16 channels because the receiver of certain channels were removed for repair.

In the calibration data several different kinds of mistakes might be made by the operator. They are: (1) it is out of dynamic range (60 db), (2) the calibration level is not a 5 db multiple, and finally, the same calibration level is repeated.

III The data processing

(1) The first stages of the data processing

The first stages of data processing were done before the end of 1977. The aim was to produce preliminary results. The station log data had not been received at that time. Therefore a reasonable noise level was used to determine off air times. The precise antenna gain and cable loss also were not known. In processing the data the calibration calculation was separated from the main program. Instead of reading the input data of calibration from the data tape, it was inserted from the teletype and the calibrations were assumed to be the same for the entire data tape. The block diagram for the organization of the programs in this stage is shown in Fig.C-1.The organization of the programs in the first stage data

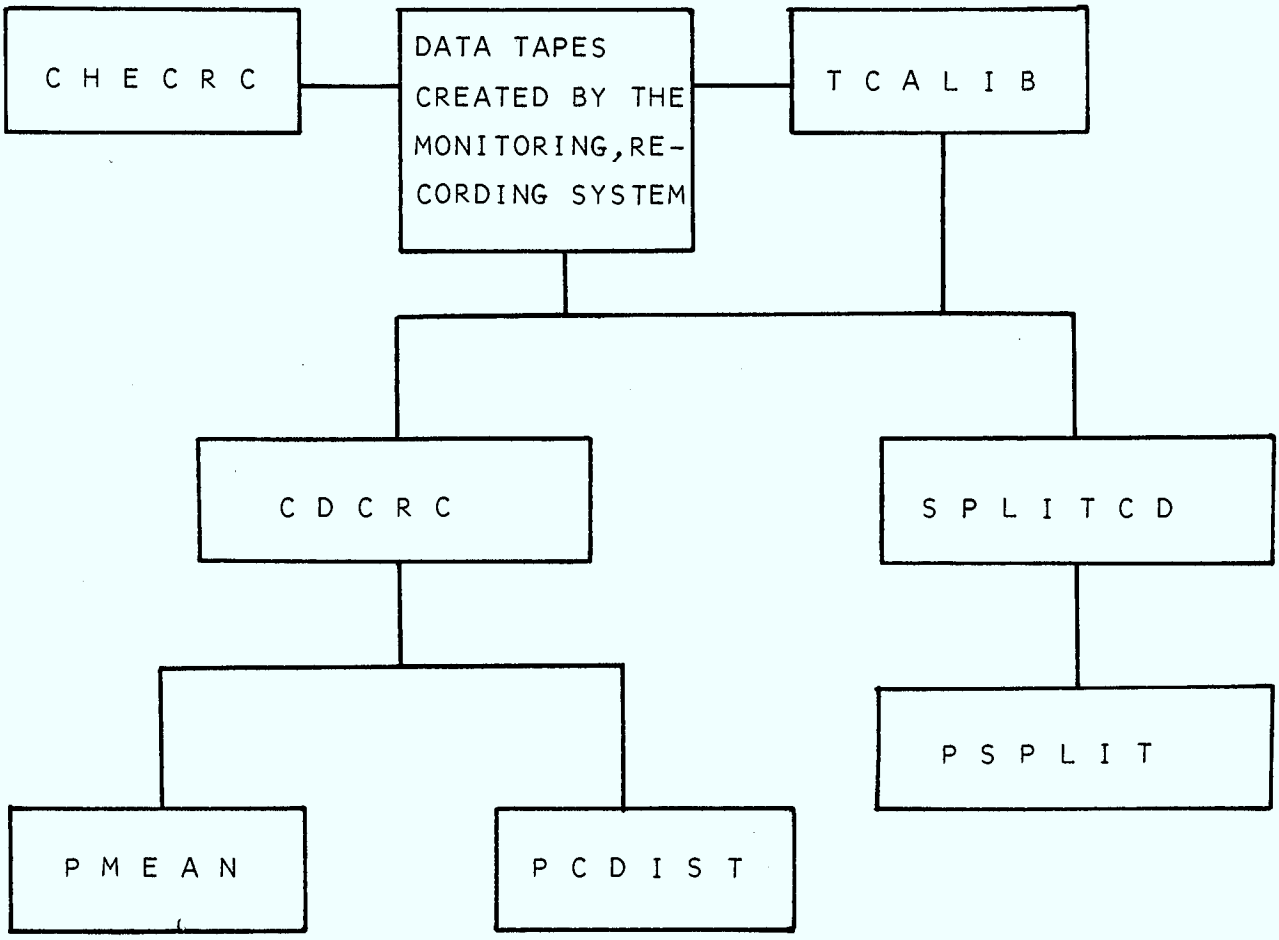

FIG. C-1 THE ORGANIZATION OF THE PROGRAMS IN THE FIRST STAGE DATA PROCESSING

processing. The main objectives are to plot the 5 minute mean (PMEAN), overall cumulative distribution over a certain period (one month)(PCDIST) and the half hour diurnal path loss (PSPLIT).

CHECRC is the program to check the file mark, to count the number of blocks in the data tape and to develop a subroutine to read the input data tape.

TCALIB is the program to calculate the calibration. 13 pair of the input data (calibration value) are taken from the teletype. The third order spline least square fit is used. The output of the calibration is used for the CDCRC and SPLITCD programs.

CDCRC calculates the 5 minute mean for each day, the cumulative distribution, and D(50, 10) over one data tape period. The input data are the data tape created by the recording system and the calibration from the output of the program TCALIB. The output results were stored in the permanent disk file for further use.

PMEAN is the plot of 5 minute mean for every day. The input data are in the permanent disk file created by CDCRC.

PCDIST is to combine the results from the various disk files created by CDCRC and plot the overall cumulative distribution.

SPLITCD is to calculate the half hour diurnal cumulative distribution over one data tape period. The results are written in the permanent disk file.

PSPLIT is to combine the split cumulative distribution

results from several disk files created by SPLITCD and the overall one month half hour split cumulative distribution are obtained. The path loss in different percentage, namely 99, 90, 50, 10, 1%, are calculated. The curves of diurnal path loss are plotted.

(2) The final stage of the data processing

The aim is to take care of all the problems which were mentioned in section II and to create intermediate magnetic tapes which will store the half hour cumulative distribution data. The intermediate tape will be used to plot the half hour median for comparison with the chart from the chart recorder, the monthly diurnal cumulative distribution curve, and the monthly diurnal path loss. The tapes also can be saved for future use. In order to save space as much as possible in the intermediate tapes a special data format is adopted. It is similar to the data tape created by the UHF monitoring recording system. The only difference is the bit structure of the heading. The cumulative distribution data for all 16 channels in the intermediate tapes are not interrupted even in the period which the recording system is off or the transmitted station is off the air. For one year's information 6 tapes are required, so every tape will have two month half hour cumulative distribution data. The organization of these programs is presented in the figure: C-2, the organization of the programs in the final stage data processing.

PCRCCD is to process the data tape created by the UHF monitoring recording system which includes the calibration data and 5 minute signal strength distribution data. The output is

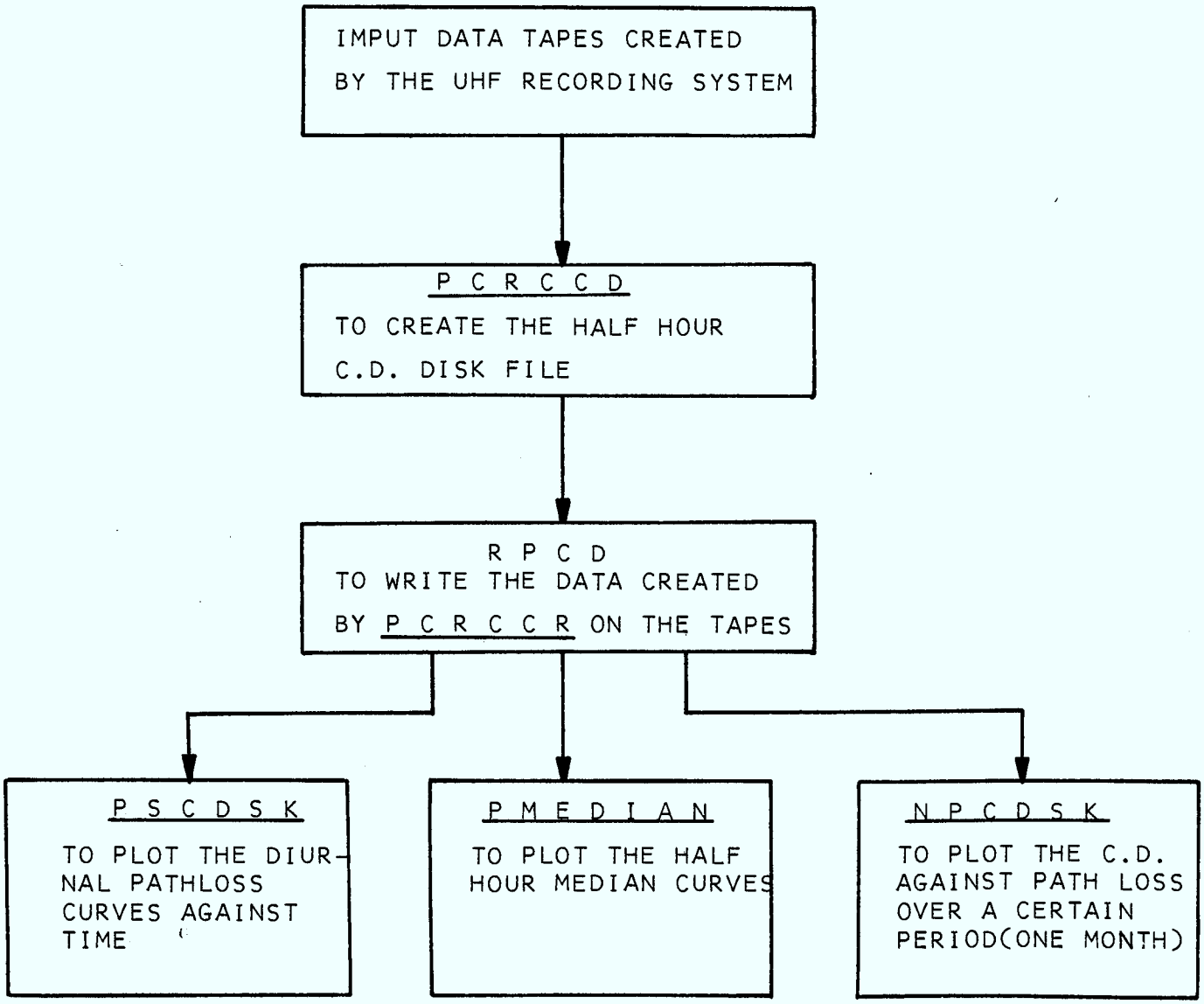

C.D.: CUMULATIVE DISTRIBUTION

FIG.C-2 THE ORGANIZATION OF THE PROGRAMS IN THE FINAL STAGE DATA PROCESSING.

the half hour diurnal cumulative distribution which were written on the permanent disk file. The heading and the cumulative distributions were assigned when the transmitting station is off the air or the recording system is off.

RPCD writes the half hour cumulative distribution data from the permanent disk files created by PCRCCD on the intermediate tapes. The order of the channels in the intermediate tape is increasing from 0 to 15. This contrasts to the disk file where the order is arbitrary.

PMEDIAN calculates the half hour median and the half hour median path loss curves for each channel for plotting.

NPCDSK is to calculate the cumulative distribution over a certain period of time (for example, one month). The curve, the cumulative distribution against path loss, also is presented.

PSCDSK calculates the diurnal cumulative distribution and plots the corresponding curves. The table which indicates the on and off period of the transmitted station or recording system is also given.

More details for the program PCRCCD, RPCD, PMEDIAN, NPCDSK and PSCDSK can be found in the document of the respective program.

Acknowledgement: The computer programs of the first stage data processing were developed by Dr. F.C. Choo. The conversion of the plot subroutine from Cyber 73 to Xerox machine was done by Joan Thomas.

Documentation of Program PCRCCD

Purpose: To process the tapes created by the CRC data acquisition system on the project UHF-VHF TV signal monitoring measurements across the Great Lakes. It calculates the half hour cumulative distribution. The results will be written on the permanent files (tapes) for further use.

Description of the block diagram:

Step 1: A. Read in all information. The parameters are:

(1) NFILE: number of blocks allowed to process the input tape (normally it is 5000)

NFILES: number of blocks to be skipped initially (normally 0)

TIME1: number of seconds allowed to process the input tape

NBYPASS:
NOSKIP: for use of buffer in

(2) NCHANL: number of channels to be processed (16)

NSEGM: number of segments in one day (48)

MINSEG: number of minutes in each segment (30)

IAABB: monitoring site (London or Ottawa)

(3) ITAPE: name of the input tape

IPT: the IPT th input tape to be processed

I0T: the I0T th output tape to be created

(4) ICHALC: computer channel number (0 - 15)

(5) ICHAIR: real channel number

(6) NOISEL: bin number of the noise level

(7) IAB: UHF station site

(8) SPAN: the strength of first bin (example:110)

(9) ANTLAB: antenna and cable correction

(10) ERP: effective radiated power

(11) MCB: Mode of calibration data status. If MCB = 0 the calibration will be calculated from the input data tape otherwise from the data card. (only when MCB = 1)

(12) NYCB, MONCB, NDCB, NHRCB, MINCB, DDLCB
They are the time (year, month, day, hour and minute) to read the calibration data card. DDLCB are the calibration data cards.

(13) NBY, NBM, NBD, NBHR, NBMIN
The starting time (year, month, day, hour and minute) in the output C.D. tape

(14) NEY, NEM, NMD, NEHR, NEMIN
The ending time (year, month, day, hour and minute) in the output C.D. tape.

B. Initialize

C. Write out the heading

Step 2 Read the input file to obtain the following information:

A. the last calibration fit

B. the time of the last block the last input tape had been processed

C. the C.D. of the last half hour the last input tape had been processed

and some other control parameters.

Step 3 Buffer in one block of input data tape.

Step 4 Start to process the 5 min. block to fix the recording time at 5 mult. minute.

Step 5 Test the block whether it is the calibration block

Step 6 do the calibration fit

Step 7 Test whether the recording system is off.

Step 8 Fill in the dummy C.D. data when the recording system is off and write out on the output permanent file.

Step 9 Test the time of the block whether it is the end of the every half hour.

Step 10 Calculate the half hour C.D. and write out on the permanent file.

Step 11 Test whether it is changing

Step 12 Read in the station log data. It includes the mode of the on-off air status (MRT), on-off air time and percentage power. If MRT = 0 there are log station data. If MRT = 1 there are no station log data. The noise level will be the on-off air criterion.

Step 13 Continue to process the 5 minute data

Step 14 Test whether the ending time has been reached.

Step 15 Write out the last calibration fit and some information of last half hour on another permanent file for the input of the next run.

Step 16 If it is the end of the input tape then go to Step 15 otherwise process next block (go back to Step 3)

Remark: This program is systematically organized.

Statement No.	Description
0 - 99	General: Read in, initialized, buffer in. Read from the permanent file (tape 14). Write the calibration and other information in the permanent file (tape 4) at the end of the program.
100 - 199	Read format
200 - 299	Write format
300 - 399	Recording system is off
400 - 499	To calculate the calibration
500 - 599	To calculate the half hour cumulative distribution and write out the result on the permanent file (tape 9).
600 - 699	Day changing
700 - 799	Tp process 5 minute block

80 - 90 in each 100 statements are reserved for minor corrections. The statement number larger than 1000 will be introduced if there is major change or further modification.

BLOCK DIAGRAM FOR P C R C C D

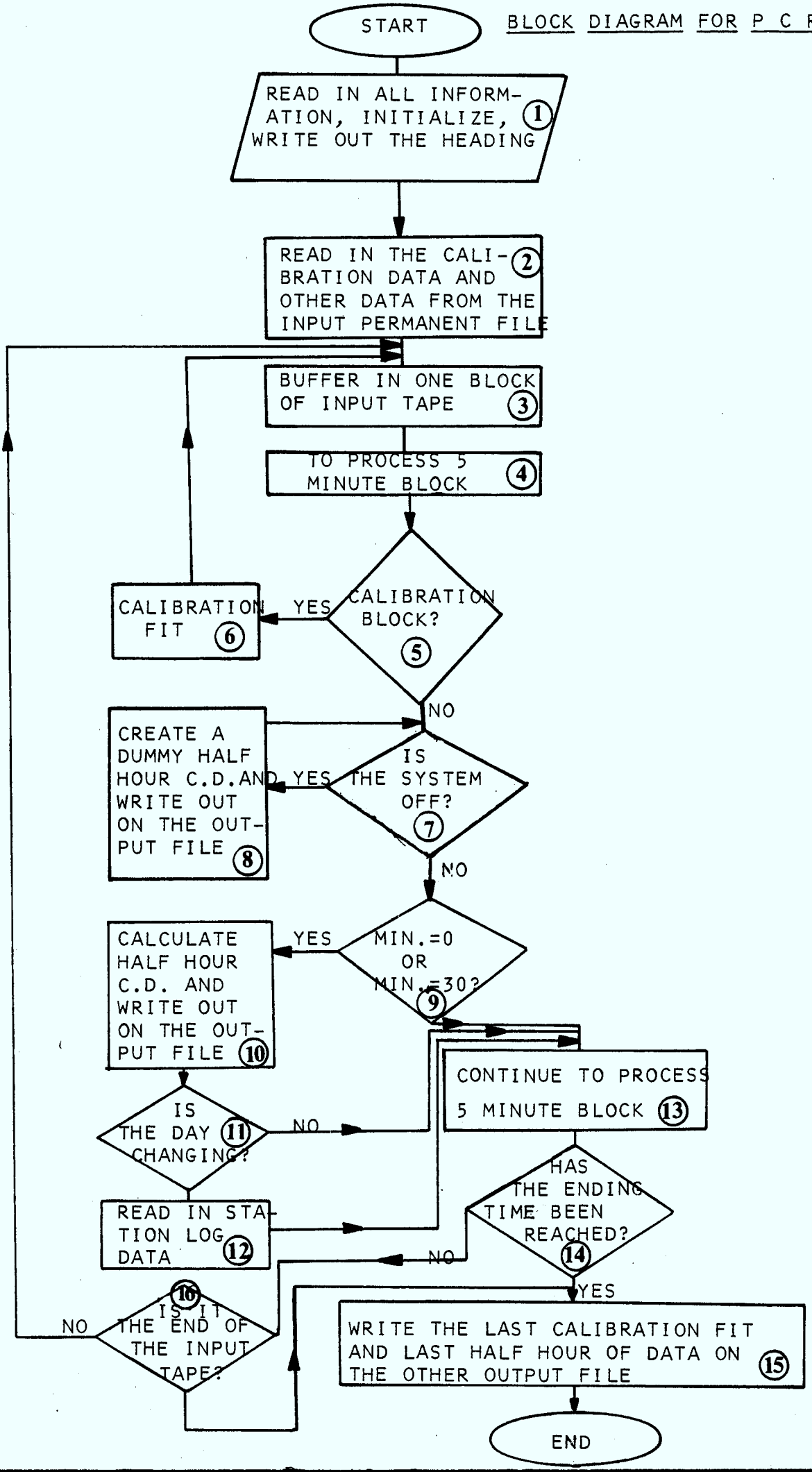

Input data:

1st card: Format (2I5, F10.2, 2I5)

NFILE, NFILES, TIME 1, NBYPASS, NOSKIP

NFILE: number of blocks allowed to be processed (normally 5000)

NFILES:number of blocks to be skipped initially (0)

NBYPAS: 0

NOSKIP:0

2nd card: Format (3I5, A10)

NCHANL, NSEGM, MINSEG, IAABB

NCHANL: number of channel to be processed (1 - 16)

NSEGM: number of segments in one day (48 for half hour resolution)

MINSEG: number of minutes in one segment (30)

IAABB: monitoring site (London or Ottawa)

3rd card: Format (8I5)

ICHALC(I), I - 1, NCHANL

ICHALC: computer channel number (0 - 15)

4th card: Format (8I5)

ICHALR(I), I = 1, NCHANL

ICHALR: Real channel number

5th card: Format (8I5)

NOISE1(I), I = 1, NCHANL

NOISE1: Noise level

6th card: Format (8A10)

IAB(I), I = 1, NCHANL

IAB: UHF station site

7th card: Format (8F10.3)

SPAN(I), I = 1, NCHANL

SPAN: The strength (in DB) of the first bin (ex.110)

8th card: Format (8F10.3)

ANTCAB(I), I = 1, NCHANL

ANTCAB: The antenna and cable correction

9th card: Format (8F10.3)

ERP(Z), I + 1, NCHANL

ERP: Effective radiative power

10th card: Format (A10,2I2)

ITAPE, IPT, IOPT

ITAPE: name of the input tape

IPT: input tape number

IOPT: output tape number

*This card has to be changed in each run since the name of the input tape and input tape number are different.

11th card: Format (I2)

MCB

MCB: The mode of calibration data status

If MCB = 0 read the calibration data from input tape

If MCB = 1 read the calibration data from input cards

1st card: Format (I2)

when MCB=1

MCHANL

MCHANL: number of channels which the calibration data be read in from cards

2nd card: Format (5I2)

NYCB, MONCB, NDCB, NHRCB, MINCB

These are the time (year, month, day, hour and minute) for calculating the calibration

DO I = 1, MCHANL

1st: Format (I2)

I

2nd: Format (I2)

ICHALC(I)

3rd: Format (13F5.1)

DDLCB(I,K), K = 1,13

DDLCB: The calibration data continue

12th card: Format (5I2)

NBY, NBM, NBD, NBHR, NBMIN

These are the starting time (year, month, day, hour and minute) of the output tape.

13th card: Format (5I2)

NAY, NEM, NED, NEHR, MENIN

These are the ending time (year, month, day, hour and minute) of the output tape

next set of cards: DO 1 I = 1, MNS

DO 2 J = 1, MCHANL

READ(5,107)MRT(J)ICHALC(J) MY, MMON, MDAY,

(MHRB(J,K), MINB(J,K), MHRS(J,K), MINS(J.K)

PCTP(J,K), K = 1.6)

```
107 FORMAT (I1, 4I2,6(4I2,I3))
2  continue
1  continue
MRT: mode of log data
     if MRT = 0  There is log data
     if MRT = 1  There is no log data
ICHALC: computer channel number
MY, MMON, MDAY: Time (year, month and day)
MHRB, MINB:  starting time (hour and minute)
             of the UHF station on-air period
MHRS, MINS:  Ending time (hour and minute)
             of the station on-air period
PCTP:        percentage power transmitted at
             that on-air period
```

Documentation of Program RPCD

Purpose: To write the cumulative distribution data created by PCRCCD on the magnetic tape.

On the output tape there are there are no interruptions o f data. Any missing data in the original data tape will be filled in with dummy data.

Notes for the Block Diagram:

Step 1: Read in the information. The parameters are:

A MBPW: number of bits per word for the computer system (60 for Cyber; 32 for Xerox)

MSEG: number of segments in one day (normally it is 48)

B MDAY: number of days data in the output tape before one file mark. (Usually we put one file mark after the one month data. This means MDAY = 30 or 31 in normal month)

MMDAY: number of days data in the output tape (usually we store two months data on the intermediate tape. It means MMDAY = 61 in normal case).

Step 2. If there are some data already in and it is needed, position the end of existing data at the beginning of the new data.

Step 3. 137 words for one half hour of one channel data from the disk file created by PCRCCD be read in.

Step 4. Pack these 137 words in the more compact form in order to save the space on the magnetic tape. The format of the packed word is shown in the appendix.

Step 5. Test whether all data in the same time is in.

Step 6. Save this information for next block output data.

Step 9. Test whether there is 16 channel data in that half hour.

Step 10. Fill in dummy C.D. data for missing data of the channel.

Step 11. Buffer out 16 channel half hour packed C.D. data as one block in the magnetic tape.

Step 12. Decide whether to put the file mark or end of the program in.

Step 13. Prepare for the next output block.

BLOCK DIAGRAM FOR R P C D

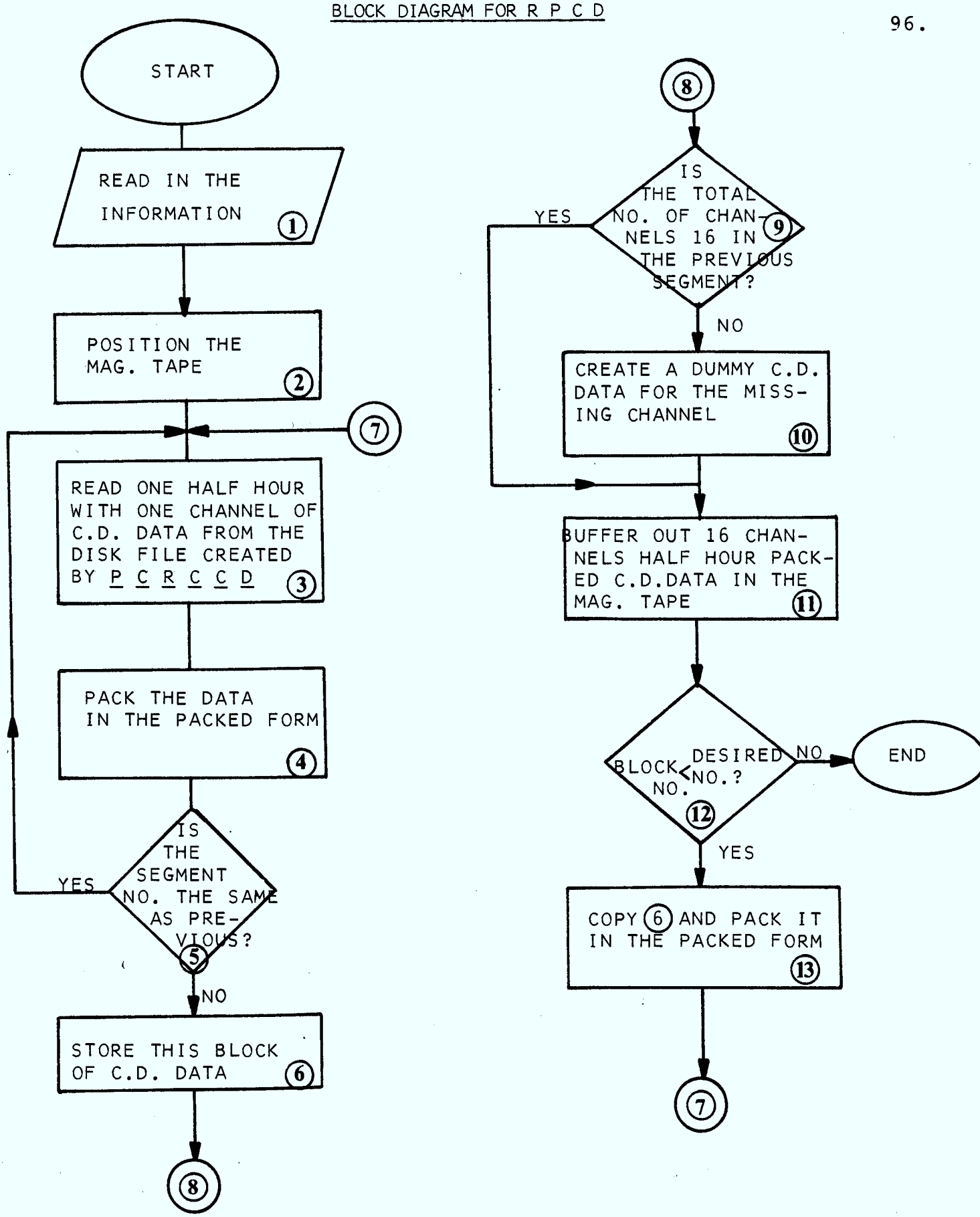

Input data:

1st card: Format (2I5)

MBPW, MSEG

MBPW: number of bits per word for the computer system (60 for Cyber, 32 for Xerox)

MSEG: number of segments each day (48 for half hour resolution)

2nd card: Format (2I5)

MDAY, MMDAY

MDAY: number of days before one file mark (30 or 31 normally)

MMDAY: number of days before two file mark (61 normally)

One disk file:

NI: Number of input file already in the magnetic tape

NF: Number of data block already in the magnetic tape

One magnetic tape:

There are some data already in this tape

Appendix

The format of the cumulative distribution data tape is similar to the data tape extended by the CRC data acquisition system on the UHF monitoring project. That is, there are 16 blocks in each record and each block consists of 128 - 16 bits words of which the first 8 words are used for heading. The 16 channel half hour cumulative distribution data are stored in one record. The details of the format for each block are shown in block format.

BLOCK FORMAT

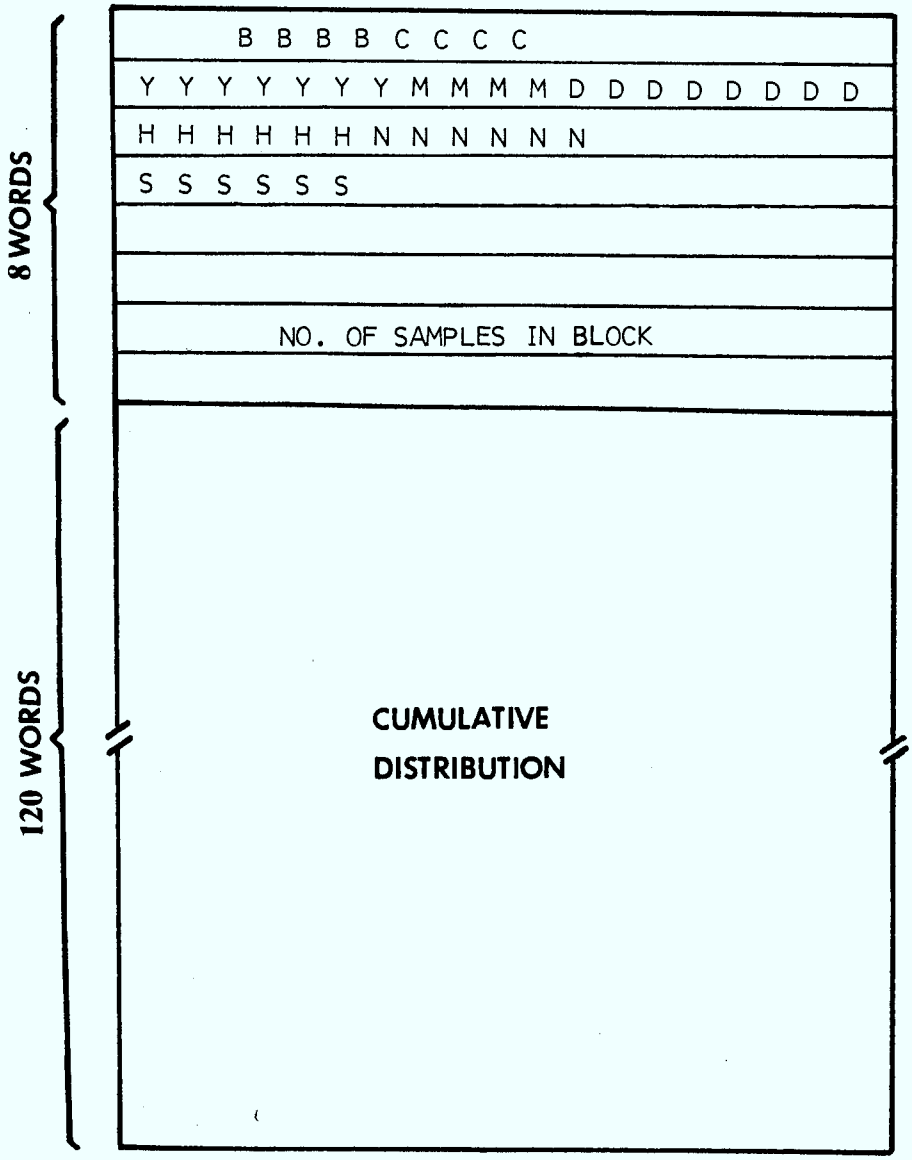

B=BLOCK TYPE (0-4)
(DETAIL BELOW)

C=CHANNEL NUMBER (0-15)

Y=YEAR FIELD (0-99)

M=MONTH FIELD (1-12)

D=DAY FIELD (1-31)

H=HOUR FIELD (0-23)

N=MINUTE FIELD (0-59)

S=SEGMENT NUMBER

WHEN B=0: IT IS CUMULATIVE DISTRIBUTION

B=1: THE STATION IS OFF THE AIR

B=2: THE RECORDING SYSTEM IS OFF

Documentation of Program: NPCDSK

Purpose: To plot a curve, the cumulative distribution over a certain period (for example, one month) against the path loss (in DB), from the half hour cumulative distribution data tape created by the programs PCRCCD and RPCD.

The notes for the Block diagram:

Step 1. Read in all the information. The parameters are:

A. MBPW: number of bits per word for the computer system (60 for Cyber; 32 for Xerox)

NFILE:Maximum number of blocks allowed to be processed

NFILES:Number of blocks to be skipped initially

TIME1: Time allowed to process the tape

B. NCHANL: number of channels to be processed

IAABB: UHF Recording station site (Ottawa, London)

ITAPE: name of the cumulative distribution data tape

C. ICHALC: computer channel number (0 - 15)

D. ICHALR: real channel number

E. IAB: : UHF transmitted station site

F. SPANI: the strength (in DB) of the first bin

G. ANTCAB: the correction of the antenna gain and cable loss

H. ERP: effective radiative power

I. NYB, MONB, NDB, NHRB, MINB:

The starting time, (year, month, day, hour and minute) of the data processing period.

J. NYE, MONE, NDE, NHRE, MINE:

The ending time (year, month, day, hour and minute)

of the data processing period.

Write out for heading.

Step 2. Read one block of the input tape

Buffer in one block of data. Every block has 16 channels half hour cumulative distribution data. If one file mark is encountered the next block data may be processed continuously. If the two file marks are encountered the result will be written out (go to Step 9).

Step 3. Unpack the words of one channel which will be processed at one time.

Step 4. and Step 5.

If the time information in the data block is within the processing time range go to next step (Step 6) and process the data. If the time is before the processing time then go back to Step 2 and read the next block data. It continues until they match. If the time is after the processing time then go to step 8.

Step 6. To accumulate the cumulative distribution, the total number of signals, the total number of signals when the UHF station and recording system are on the air.

Step 7. To test whether all the channels in the data block have been processed. If it is, then read the next block (i.e. go back to step 2). Otherwise, unpack the words of another channel (i.e. go back to step 3.)

Step 8. junction

Step 9. To calculate the cumulative distribution in percentage (i.e. normalization for the cumulative distribution over a certain period).

Step 10. To calculate the Rayleigh distribution (-log(-lnP) when P is the normalized cumulative distribution) and the normalization. To calculate the percentage which the UHF station and recording system are on the air.

Step 11. Write out the percentage time the UHF station and the recording system are on the air, the normalized cumulative distribution, the normalized Rayleigh distribution and the strength (in DB) in every bin.

Step 12. Plot the curve which the normalized cumulative distribute against path loss (in DB).

Input data

1st card: Format (3I5, F10.5)

MBPW, NFILE, NFILES, TIME 1

MBPW: number of bits per word in the computer system (60 for Cyber, 32 for Xerox)

NFILE:number of blocks allowed to be processed

NFILES:number of blocks to be skipped initially (normally 0)

TIME1 :number of seconds allowed to process the tape

2nd card: Format (2I5), 2A10)

NCHANL, IAABB, ITAPE

BLOCK DIAGRAM FOR N P C D S K

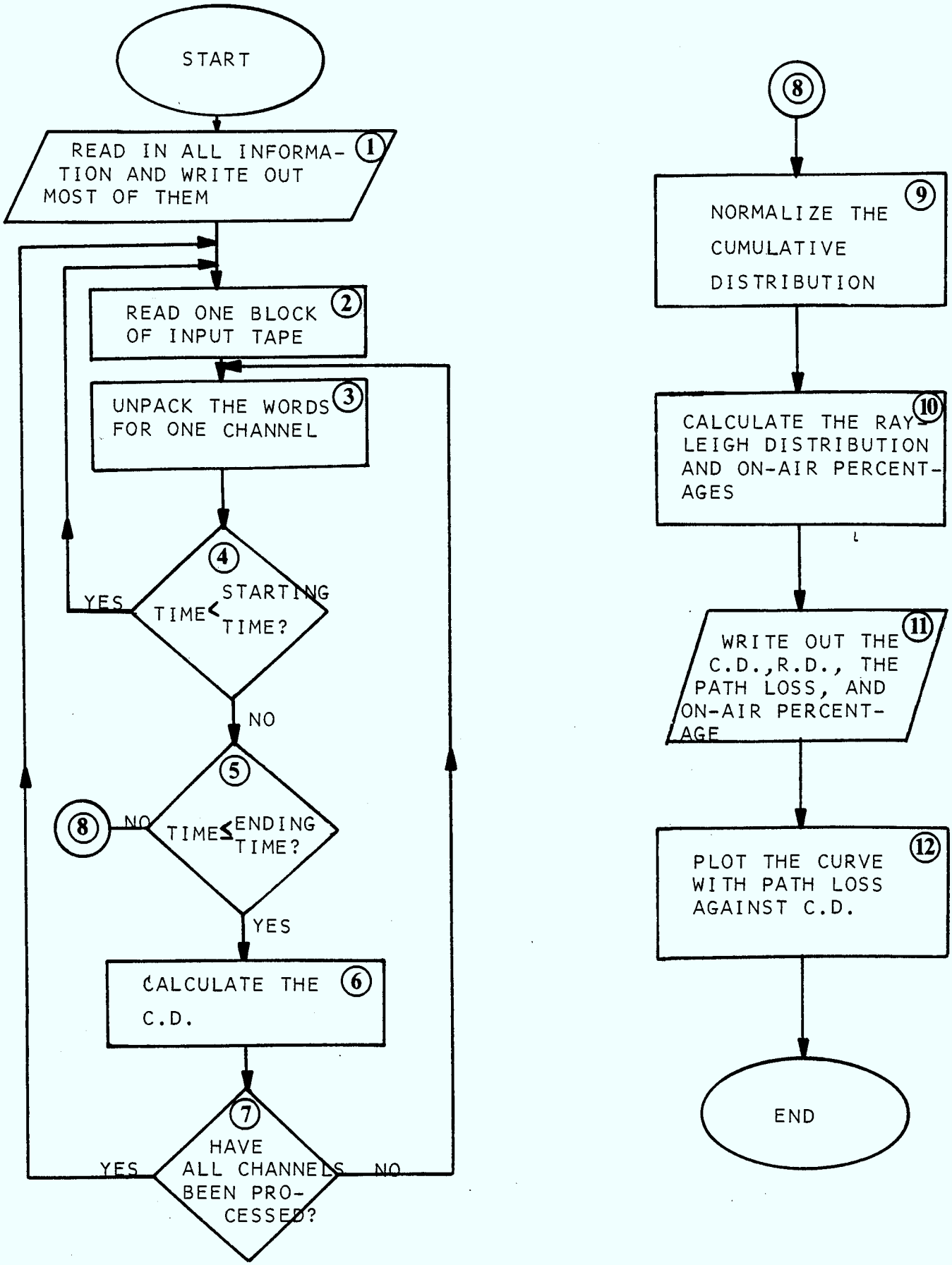

NCHANL: number of channels to be processed (from 1 - 16)

IAABB: recording site (London or Ottawa)

ITAPE: the name of the processing tape (ex.CRS002)

3rd card: Format (16I5)

ICHALC(I), I = 1, NCHANL

ICHALC: computer channel number

4th card: Format (16I5)

ICHALR(Z), I = 1, NCHANL

ICHALR: Real channel number

5th card: Format (8A10)

IAB(I), I = 1, NCHANL

IAB: UHF station site

6th card: Format (8F10.5)

SPAN(I), I = 1, NCHANL

SPAN: the beginning of the span (the strength of the first bin)

7th card: Format (8F10.5)

ANTCAB(I), I = 1, NCHANL

ANTCAB: The cable and antenna corrections

8th card: Format (8F10.5)

ERP(I), I = 1, NCHANL

ERP: the effective radiative power

9th card: Format (5IZ)

NYB, MONB, NDB, NHRB, MINB

The starting time (year, month, day, hour and minute) of the period to be processed.

10th card: Format (5IZ)

NYE, MONE, NDE, NHRE, MINE

The ending time (year, month, day, hour and minute) of the period to be processed.

Documentation of Program PSCDSK

Purpose: To plot the curves which are the path loss against the time of the day from the half hour cumulative distribution data tape created by the programs PCRCCD and RPCD. The table about whether the UHF and recording system are or are not on the air at every half hour within the processing period is written out.

The notes for the block diagram:

Step 1. Read in all information. The parameters are:

A MBPW

NFILE

NFILES Same as program NPCDSK

TIME 1

NJ = number of the different percent path loss to be processed

B,C,D,E,F,G,H,I and J are the same as NPCDSK

K XN: the percent of the path loss

L PRTCUT: the criterion for whether the points will appear in the output curves

(for example, if PRTCUT = 20 it means if the on-air percent is less than 20% in that segment then the data is not reliable (poor statistics). The point represented in the path loss at this segment will

be ignored)

Step 2,3,4,5,7 and 8 are the same as NPCDSK

Step 6.

A. To add up the cumulative distribution in which they are in the same segment (half hour) of the day. It is called " split cumulative distribution." (For example, Sept. 9-10:00 AM and Sept. 10, 10:00 AM are in the same segment of the day starting at 10:00 AM.

B. To calculate the total number of signal in each segment when the UHF station and recording system are on the air. (NCOUNT)

C. To calculate the total number of signals in each segment (MCOUNT)

D. To store the information about which the UHF station and recording system are on the air for every half hour. Since there are 5 minute distribution data in the original data tapes created by the monitoring recording system, the number (LCOUNT) from 0 - 6 indicates how many 5 minute blocks in the half hour are on the air.

Step 9. To normalize the split cumulative distribution (i.e. in percent)

Step 10. To calculate the strength (in DB) for different percent path loss in every segment (half hour of the day)

Step 11(a) to write out the result in step 10. They are the input data for plotting.

(b) To write out the table about the on-off air in every half hour and on air percent of each segment

Step 12. If the on-air percent is less than a certain number which we desire (PRTCUT) poor statistics are assumed and the data is not reliable. These points are washed out.

Step 13. To plot the curves which the strength (in DB) for certain percent path loss against half hour of the day. The points with poor statistics are not shown in the curves.

Input data

1st card: Format (3I5, F10.5, If)

MBPW, NFILE, NFILES, TIME1, NJ

MBPW

NFILE same as NPCDSK

NFILES

TIME1

NJ: number of different percent path loss to be proessed (1 - 10)

2nd, 3rd - - - and 10th card

Same as Program NPCDSK

11th card: Format (10F5.2)

XN(I), I = 1, NJ

XN: percentage of path loss (for example: 1, 10, 50, 90, 99 - - - -)

12th card: Format (F5.2)

PRTCUT

PRTCUT: cut off criterion (15 or 20)

BLOCK DIAGRAM FOR P S C D S K

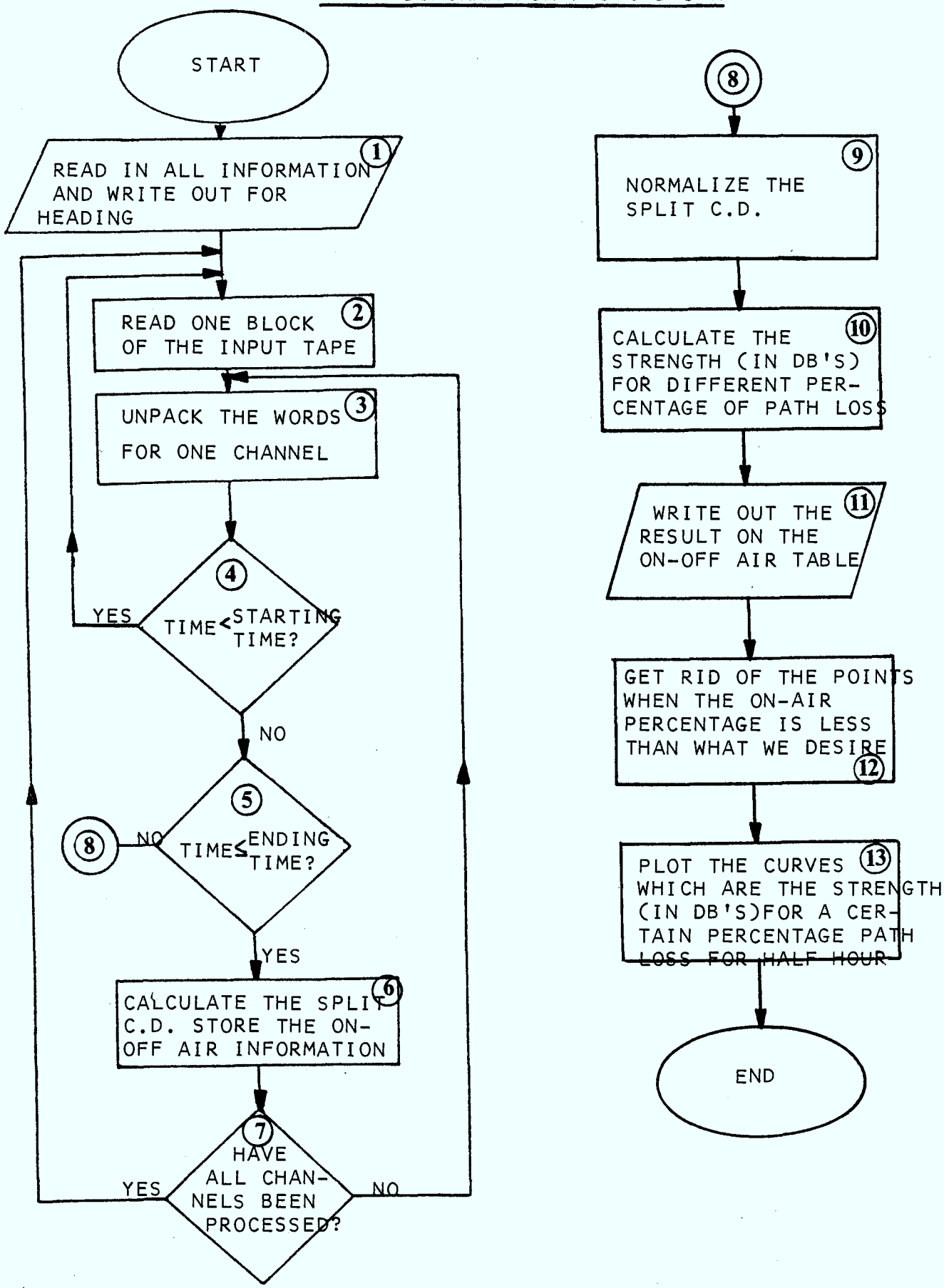

Documentation of Program PMEDIAN

Purpose: to plot the curves, the median path loss (in DB) against the time of the day, from the half hour cumulative distribution data tapes created by the programs PCRCCD and RPCD

The notes for the block diagram

Step 1, 2, 3, 4, 5, 7 and 8 are the same as Program NPCDSK

Step 6. Calculate the strength (in DB) of median path loss for every half hour. They are the input of the plotting.

Step 9. Plot the median against time for every day.

Input data:

They are the same as Program NPCDSK

BLOCK DIAGRAM FOR P M E D I A N

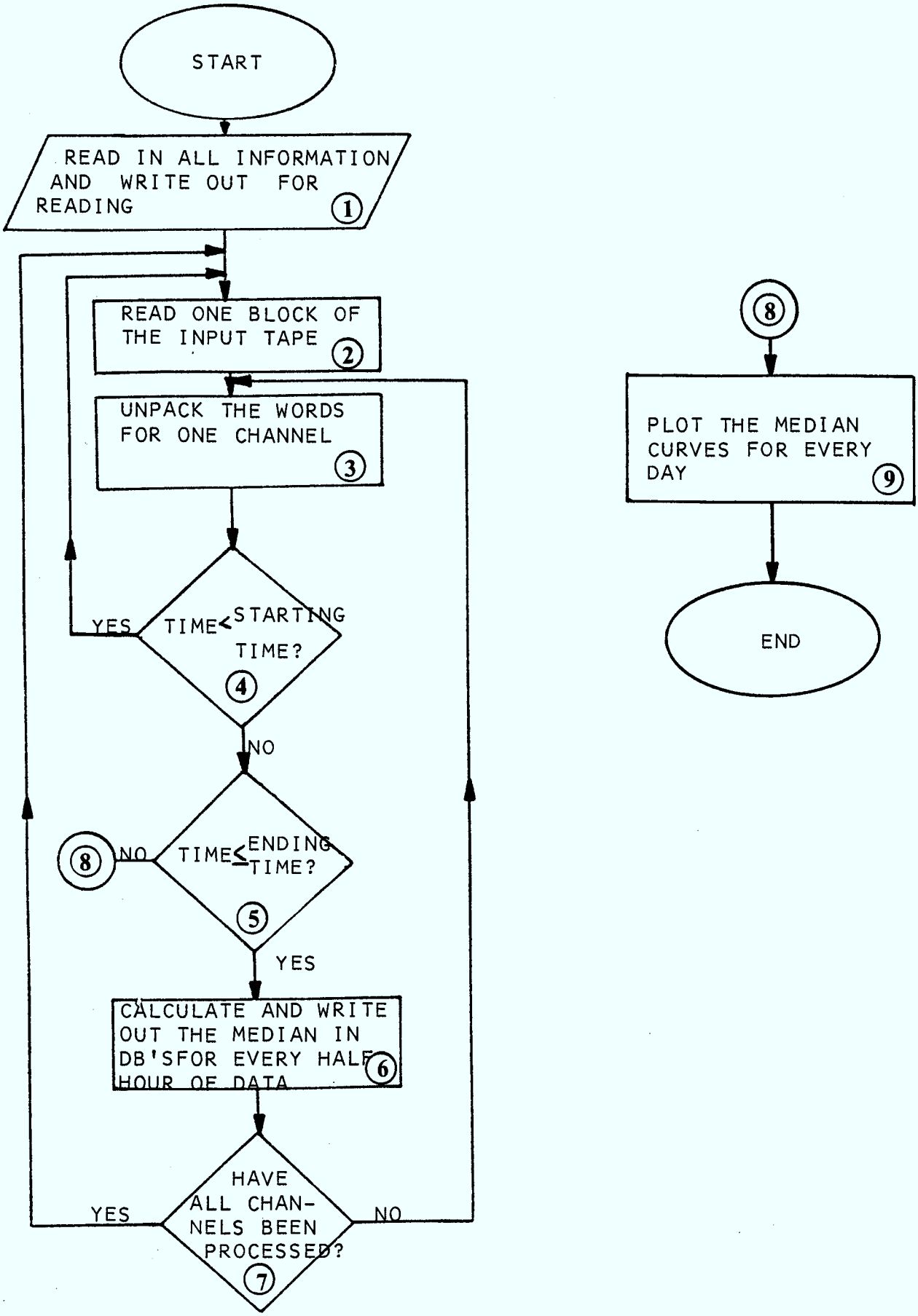

MEASUREMENTS OF ANOMALOUS PROPOGATION OF UHF/VHF USING TV TRANSMITTERS